

**Exploring the potential of MSC secretome to counteract
APAP-induced hepatic injury *in vitro***

Daniela Sofia Nunes Ribeiro

Thesis to obtain the Master of Science Degree in

Biological Engineering

Supervisor(s): Professor Joana Paiva Gomes Miranda
and Professor Cláudia Alexandra Martins Lobato da Silva

Examination Committee

Chairperson: Professor Gabriel António Amaro Monteiro

Supervisor: Professor Joana Paiva Gomes Miranda

Member of the Committee: Professor Susana Zeferino Solá da Cruz

November 2021

Preface

The work presented in this thesis was performed at the Research Institute of Medicines (iMED.Ulisboa), Faculty of Pharmacy, University of Lisbon (Lisbon, Portugal), during the period April-November 2021, under the supervision of Prof. Joana Miranda. The thesis was co-supervised at Instituto Superior Técnico by Prof. Cláudia Lobato.

Declaration

"I declare that this document is an original work of my own authorship and that it fulfils all the requirements of the Code of Conduct and Good Practices of the Universidade de Lisboa."

Acknowledgements

First and foremost I would like to express my gratitude to Professor Joana Miranda for welcoming me during these past months in the Advanced Cell Models for Predictive Toxicology & Cell-based Therapies group, in iMed.Ulisboa, Faculdade de Farmácia, Universidade de Lisboa. I am thankful for this opportunity to broaden my knowledge and insights regarding laboratory investigation.

Also I would like to express my appreciation to Professor Cláudia Lobato for being always available, patient and kind throughout my time at Técnico, but specially during this master thesis.

To all members of the laboratory group, this thesis would not be possible without your precious help and patience, teaching me all the cell culture principles and guiding me when things did not go as expected. If during these five years of Técnico I have not learnt enough about resilience, then these past months are the culmination of a long and tough journey.

I am grateful to say that the best I take from Técnico are the friends I made. To all of you, for always being present, in the good, in the bad and in the crazy moments, I am truly thankful and I hope that we continue to make many more memories together.

To the girls I carry with me since high school or even before that, with whom I grew up and became the person I am today, thank you for always being there cheering me up.

To my family, specially my parents, thank you for sponsoring all my studies and many of my wills, for believing in me and for always being there when I needed. To my not so little brother, thank you for all the funny moments that were so much needed throughout these years. And, of course, to my dogs who always greeted me with happy tails and in seconds made all the problems disappear.

Last but not least, to my favourite nerdy goofer, it is to you I must thank for having this thesis done. For always listening to all my vents, to keep pushing me up to be a better person and to making me laugh every day! I hope that you are so proud of me as I am of you and I hope that you continue to think that I am amazing for many more years.

I will always remember these Técnico years with an emotional smile, certain that I collected some tools to unravel what life is and what is about to begin, and confident that I have the right people by my side to overcome the next challenges.

Resumo

O paracetamol é a principal causa de lesão hepática induzida por fármacos, correspondendo a 40-70% da insuficiência hepática aguda na Europa. As terapias atuais não cumprem com a necessidade global ou apresentam uma estreita janela terapêutica. Assim, as células estaminais mesenquimais (CEM) e os seus fatores parácrinos surgem como alternativa, potenciando a regeneração hepática.

Estudos recentes evidenciam a alteração do comportamento das CEM em resposta ao nicho microambiental. Assim, preconditionou-se CEM com meio de células hepáticas lesadas (meio SOS) produzindo-se um secretoma mais direcionado para lesão hepática. O meio de um modelo *in vitro* de lesão hepática induzida por APAP (meio SOS) foi produzido incubando células-tipo hepatócito (CTH) com o DL₅₀ estimado para APAP durante 8 horas. Após incubação com APAP, as CTH alteraram a morfologia, expressando genes de stress reticular endoplasmático e apoptose. Adicionalmente, o modelo de lesão foi caracterizado em culturas 3D, sugerindo maior efeito hepatoprotetor do que em culturas 2D.

Posteriormente, preconditionou-se CEM com o meio SOS, modulando o secretoma para um fenótipo mais angiogénico, sobreexpressando *SDF-1* e *TNF-A*. Salienta-se que, após exposição ao secretoma preconditionado, CTH lesadas com APAP exibiram efeitos pró-regenerativos, sobreexpressando *CCND1*, *C-MET*, *VEGF-A* e *FGF-2*. Ademais, observou-se aumento da proliferação celular em CTH expostas a 5 e 15 mM APAP durante 24 horas incubadas com o secretoma preconditionado. Efetivamente, o condicionamento exibiu relevância terapêutica em CTH com 15 mM APAP.

Resumindo, o modelo *in vitro* de lesão hepática induzida por APAP mimetizou o microambiente lesionado, aumentando o potencial do CEM-secretoma na regeneração hepática.

Palavras-chave: células-tipo hepatócito (CTH); paracetamol; lesão hepática induzida por fármacos; secretoma; células estaminais mesenquimais (CEM); regeneração hepática.

Abstract

Acetaminophen (APAP)-induced hepatotoxicity is the major cause of drug-induced liver injury (DILI), accounting for 40-70 % of acute liver failure in Europe. Current therapies do not meet the global need or display a narrow therapeutical window. Thus, mesenchymal stem cells (MSCs) and their paracrine factors emerge as alternative therapeutical approaches to enhance liver regeneration.

Emerging evidence sustains that MSC behaviour is altered in response to the microenvironmental niche. Thus, priming MSCs with medium from hepatic injured cells (SOS medium) was attempted to produce an MSC-secretome more targeted for liver injury. Herein, medium from an APAP-induced hepatic injury *in vitro* model (SOS medium) was produced by incubating human hepatocyte-like cells (HLCs) with the estimated APAP IC₅₀ value for 8 hours. Upon APAP incubation, HLCs altered their morphology, expressing APAP-induced hepatotoxicity genes related with endoplasmic reticulum stress and apoptosis. Additionally, the injury model was characterized in 3D cultures, suggesting a higher hepatoprotective effect than in 2D cultures.

Afterwards, MSCs were primed with the SOS medium, modulating their secretome into a more angiogenic phenotype, up-regulating *SDF-1* and *TNF-A*. Importantly, upon exposure to MSCs-primed secretome, APAP-injured HLCs displayed pro-regenerative effects, up-regulating *CCND1*, *C-MET*, *VEGF-A* and *FGF-2*. Results also showed increased cell proliferation in HLCs exposed to 5 and 15 mM APAP for 24 hours incubated with the MSCs-primed secretome. Indeed, the priming strategy displayed therapeutic relevance in 15 mM APAP-injured HLCs.

In sum, the APAP-induced liver injury *in vitro* model mimicked the injury microenvironment and increased the MSC secretome potential for enhanced hepatic regeneration.

Keywords: hepatocyte-like cells (HLCs); APAP; DILI; secretome; mesenchymal stem cells (MSCs); liver regeneration.

Index

Acknowledgements.....	IV
Resumo.....	VI
Abstract.....	VII
Index.....	VIII
List of figures.....	X
List of tables.....	XIII
List of abbreviations.....	XIII
1. Introduction.....	1
1.1. Liver structure and function.....	1
1.1.1. Metabolic zonation.....	1
1.1.2. Drug metabolism.....	3
1.2. Liver failure.....	4
1.3. Drug-induced liver injury.....	5
1.3.1. APAP metabolism.....	6
1.4. Liver regeneration.....	10
1.4.1. Intrinsic hepatic regeneration.....	10
1.4.2. Signals behind the liver regeneration process.....	10
1.5. Cell-based therapies for liver regeneration.....	13
1.5.1. Mesenchymal stem cells therapy for liver regeneration.....	14
1.5.1.1. Extracellular vesicles and exosomes.....	18
1.5.1.2. Priming strategies to improvement the clinical outcome of MSCs.....	18
1.6. Motivation and aims.....	21
2. Materials and methods.....	22
2.1. Reagents.....	22
2.2. Cell culture.....	22
2.3. Collagen coating.....	22
2.4. Hepatocyte differentiation protocol.....	22
2.5. Conditioned medium production.....	24
2.5.1. SOS medium.....	24

2.5.2.	Pre-conditioning of hnUCM-MSCs: production of conditioned medium (MSC-CM).....	24
2.6.	Cell viability assays	26
2.7.	Gene expression	26
2.8.	Protein quantification	27
2.9.	Statistical analysis	27
3.	Results and discussion	28
3.1.	APAP toxicity in hepatocyte-like cells (HLCs)	28
3.2.	APAP-induced injury in 2D and 3D HLC <i>in vitro</i> cultures reveal differential liver injury-related gene expression levels	30
3.2.1.	APAP induced morphological changes and altered gene expression in 2D-cultured HLCs	30
3.2.2.	3D culturing of HLCs to establish an <i>in vitro</i> APAP-induced liver injury model.....	33
3.3.	Priming with the SOS medium exerted pro-angiogenic and regenerative effects in hnUCM-MSCs	36
3.4.	Evaluation of the regenerative effect of primed MSC secretome in APAP-induced liver injury <i>in vitro</i> model	39
3.4.1.	Inducing liver injury through APAP exposure	39
3.4.2.	pMSC-CM displayed a regenerative effect in APAP-induced injury <i>in vitro</i> model	40
4.	Conclusions and future perspectives	44
5.	References	46
6.	Annexes.....	54

List of figures

Figure 1 - Schematic representation of the liver acinus. Identification of the distinct cell-types and structures presented as well as the blood flux from the portal vein and hepatic artery to the central vein.

Figure 2 - Representation of biochemical pathway zonation in the liver. Distribution preference through periportal or perivenous regions in the liver. Abbreviations: TG (triglyceride).

Figure 3 - APAP metabolism in the liver. This xenobiotic is metabolized through sulfation, glucuronidation and oxidation into APAP-sulfate, APAP-gluc and NAPQI, respectively. The latter is a reactive metabolite detoxified by intracellular GSH and excreted as APAP-cys. Abbreviations: APAP-sulfate (APAP with a sulfate group); APAP-gluc (APAP inactive glucuronide form); SULT (sulfotransferases); UGT (5'-diphosphate-glucuronosyltransferases); CYP450 (cytochrome P450); NAPQI (*N*-acetyl-*p*-benzoquinone imine); GSH (glutathione); GST (Glutathione-S-transferases); APAP-cys (APAP nontoxic conjugates of cysteine and mercapturic acid).

Figure 4 - Mechanism of the APAP-induced hepatotoxicity. Under excessive doses, higher amounts of APAP are oxidated into NAPQI, which covalently binds to mitochondrial proteins, forming NAPQI-adducts. As a result, free radicals such as superoxide are formed, inducing the mitochondrial oxidative stress. Hence, Trx is oxidated, detaching from ASK1 and activating the latter. Parallely, MLK3 is activated and, together with ASK1, phosphorylate MKK4. Sequentially, MKK4 and JNK are phosphorylated. The presence of JNK and Bax in the mitochondria increases its oxidative stress, promoting DNA fragmentation and cell necrosis. Abbreviations: NAPQI (*N*-acetyl-*p*-benzoquinone imine); Trx (thioredoxin); ASK1 (apoptosis signal-regulating kinase 1); MLK3 (mixed-lineage kinase 3); MKK4 (mitogen-activated protein kinase kinase 4); JNK (c-jun N-terminal kinase); Bax (Bcl-2-associated X protein).

Figure 5 - Liver regeneration process. Identification of the soluble mediators that potentiate the different stages of the cell cycle. Abbreviations: TNF- α (tumour necrosis factor alpha); IL-6 (interleukin 6); HGF (hepatocyte growth factor); EGF (epidermal growth factor); (HB)-EGF (heparin-binding epidermal growth factor); TGF- α (transforming growth factor alpha); TGF- β (transforming growth factor beta); G0, G1, S (synthesis), G2 and M (mitosis) are phases of the cell cycle.

Figure 6 - Mesenchymal stem cell homing mechanism. Steps and molecules involved in the tethering/rolling, activation and arrest, transmigration/diapedesis and migration. Abbreviations: VCAM-1 (vascular adhesion molecule-1); VLA-4 (very late antigen 4); MMPs (matrix metalloproteinases).

Figure 7 - Hepatocyte differentiation protocol. Description of the three-step differentiation protocol consisting on endoderm commitment/foregut induction, hepatoblast and liver bud formation and hepatoblast differentiation/hepatocyte maturation. Abbreviations: α -MEM (minimum essential medium eagle alpha modification); BM (basal medium); FBS (fetal bovine serum); EGF (epidermal growth factor); FGF (fibroblast growth factor); HGF (hepatocyte growth factor); ITS

(insulin-transferrin-selenium); DMSO (dimethyl sulfoxide); 5-AZA (5-azacytidine); OSM (oncostatin M); D0-D27 (days from 0 to 27 of the hepatocyte differentiation protocol).

Figure 8 - Outline of the work developed divided in three major phases: 1) production of the SOS medium from hnUCM-MSC-derived HLCs; 2) production of MSC-CM primed with SOS medium 5x concentrated (pMSC-CM); 3) evaluation of MSC-CM, either primed (pMSC-CM) or control (cMSC-CM) 10x concentrated, effect on APAP-injured hnUCM-MSC-derived HLCs through qRT-PCR and MTS assays. Abbreviations: hnUCM-MSCs (human neonatal umbilical cord matrix-derived mesenchymal stem cells); HLCs (hepatocyte-like cells); DM (differentiation medium); SOS medium (hepatocyte-like cells medium with SOS secreted signals after APAP exposure); α -MEM (minimum essential medium eagle alpha modification); pMSC-CM (human neonatal umbilical cord matrix-derived mesenchymal stem cells conditioned medium primed with the hepatocyte-like cell SOS medium); cMSC-CM (human neonatal umbilical cord matrix-derived mesenchymal stem cells conditioned medium); qRT-PCR (quantitative real-time polymerase chain reaction).

Figure 9 - APAP toxicity in HLCs. The HLCs were incubated with 5, 10, 15, 20, 30, 50 and 60 mM of APAP for 24 hours (n=2) at D27. The percentage of live cells is calculated relatively to non-treated HLCs at D28. Abbreviations: IC₅₀ (half-maximal inhibitory concentration).

Figure 10 - APAP altered HLCs' polygonal shape morphology and caused detachment. a) morphological changes in 2D-cultured HLCs throughout the differentiation protocol, from D1 to D27; b) HLCs' morphology after an 8-hour exposure to 30 mM APAP; b) HLCs' morphology at the end of the conditioning period to produce the SOS medium. HLCs were exposed to APAP at D27. After APAP exposure, the medium was replaced by fresh medium without APAP. Scale bar = 100 μ m. Abbreviations: D1 - D27 (days 1 to 27 of the hepatocyte differentiation protocol).

Figure 11 - Endoplasmic reticulum stress and apoptosis were induced in HLCs following APAP exposure. Gene expression of HLCs with an 8-hour exposure to 30 mM APAP, at D27, followed by a 24-hour conditioning with fresh medium without APAP, relative to non-injured HLCs recovered at D28. Data represented as average \pm SD (n=1-3). **, *** significantly differed from the non-injured HLCs gene expression with $p < 0.01$ and $p < 0.001$, respectively. Abbreviations: *ASK1* (apoptosis signal-regulating kinase 1); *RIPK3* (receptor-interacting protein kinases 3); *ATF-6* (activating transcription factor 6); *BAX* (Bcl-2-associated X protein); *HNF4-A* (hepatocyte nuclear factor 4 alpha); *TNF-A* (tumour necrosis factor alpha).

Figure 12 - HLCs aggregates' morphological changes in 3D culturing. a) morphological variation of hnUCM-MSC-derived HLCs aggregates at D21 and D27 cultured in ultra-low attachment plates; b) HLCs aggregates' morphology after an 8-hour exposure to 30 mM APAP, at D27; c) HLCs aggregates' morphology at the end of the 24-hour conditioning period. Scale bar = 100 μ m. Abbreviations: D21, D27 (days 21 and 27 of the hepatocyte differentiation protocol).

Figure 13 - HLCs aggregates reduced their diameter upon APAP exposure. HLCs aggregates' diameters, in μ m, at D21, D27, after an 8-hour exposure to 30 mM APAP at D27 (D27 + APAP) and at D28 at the end of the 24-hour conditioning period. The diameters were measured through phase

contrast microscopy images of HLCs inoculated in ultra-low attachment culture plates. Abbreviations: D21 - D28 (days 21 to 28 of the hepatocyte differentiation protocol).

Figure 14 - 3D-cultured HLCs inhibited APAP-related pathways. Gene expression of 3D-cultured HLCs is presented relative to 2D-cultured HLCs both exposed to 30 mM APAP for 8 hours and recovered at the end of the conditioning period. Data represented as average \pm SD (n=1-3). **, *** significantly differs from 2D and 3D-cultured HLCs with $p < 0.01$ and $p < 0.001$, respectively. Abbreviations: *ASK1* (apoptosis signal-regulating kinase 1); *RIPK3* (receptor interacting protein kinases 3); *ATF-6* (activating transcription factor 6); *BAX* (Bcl-2-associated X protein); *HNF4-A* (hepatocyte nuclear factor 4 alpha); *TNF-A* (tumour necrosis factor alpha).

Figure 15 - Priming with the SOS medium increased hnUCM-MSCs' confluency. a) hnUCM-MSCs' morphology 2 days post-inoculation; b) hnUCM-MSCs' morphology 5 days post-inoculation and 72 hours after the priming with the SOS medium; c) non-primed hnUCM-MSCs' morphology 5 days post-inoculation. Scale bar = 100 μ m.

Figure 16 - Enhanced pro-angiogenic effects in hnUCM-MSCs primed with the SOS medium. Gene expression of hnUCM-MSCs primed for 24 hours with the SOS medium following a 48-hour incubation with fresh medium is presented relative to non-primed hnUCM-MSCs. Data represented as average \pm SD (n=2-3). *** significantly differs from the non-primed hnUCM-MSCs gene expression with $p < 0.001$. Abbreviations: *IL-6* (interleukin 6); *VEGF-A* (vascular endothelial growth factor alpha); *HGF* (hepatocyte growth factor); *SDF-1* (stromal cell-derived factor 1); *TNF-A* (tumour necrosis factor alpha).

Figure 17 - Mitochondrial and oxidative stress were induced in HLCs following APAP exposure. Gene expression of HLCs exposed to 30 mM APAP for 24 hours is presented relative to non-injured HLCs recovered at D28. Data represented as average \pm SD (n=1-3). *, *** significantly differs from the non-injured HLCs gene expression with $p < 0.05$ and $p < 0.001$, respectively. Abbreviations: *ASK1* (apoptosis signal regulating kinase 1); *RIPK3* (receptor-interacting protein kinases 3); *ATF-6* (activating transcription factor 6); *BAX* (Bcl-2-associated X protein); *HNF4-A* (hepatocyte nuclear factor 4 alpha); *TNF-A* (tumour necrosis factor alpha).

Figure 18 - Regenerative genes were up-regulated in HLCs exposed to the MSC secretome. Gene expression of HLCs with cMSC-CM and pMSC-CM 10x concentrated, after a 24-hour exposure to 30 mM APAP, is presented relative to HLCs exposed to 30 mM APAP for 24 hours incubated with their basal medium (control) for other 24 hours. Data represented as average \pm SD (n=2-3). *, *** significantly differs from the control gene expression with $p < 0.05$ and $p < 0.001$, respectively. ##, ### significant difference between injured HLCs with cMSC-CM and with pMSC-CM with $p < 0.01$ and $p < 0.001$, respectively. Abbreviations: HLCs (hepatocyte-like cells); *BAX* (Bcl-2-associated X protein); *CCND1* (cyclin D1); *VEGF-A* (vascular endothelial growth factor alpha); *FGF-2* (fibroblast growth factor 2); cMSC-CM (human neonatal umbilical cord matrix-derived mesenchymal stem cells conditioned medium not primed); pMSC-CM (human neonatal umbilical cord matrix-derived mesenchymal stem cells conditioned medium primed with the hepatocyte-like cell SOS medium).

Figure 19 - MSC secretome enhanced HLCs proliferation in lower APAP concentrations. Cell viability of HLCs exposed to different APAP concentrations for 24 hours and incubated with cMSC-CM or pMSC-CM, 10x concentrated, or with their basal medium, for 24 hours. Cell viability percentage was normalized to the positive control (HLCs not exposed to APAP). Data represented as average \pm SD (n=1). *, **, *** significantly differs from the injured HLCs with IMDM, cMSC-CM or pMSC-CM gene expression with $p < 0.05$, $p < 0.01$ and $p < 0.001$, respectively. Abbreviations: HLCs (hepatocyte-like cells); cMSC-CM (human neonatal umbilical cord matrix-derived mesenchymal stem cells conditioned medium); pMSC-CM (human neonatal umbilical cord matrix-derived mesenchymal stem cells conditioned medium primed with the hepatocyte-like cell SOS medium).

List of tables

Table 1 - Effect of different priming agents in MSCs.

List of abbreviations

2D	Two-dimensional
3D	Three-dimensional
5-AZA	5-azacytidine
ABC	Adenosine triphosphate-binding cassette
ACLV	Acute-on-chronic liver failure
AKT	Protein kinase B
ALF	Acute liver failure
ALT	Alanine aminotransferase
Ang	Angiopoietin
ANXA 1	Anti-inflammatory molecule annexin-A1
APAP	4-acetamidophenol
APAP-cys	APAP nontoxic conjugates of cysteine and mercapturic acid
APAP-gluc	APAP glucuronide form
ASK1	Apoptosis signal-regulating kinase 1
AST	Aspartate aminotransferase
ATF	Activating transcription factor
ATF-6N	Active N terminus cytosolic fragment
ATP	Adenosine triphosphate
Axin2	Axis inhibition protein 2
Bax	Bcl-2-associated X protein
BM	Basal medium
BM-MSCs	Bone marrow-derived mesenchymal stem cells

BSA	Bovine serum albumin
ccCK18	Caspase-cleaved cytokeratin-18
CCL25	C-C chemokine ligand 25
CCl₄	Carbon tetrachloride
CCR9	C-C chemokine receptor type 9
CD	Cluster of differentiation
CDKs	Cyclin-dependent kinases
CHOP	C/EBP homologous protein
CK18	Cytokeratin-18
CLF	Chronic liver failure
CM	Conditioned medium
CO₂	Carbon dioxide
CRISPR	Clustered regularly interspaced short palindromic repeat
CX43	Connexin 43
CXCR4	C-C chemokine receptor type 4
CYP450	Cytochrome P450
DAMPs	Damage-associated molecular patterns
DILI	Drug-induced liver injury
DKK1	Dickkopf Wnt signaling pathway inhibitor
DM	Differentiation medium
DMSO	Dimethyl sulfoxide
DPP4	Dipeptidyl peptidase-4
DSG2	Desmoglein 2
ECM	Extracellular matrix
EGF	Epidermal growth factor
EGFR	Epidermal growth factor receptor
eIF2α	Eukaryotic initiation factor-2-alpha
ER	Endoplasmic reticulum
ERK	Extracellular signal-regulated protein kinase
ESCs	Embryonic stem cells
EVs	Extracellular vesicles
Exo	Exosomes
FBS	Fetal bovine serum
FGF	Fibroblast growth factor
GLDH	Glutamate dehydrogenase
GSH	Glutathione
GSTs	Glutathione-S-transferases
HBV	Hepatitis B virus
HCC	Hepatocellular carcinoma
HGF	Hepatocyte growth factor

HIF	Hypoxia-induced factor
HLA	Human leukocyte antigen
HLCs	Hepatocyte-like cells
HMGB1	High mobility group box-1 protein
HNF	Hepatocyte nuclear factor
hnUCM-MSCs	Human neonatal umbilical cord matrix-derived mesenchymal stem cells
HO	Heme oxygenase
HSCs	Hepatic stellate cells
HybHPs	SRY-related high-mobility-group box transcription factor 9 hybrid hepatocytes
IDO	Indoleamine
IFN-γ	Interferon gama
IGF	Insulin-like growth factor
IL	Interleukin
IMDM	Iscove's modified Dulbecco's medium
iPSCs	Induced pluripotent stem cells
IRE1α	Inositol-requiring enzyme 1 alpha
ITS	Insulin-transferrin-selenium
JNK	c-jun N-terminal kinase
K18-FL	Full-length cytokeratin 18
K19	Keratin 19
LDLT	Living donor liver transplantation
LPCs	Liver progenitor cells
LPS	Lipopolysaccharide
LSECs	Liver sinusoidal endothelial cells
MAPK	Ras-Raf-mitogen-activated protein kinase
Mfsd2a	Major facilitator super family domain containing 2a
miR	MicroRNA
MKK4	Mitogen-activated protein kinase kinase 4
MLK3	Mixed-lineage kinase 3
MMPs	Matrix metalloproteinases
MSC-CM/	Human neonatal umbilical cord matrix-derived mesenchymal stem cells
cMSC-CM	conditioned medium
MSCs	Mesenchymal stem cells
NAC	<i>N</i> -acetylcysteine
NAFLD	Non-alcoholic fatty liver disease
NaOH	Sodium hydroxide
NAPQI	<i>N</i> -acetyl- <i>p</i> -benzoquinone imine
NF-κB	Nuclear factor kappa light chain enhancer of activated B cells
NGF	Nerve growth factor
NK	Natural killer

NO	Nitric oxide
NPC	Non-parenchymal cells
Nrf-2	Nuclear factor-erythroid factor 2-related factor
NRG	Neuregulin
OATPs	Organic anion-transporting polypeptides
OATs	Organic anion transporters
OCTs	Organic cation transporters
OSM	Oncostatin M
PBS	Phosphate buffered saline
PDL-1	Programmed death-ligand 1
PERK	The double-stranded RNA dependent protein kinase like ER kinase
PGE	Prostaglandin E
PHH	Primary human hepatocytes
PHx	Partial hepatectomy
PI3K	Phosphatidylinositol 3-kinase
pMSC-CM	Human neonatal umbilical cord matrix-derived mesenchymal stem cells conditioned medium primed with the hepatocyte-like cell SOS medium
qRT-PCR	Quantitative real-time polymerase chain reaction
RIPK	Receptor-interacting protein kinases
RT	Room temperature
SD	Standard deviation
SDF-1	Stromal cell-derived factor 1
SLC	Solute carrier
SOS medium	Hepatocyte-like cells medium with SOS secreted signals after APAP exposure
Sox9	SRY-related high-mobility-group box transcription factor 9
STAT	Janus kinase-signal transducer and activator of transcription
STM	Septum transverse mesenchyme
SULT	Sulfotransferases
TAA	Thioacetamide
TG	Triglyceride
TGF-α	Transforming growth factor alpha
TGF-β	Transforming growth factor beta
TNF-α	Tumour necrosis factor alpha
Treg	Regulatory T cells
Trx	Thioredoxin
TSG	Tumour necrosis factor stimulated gene
UC-MSCs	Umbilical cord-derived mesenchymal stem cells
UDG	Uracil-DNA glycosylase
UGT	5'-diphosphate-glucuronosyltransferases
US	United States

VCAM 1	Vascular adhesion molecule-1
VEGF-α	Vascular endothelial growth factor alpha
VLA-4	Very late antigen-4
XBP1	X-box binding protein 1 spliced
YAP	Hippo/yes-associated protein
α-MEM	Minimum essential medium eagle alpha modification

1. Introduction

1.1. Liver structure and function

The liver is the largest internal organ by mass in the human body, lying in the upper right quadrant of the abdomen. This central metabolic organ interacts with several other organ systems in the body, such as the endocrine and the gastrointestinal systems, and is responsible for numerous physiological processes, namely, macronutrient metabolism, ammonia detoxification, blood volume regulation, storage of iron and copper, protein synthesis, bile synthesis and, importantly, biotransformation of xenobiotic compounds and endogenous metabolic by-products.^{1,2}

The hepatic function is regulated by several cell types classified as parenchymal cells (the hepatocytes) and non-parenchymal cells (NPC). Hepatocytes are responsible for numerous functions, composing up to 80 % of the hepatocellular mass and are classified as the liver's primary epithelial cell population. Biliary epithelial cells or cholangiocytes, hepatic stellate cells (HSCs), Kupffer cells and liver sinusoidal endothelial cells (LSECs) constitute the NPC population. Cholangiocytes are the second most abundant epithelial cells and have the main physiologic function of modifying the hepatocyte-derived bile. Stellate cells in the quiescent state are able to store the vitamin A in lipid droplets. In the presence of liver damage, these cells are activated, proliferate and lose the vitamin A stores, producing excessive amounts of collagen in the injured liver which resulted in liver fibrosis. Pro- or anti-inflammatory roles in the liver wound healing are performed by Kupffer cells, as the resident macrophage population. Lastly, LSECs form fenestrated sieve plates at the sinusoidal lumen, crucial for particle exchange between plasma and the cell types of the liver, without losing the barrier function.^{2,3}

1.1.1. Metabolic zonation

Liver's histological structural unit is the lobule of hexagonal shape in which the hepatocytes are arranged radially in cords from the central vein towards the portal triads at each corner, comprising the hepatic artery, portal vein and bile duct. The functional unit of the liver is named liver acinus and involves segments of two lobules, comprising the portal triad and the central vein (Figure 1). Within the lobule, in between the cords, there are liver sinusoids which are blood vessels with discontinuous endothelium, exposing hepatocytes to nutrients, toxins and oxygen. In between the sinusoidal lumen and the apical membrane of hepatocytes there is the space of Disse, where Kupffer and HSCs are located. Through this space hepatocytes are in contact with the wall of sinusoids.^{1,2,3}

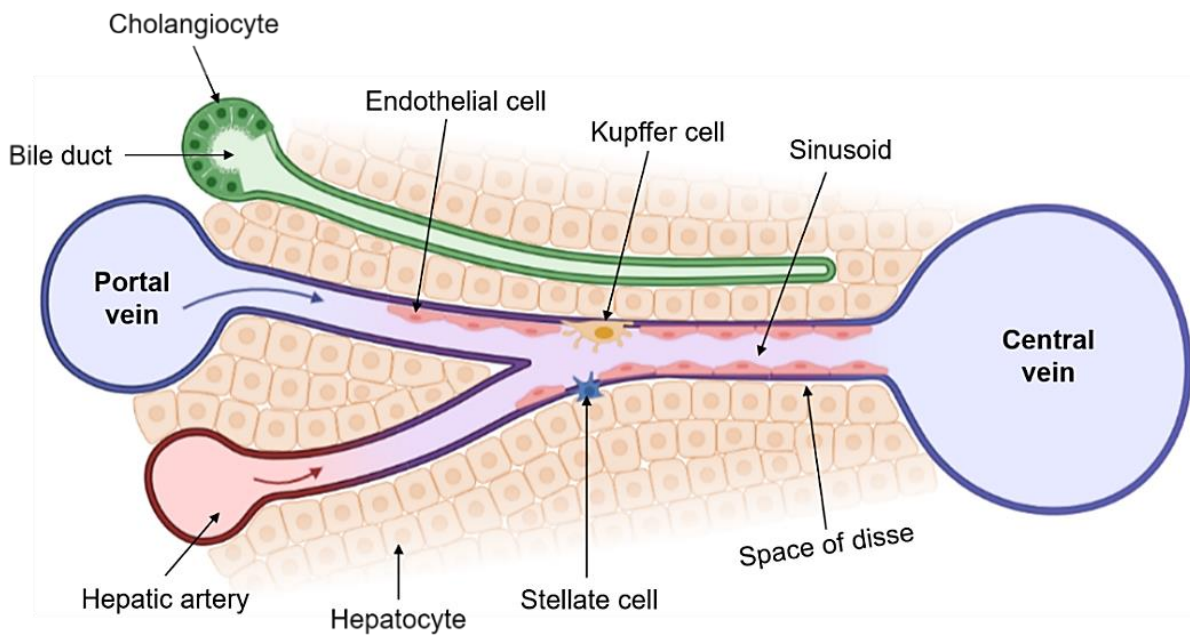


Figure 1 - Schematic representation of the liver acinus. Identification of the distinct cell-types and structures presented as well as the blood flux from the portal vein and hepatic artery to the central vein.

Characterized by being a very vascular organ, the liver receives up to 25 % of total cardiac output. The portal vein supplies 75 % of the liver's blood, rich in nutrients from the intestine, the pancreas and the spleen. The oxygen-rich blood, about 25 % of the blood supply, arises from the hepatic artery.⁴ These two types of blood are mixed in the liver sinusoids before flowing over the cells of the hepatic acinus and draining into the central vein. As cells consume oxygen and process nutrients, producing metabolites and waste products, blood composition varies and, consequently, gradients of oxygen, nutrients and waste are created throughout the liver acinus. These gradients influence gene expression and metabolism and result in hepatocyte functional heterogeneity, a phenomenon named 'metabolic zonation' (Figure 2). Thus, the liver lobule is divided into three distinct zones, in which there is a decreasing gradient of the oxygen level from zone 1 (periportal region) to zone 3 (perivenous region).^{2,4} As such, oxygen-dependent pathways are preferentially located in the periportal region, namely, mitochondrial β -oxidation, gluconeogenesis, cholesterol formation and amino acid catabolism. On the other hand, triglyceride (TG) synthesis, lipogenesis/ketogenesis, glycolysis and biotransformation of drugs are predominantly active in the perivenous region.^{2,4} This distribution allows for simultaneous performance of different and opposing metabolic pathways, avoiding interference and waste of energy. However, some enzymatic distribution gradients involved in certain pathways may change according to physiological circumstances.⁵

The Wnt/ β -catenin signalling pathway has a significant role in liver zonation, being related with the elevated transcription levels of perivenous genes under β -catenin control, namely, cytochromes P450 (CYP450) 2E1, CYP2C and glutathione-S-transferase (GST). Negative regulators of the Wnt signalling, including the adenomatous polyposis coli tumour suppressor protein, suppress β -catenin activity,

resulting in higher expression of periportal genes.⁶ Abnormal Wnt/ β -catenin signalling is related with many diseases development and/or progression, including hepatocellular carcinoma (HCC).⁷

Due to its position, the liver is susceptible to numerous types of injuries, from metabolic (non-alcoholic fatty liver disease, NAFLD), viruses (hepatitis A, B or C), toxic substances (alcohol or drugs) to tumoral diseases (HCC). Several diseases have zonal preferences in the liver, as cells differentially express zone-specific genes and are exposed to different metabolic processes and toxins depending on their location.⁸ For example, drug-induced liver injury (DILI) has different zonation patterns depending on the drug. 4-acetamidophenol (APAP), carbon tetrachloride (CCl₄) and ethanol are associated with perivenous damage while doxorubicin, galactosamine and allyl alcohol are predominantly related with periportal damage. Moreover, fatty liver disease and malaria are linked with perivenous damage whereas autoimmune hepatitis and primary biliary cirrhosis with periportal injury.⁹

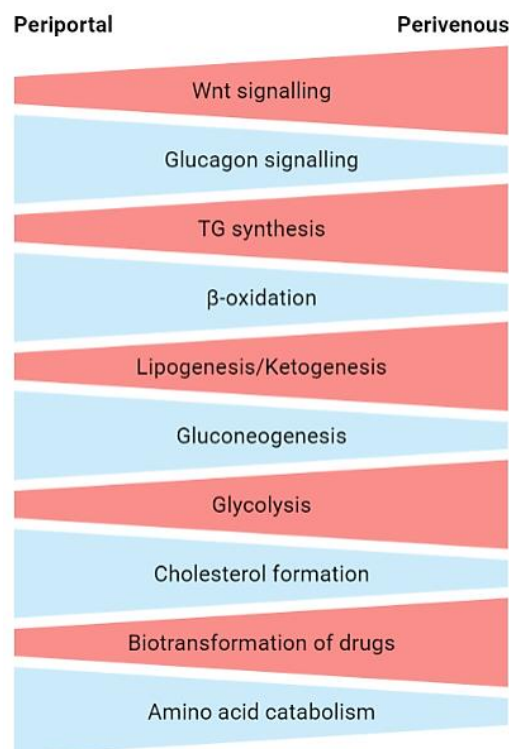


Figure 2 - Representation of biochemical pathway zonation in the liver. Distribution preference through periportal or perivenous regions in the liver. Abbreviations: TG (triglyceride).

1.1.2. Drug metabolism

Xenobiotics are compounds foreign to the human body (e.g. drugs, alcohol), metabolized by biotransformation of a lipophilic form to a hydrophilic form which is more easily excreted. This process of drug metabolism is divided in phases I, II and III and although more abundant in the liver, it is a ubiquitous process.¹ Indeed, liver is highly exposed to xenobiotics entering the organ through the portal vein. Therefore, this organ has a crucial function in detoxification of xenobiotics in the human body,

since phase I and II of the drug-metabolizing process occurs mostly in the smooth endoplasmic reticulum (ER) of hepatocytes.¹⁰

Phase I involves the activity of the drug-metabolizing enzymes belonging to the CYP450 family, being CYP3A4 the most abundant one in the human liver. The CYP450 enzymes convert drugs into water-soluble products, through oxidation (the primary reaction), sulfoxidation, aromatic hydroxylation, aliphatic hydroxylation, *N*-dealkylation, *O*-dealkylation and deamination, facilitating their excretion by the kidney or the liver.^{1,10}

During phase II, the transferase enzymes, such as, uridine 5'-diphosphate-glucuronosyltransferases (UGT), sulfotransferases (SULT), GST and *N*-acetyltransferases, aid the conjugation of metabolites from phase I or parent compounds to hydrophilic endogenous compounds, facilitating its secretion into blood and bile. This conjugation can be performed resorting to glucuronate, glutathione (GSH) or sulfate.¹⁰

Lastly, the phase III of drug metabolism consists in the transportation out of the cells of metabolites through efflux transporters that contribute to bile secretion and xenobiotic clearance. These transporters are located in the apical/canicular membrane and include adenosine triphosphate (ATP)-binding cassette (ABC) family of drug transporters, which consume ATP energy to actively transport the drug from one side of the cell membrane to another. Other type of transporters are the influx transporters (also designated as phase 0), located on the basolateral/sinusoidal membrane, that are responsible for the uptake of molecules from blood, comprising organic anion transporters (OATs), organic cation transporters (OCTs) and organic anion-transporting polypeptides (OATPs). These transporters mediate drug accumulation within cells, which is related with their therapeutic efficacy, toxicity and drug-drug interactions.^{10,11}

1.2. Liver failure

A punctual liver injury, either metabolic, viral, chemical or tumoral, in healthy individuals activates an intrinsic regenerative hepatic response, intending to re-establish homeostasis. However, under repeated injuries, hepatocyte damage induces HSCs and myofibroblasts activation, resulting in the excessive accumulation of extracellular matrix (ECM) proteins. Therefore, the regeneration process is hindered and fibrosis is developed, which leads to scarring and tissue stiffness changes. If no further damage occurs the tissue has the ability to recover with time, resorting to matrix metalloproteinases (MMPs) capable of removing ECM deposition.^{12,13}

The progression of hepatic parenchymal dysfunctions leads to increasing degrees of insufficiency resulting in liver failure which can be classified in three types, namely, chronic, acute and acute-on-chronic.

Chronic liver injury is characterized by repeated injuries which lead to an inflammatory status and progressive degrees of hepatic parenchymal dysfunctions. Consequently, this functional insufficiency

develops into chronic liver failure (CLF), a common outcome of hepatic cirrhosis which is characterized by the infiltration of T cells, B cells and monocytes along with progressive ECM deposition. At this stage, an acellular mesh of connective tissue replaces the functional hepatic parenchyma, hampering the activity of MMPs and hindering repairment.¹³

Acute liver failure (ALF) is caused by a sudden decompensation of the hepatic function which triggers inflammatory or fibrotic responses, after exposure to toxic doses of drugs (DILI) or viral infections. Depending on the time frame of appearance of symptoms, namely, encephalopathy and coagulation alterations, ALF is categorized into hyperacute if symptoms appeared within one week; acute if symptoms showed between one and three weeks; or subacute if symptoms showed between three and twenty-six weeks.¹⁴

Lastly, acute-on-chronic liver failure (ACLV) arises frequently in patients with chronic hepatitis B or hepatitis B virus (HBV)-related cirrhosis and acute decompensation, associated to ascites, hepatic encephalopathy, gastrointestinal haemorrhage and bacterial infection. ACLV is an end-stage liver disease owing to the quick progression of multiorgan failure and the high mortality rates.¹⁵

1.3. Drug-induced liver injury

The strategic anatomic position of the liver close to the gastrointestinal tract, the structural organization of the liver sinusoidal space and the blood supply from the portal vein make the liver an organ highly exposed to xenobiotics, namely, prescription-only or over-the-counter medicines. The xenobiotics biotransformation within hepatocytes may generate reactive metabolites that interfere with specific cell functions. The mechanisms behind hepatotoxicity depend on the used drug, being the most common related with the increase of oxidative or redox stress (e.g. acetaminophen), mitochondrial dysfunction (e.g. amiodarone, troglitazone, valproic acid), DNA damage (e.g. nevirapine), depletion of enzymes and co-factors (e.g. acetaminophen) and dysfunction of cell repairing mechanisms (e.g. valproic acid, retinol).¹⁶ The stressed and dying hepatocytes release damage-associated molecular patterns (DAMPs) that trigger the innate immune system by interacting with pattern recognition receptors. Then, resident liver Kupffer cells, natural killer (NK) and NK T cells are activated to produce cytokines and chemokines which induce leukocytes infiltration in the liver. Although DAMPs are crucial for the host's defence, the promoted inflammatory response may increase the hepatic injury.^{17,18}

The liver susceptibility for drug-induced hepatotoxicity may lead to DILI, the most common cause of ALF in the western world and for the withdrawal of drugs from the market, since 43 % of human toxicities are not predicted in animal studies.^{19,20,21} DILI can be classified as intrinsic or idiosyncratic. The intrinsic hepatotoxicity is direct, common, dose-dependent, reproducible in animal models, affects all individuals at the same dose and has a predictable short latent period after exposure, commonly caused by high doses of acetaminophen, aspirin, niacin and cancer chemotherapy, for instance.²² Conversely, the idiosyncratic DILI is unpredictable, non-dose-dependent, not reproducible in animal models and occurs in less than 1 of every 10 000 exposed individuals.¹⁷ Preclinical tests fail to identify most of the drug

candidates responsible for the unpredictable stress that increase the liver's sensitivity to injury with lower doses of a given drug. Age, gender, genetic polymorphisms, immunologic reactions, coexisting diseases and nutritional status are some examples of factors crucial for individual sensitivity to xenobiotics.²³ Additionally, idiosyncratic DILI is also categorized as acute or chronic depending on the duration, as hepatitis (related with hepatocyte necrosis), cholestatic (due to bile duct damage) or as mixed injury.^{16,22} Drugs that induce idiosyncratic hepatotoxicity include amoxicillin-clavulanate, macrolide antibiotics, diclofenac and troglitazone.²²

The diagnosis for DILI is difficult due to its variable phenotype and the lack of specific biomarkers, resulting in an exclusion-based diagnosis.¹⁶ The serum activities of alanine aminotransferase (ALT) and aspartate aminotransferase (AST) have been used as standard biomarkers for hepatocellular injury since they are released by liver cells into the bloodstream under damage or inflammation. However, these biomarkers are also present in significant amounts in myocytes and may be released in situations of muscle injury.²⁴ Therefore, new liver specific biomarkers capable of predicting DILI have been investigated. For example, glutamate dehydrogenase (GLDH) is a mitochondrial enzyme mainly expressed throughout the liver lobule and in fewer amounts in the kidney, pancreas, brain and intestine. Upon the loss of hepatocellular membrane integrity, GLDH enzyme is released from the damaged hepatocytes into the circulation. Therefore, GLDH might be a biomarker for mitochondrial toxicity as a result of DILI.^{17,18} Another biomarker for DILI is the type-I intermediate filament protein cytokeratin-18 (CK18), which is abundant in hepatocytes. Necrotic cells release full-length CK18 into their plasma upon cell membrane disintegration, while apoptotic cells release caspase-cleaved CK18 (ccCK18) fragments into circulation. Thus, the ratio between full-length CK18 and ccCK18 indicates the degree of necrotic versus apoptotic hepatocellular injury.²⁵ Additionally, the high mobility group box-1 protein (HMGB1), which is located in the cell nucleus, and the microRNA (miR)-122 which is the most abundant miR in the liver, mainly up-regulated in embryonic development, are examples of DAMPs released from necrotic hepatocytes, known to induce inflammation and to act as DILI biomarkers.^{17,18}

1.3.1. APAP metabolism

Acetaminophen, also known as APAP or paracetamol, is a highly used anti-pyretic and analgesic drug, reaching the peak blood concentration within 90 minutes after ingestion. Although it is advertised as safe in doses up to 3250 mg every 24 hours in adults by the United States (US) Food and Administration and up to 4000 mg as daily maximum dosage in Europe, APAP toxicity is the most common cause of severe intrinsic DILI.^{26,27} In fact, APAP toxicity is responsible for 46 % of all ALF in the US and between 40 to 70 % of all cases in the United Kingdom and Europe.²⁸ Most of the times the APAP hepatotoxicity occurs unintentionally with doses above the maximum recommended, but the combination of factors like nutritionally depleted state, alcohol abuse, use of drugs that stimulate the CYP450 system or coexisting diseases, decrease APAP toxicity threshold.^{17,29}

APAP is metabolized by phase I and II enzymes in hepatocytes, through sulfation, glucuronidation and oxidation. Under therapeutic doses (Figure 3), APAP is catalysed by UGTs into the

pharmacologically inactive glucuronide form (APAP-gluc), which is more water soluble and constitutes about 52 to 57 % of urinary metabolites. The sulfation of APAP is performed by SULTs which transfer a sulfate group to APAP, forming the inactive metabolite APAP-sulfate, more polar and accounting for 30 to 40 % of the excreted metabolites. A minor fraction (5 to 10 %) is oxidized by the CYP450 enzymes, such as CYP2E1 and CYP1A2, into the reactive metabolite *N*-acetyl-*p*-benzoquinone imine (NAPQI). NAPQI is rapidly detoxified by the intracellular GSH. GSTs catalyse the binding of NAPQI to the sulfhydryl group of hepatic GSH forming APAP-GSH. The latter is excreted as nontoxic conjugates of cysteine and mercapturic acid (APAP-cys) in urine. Finally, less than 5 % of APAP is excreted unchanged.³⁰

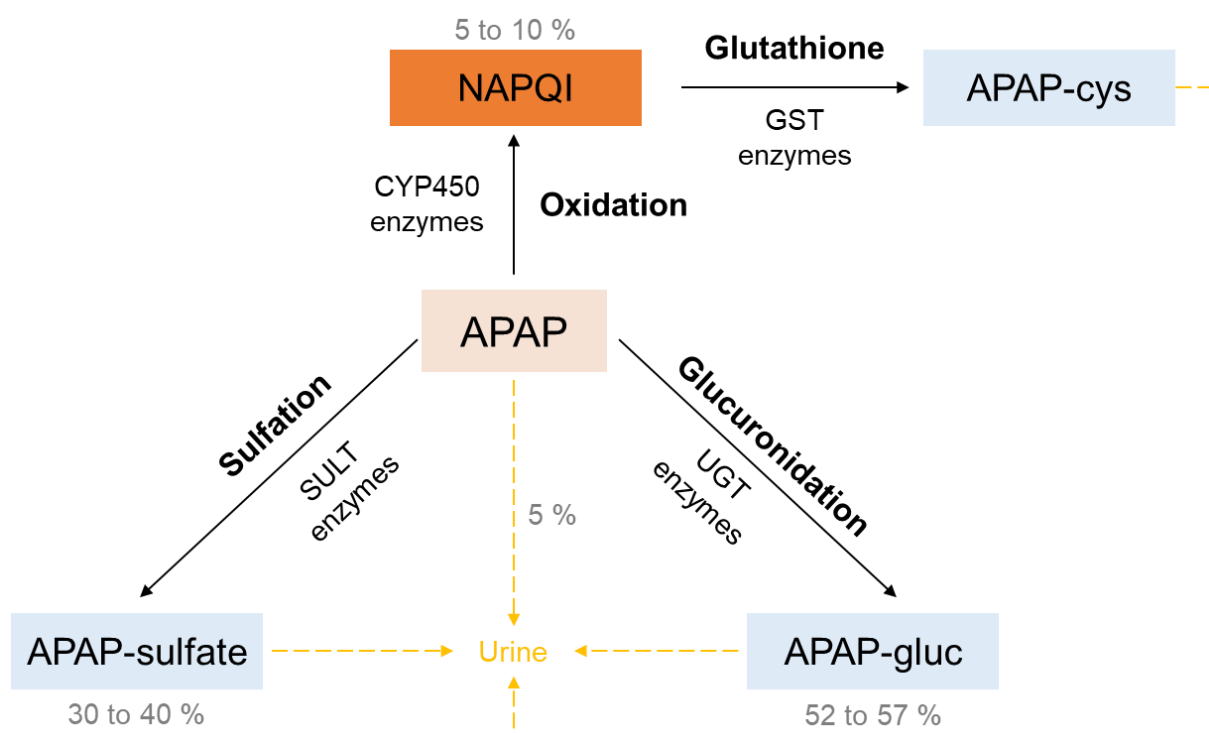


Figure 3 - APAP metabolism in the liver. This xenobiotic is metabolized through sulfation, glucuronidation and oxidation into APAP-sulfate, APAP-gluc and NAPQI, respectively. The latter is a reactive metabolite detoxified by intracellular GSH and excreted as APAP-cys. Abbreviations: APAP-sulfate (APAP with a sulfate group); APAP-gluc (APAP inactive glucuronide form); SULT (sulfotransferases); UGT (5'-diphosphate-glucuronosyltransferases); CYP450 (cytochrome P450); NAPQI (*N*-acetyl-*p*-benzoquinone imine); GSH (glutathione); GST (Glutathione-S-transferases); APAP-cys (APAP nontoxic conjugates of cysteine and mercapturic acid).

Under excessive doses of APAP (Figure 4), sulfation and glucuronidation pathways become saturated and higher amounts of APAP are oxidated into NAPQI.²⁹ The accumulation of the reactive metabolite depletes GSH stores and NAPQI covalently binds to cysteine groups on cellular proteins, especially mitochondrial proteins, modifying intracellular structures and forming NAPQI-adducts. This step is irreversible and results in dysfunctions in the mitochondrial respiration, generating free radicals, namely, superoxide. Thus, mitochondrial anti-oxidant defences are compromised leading to an initial

mitochondrial oxidative stress and oxidation of mitochondrial proteins such as thioredoxin (Trx). Therefore, Trx detaches from apoptosis signal-regulating kinase 1 (ASK1) which becomes activated in the cytosol. During APAP hepatotoxicity, mixed-lineage kinase 3 (MLK3) is also activated upon oxidative stress. The counterplay between activated ASK1 and MLK3 phosphorylates mitogen-activated protein kinase kinase 4 (MKK4) which subsequently phosphorylates c-jun N-terminal kinase (JNK) in the cytosol. The phosphorylated JNK inhibits mitochondrial electron transport in the mitochondria, increasing its oxidative stress. Additionally, Bcl-2-associated X protein (Bax) translocation from the cytosol to the mitochondria enhances oxidative stress and the release of mitochondrial intermembrane proteins, which move to the nucleus and promote DNA fragmentation. The last event induces the activation of receptor-interacting protein kinases (RIPK) 3/1 resulting in hepatocyte necroptosis.^{30,31}

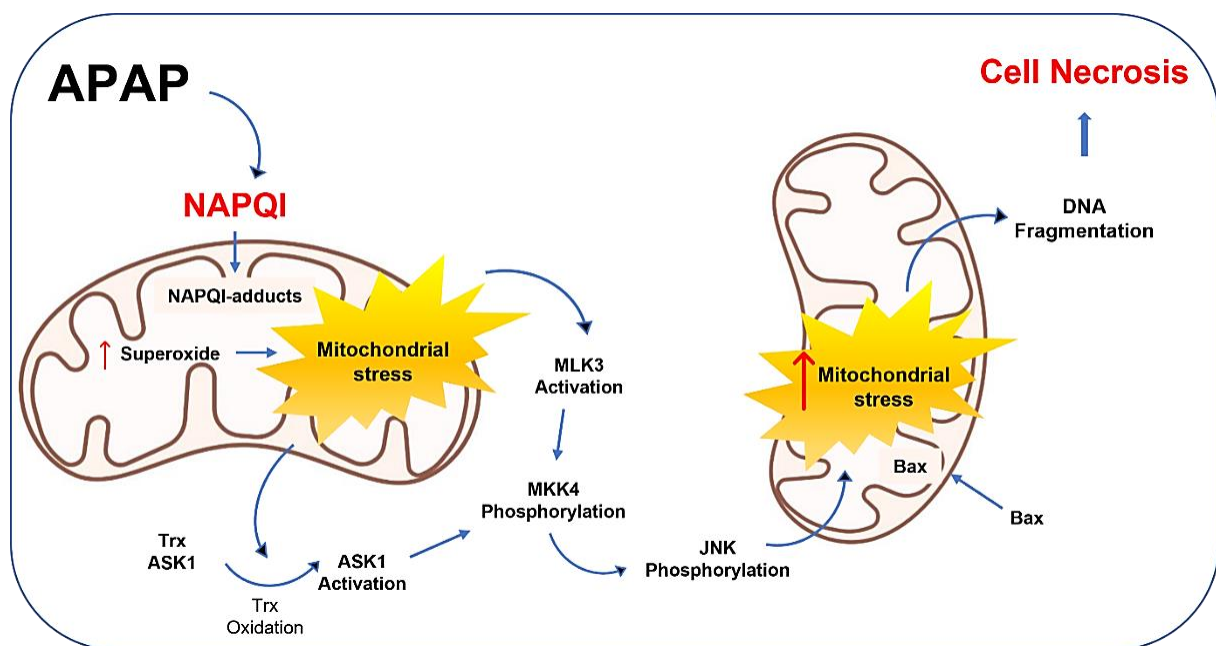


Figure 4 - Mechanism of the APAP-induced hepatotoxicity. Under excessive doses, higher amounts of APAP are oxidized into NAPQI, which covalently binds to mitochondrial proteins, forming NAPQI-adducts. As a result, free radicals such as superoxide are formed, inducing the mitochondrial oxidative stress. Hence, Trx is oxidated, detaching from ASK1 and activating the latter. Parallely, MLK3 is activated and, together with ASK1, phosphorylate MKK4. Sequentially, MKK4 and JNK are phosphorylated. The presence of JNK and Bax in the mitochondria increases its oxidative stress, promoting DNA fragmentation and cell necrosis. Abbreviations: NAPQI (*N*-acetyl-*p*-benzoquinone imine); Trx (thioredoxin); ASK1 (apoptosis signal-regulating kinase 1); MLK3 (mixed-lineage kinase 3); MKK4 (mitogen-activated protein kinase kinase 4); JNK (c-jun N-terminal kinase); Bax (Bcl-2-associated X protein).

An acute inflammatory response is triggered by the release of DNA fragments, HMGB1, mitochondrial DNA, uric acid and ATP from necrotic hepatocytes, acting like DAMPs. Pro-inflammatory cytokines, such as tumour necrosis factor alpha (TNF- α), interleukin (IL)-6, IL-1 β and IL-10, are activated in Kupffer cells directing neutrophils and monocytes to the injured regions. This inflammatory status contributes

for the progression of the initial liver injury whilst aiding the repair and regeneration of liver tissue in a late phase by removing cells debris.^{31,32}

ER stress is common in APAP-induced hepatotoxicity since NAPQI also covalently binds to ER proteins. Indeed, under ER stress, the dissociation of the ER protein chaperone binding immunoglobulin protein activates the three ER stress sensors – the inositol-requiring enzyme 1 alpha (IRE1 α), the double-stranded RNA-dependent protein kinase-like ER kinase (PERK) and the activating transcription factor (ATF)-6 – inducing the transcription of X-box binding protein 1 spliced (XBP1), ATF-4 and active *N*-terminus cytosolic fragment (ATF-6N), respectively. These proteins translocate to the nucleus and regulate the expression of ER stress target genes, such as C/EBP homologous protein (CHOP), with a pro-damage role in liver injury by inhibiting liver regeneration.^{32,33}

The perivenous hepatocyte necrosis is characteristic of the APAP hepatotoxicity, mainly due to the abundance of CYP2E1 in the perivenous region which is involved in the formation of NAPQI.²⁹ After APAP overdose, GSTs are readily released from periportal and perivenous hepatocytes, unlike ALT and AST. Therefore, elevated plasma GST levels are an indicator of APAP-induced hepatotoxicity and acute liver damage.³⁰

The susceptibility to APAP hepatotoxicity is dependent on genetic and environmental factors. In particular, genetic factors such as polymorphisms in CYP enzymes, genetic changes in UGT or SULT enzymes or even ethnic backgrounds may lead to different risks of APAP hepatotoxicity.²⁷ Additionally, upon inflammatory stress, tissue homeostasis is altered due to the release of several transcription factors, cytokines and enzymes, which may induce organ injury. Thus, this dysregulation causes the tissue to be more sensitive to the stress imposed by a toxic xenobiotic agent. Indeed, the lipopolysaccharide (LPS) from Gram-negative bacteria induce inflammatory responses and reduce the threshold for APAP hepatotoxicity.²³ Moreover, hepatitis viruses along with APAP consumption increase the risk for acute liver injury^{34,35} and in malnutrition states the GSH stores become easily saturated and the risk for APAP hepatotoxicity is higher.²⁷ Furthermore, chronic alcohol consumption increases the susceptibility for APAP-induced liver failure, since alcohol depresses mitochondrial GSH, enhances the bioactivation of APAP by increasing the activity of CYP enzymes and increases intestinal permeability of LPS to the liver.^{23,27}

The early identification of DILI and the offending drugs are essential to avoid the need for liver transplantation. For APAP overdose, the administration of *N*-acetylcysteine (NAC) within 8 hours of ingestion is an effective antidote. NAC provides cysteine and replenishes hepatic GSH stores providing more substrate for the detoxification of the accumulated NAPQI. Moreover, NAC enhances the sulfation metabolic pathway, reducing the APAP oxidation to NAPQI.^{26,29,30}

1.4. Liver regeneration

1.4.1. Intrinsic hepatic regeneration

Until a certain extension of damage, the liver has the unique ability to regenerate itself and regain its original mass through compensatory growth after surgical resection – partial hepatectomy (PHx) – or exposure to toxins that cannot metabolize. Indeed, mammals can survive with only 25 % of the liver after PHx.³⁶ This organ's capability enables the treatment of liver diseases either by removing the damaged part of a diseased liver or by transplanting a part of a healthy liver.³⁷

The intrinsic regeneration of the liver mainly resorts either to mature cells, hepatocytes and cholangiocytes, or to liver progenitor cells (LPCs) that can differentiate into hepatocytes and cholangiocytes.¹⁴ However, LPCs are rare in normal adult livers, constituting, approximately, only 0.01 % of the liver cell population, hence the regenerative response is mainly granted by distinct mature hepatocyte subpopulations.^{38,39}

The axis inhibition protein 2 (Axin2), the major facilitator super family domain containing 2a (Mfsd2a) and the SRY-related high mobility-group box transcription factor 9 (Sox9) are some examples of markers of different hepatocyte subpopulations. The Axin2 is a transcriptional β -catenin target dependent of Wnt signalling with proliferative and self-renewing properties, mainly located adjacent to the hepatic central vein.⁴⁰ Mfsd2a is a periportal marker also involved in liver regeneration. Sox9 is a specific and early marker of biliary cells and a transcription factor involved in liver development. Sox9 hybrid hepatocytes (HybHPs) around periportal region express cholangiocyte-specific genes and hepatocyte markers.

During the homeostatic regeneration process, Axin2⁺ hepatocytes expand from the central vein towards the portal vein, while Mfsd2a⁺ hepatocyte population decreases over time and the HybHPs hepatocyte population remain constant. Conversely, upon chronic injuries, Pu *et al.* (2016) demonstrated that the Mfsd2a⁺ hepatocytes were the major source responsible for liver regeneration.⁴¹ Furthermore, in this type of injury, HybHPs are also known to proliferate.³⁹

1.4.2. Signals behind the liver regeneration process

Over the past decades, efforts have been made to understand the complex network of signals responsible for the cell cycle progression of hepatocytes upon regenerative processes. Indeed, hepatic regeneration is mediated by several signalling pathways that cooperate between each other. In the case of pro-regenerative signalling pathways Wnt, Notch, Hippo/yes-associated protein (YAP), vascular endothelial growth factor (VEGF), insulin-like growth factor (IGF)-1, fibroblast growth factor (FGF), neuregulin 1 (NRG1)/ErbB and Hedgehog signalling are the main ones. Other pathways such as phosphatidylinositol 3-kinase (PI3K)/ protein kinase B (AKT) and nuclear factor kappa light chain enhancer of activated B cells (NF- κ B) signalling have dual functions in regeneration as pro-inflammatory and anti-apoptotic.⁴² Since redundancy is one important characteristic of these pathways, the loss of an individual gene leads to a delay rather than to a complete inhibition of the liver regeneration.⁴³

From the traditional rodent model of 2/3 PHx, the liver regeneration process was characterized and described in three critical phases, as seen in Figure 5, namely, priming, progression and termination.

The priming phase is the first phase of the liver regeneration and promotes the activation of numerous genes within few minutes after injury. β -catenin remains overexpressed in the hepatocyte nucleus for 24 hours. Therefore, quiescent hepatocytes convert from G0 to G1 of the cell cycle due to pro-inflammatory cytokines, namely, TNF- α and IL-6, released by Kupffer cells, which through the NF- κ B, JNK, Janus kinase-signal transducer and activator of transcription 3 (STAT3), extracellular signal-regulated protein kinase (ERK) 1/2 signalling pathways, respectively, induce the transcription of several proliferative genes, including cyclin D1.^{39,44,45}

The second phase is termed progression, in which growth factor receptors are activated and hepatocytes progress from the G1 phase to the mitosis (M), promoting proliferation. Additional signalling factors named mitogens secreted by different cell types assist this replicative cycle and can be classified as complete or auxiliary. Complete mitogens, namely, hepatocyte growth factor (HGF) and epidermal growth factor receptor (EGFR) ligands act like paracrine factors inducing hepatocyte proliferation and DNA synthesis through the Ras-Raf-mitogen-activated protein kinase (MAPK) signalling and the PI3K/Akt signalling pathway. Notably, the loss of either EGFR or c-Met, which is the HGF cell surface receptor in hepatocytes and cholangiocytes, delays liver repair and the regeneration process is completely blocked by the loss of both receptors. HGF in healthy liver is bound to the ECM of endothelial and Kupffer cells, but after injury it is released to the bloodstream and additional HGF is produced by HSCs and endothelial cells. This additional HGF production is detected by c-Met, which induces cyclin and cyclin-dependent kinases (CDKs) activation, responsible for cell cycle regulation and the initiation of DNA synthesis. Regarding the EGFR ligands, heparin-binding (HB)-EGF is produced by Kupffer and endothelial cells in the liver, EGF is secreted by Brunner's gland in the duodenum and transforming growth factor (TGF)- α is secreted by hepatocytes. In turn, auxiliary mitogens, such as bile acids, norepinephrine, insulin, TNF- α , IL-6, estrogen and serotonin, promote and accelerate the proliferation step cell cycle entry by boosting the effect of direct mitogens.^{39,44,46}

Another mechanism behind liver regeneration during the priming and proliferation phases is angiogenesis. The cross-talk between LSECs, HSCs and hepatocytes induces the formation of new microvasculature from pre-existing blood vessels and mature endothelial cells. In a hypoxia-stimulated environment, hypoxia-induced factors (HIFs) react to reduced oxygen levels by up-regulating VEGF, VEGF receptors, endothelial nitric oxide synthase, vascular endothelial cadherins, platelet endothelial cell adhesion molecule-1, MMPs, angiopoietins (Ang) and integrins, for example. These factors mediate vasodilation, increase vascular permeability and endothelial cell membrane remodelling, allowing for endothelial cell migration, proliferation and organization of new vessels.⁴⁷

Lastly, termination is the last step and is related to the cessation of proliferation through the activation of key factors. For example the TGF- β , released by hepatocytes, stellate, endothelial and Kupffer cells is a pro-inhibitory cytokine that inhibits hepatocyte proliferation by blocking the function or production of CDKs and cyclins. Similarly, activin A produced by hepatocytes also hinders hepatocyte proliferation.^{39,44} Moreover, the hepatocyte nuclear factor (HNF)4- α , which is a transcription factor

essential for the maintenance of the hepatic functions, plays a key role in the hepatocytes exit from the cell cycle, aiding the termination of the liver regeneration.⁴⁸

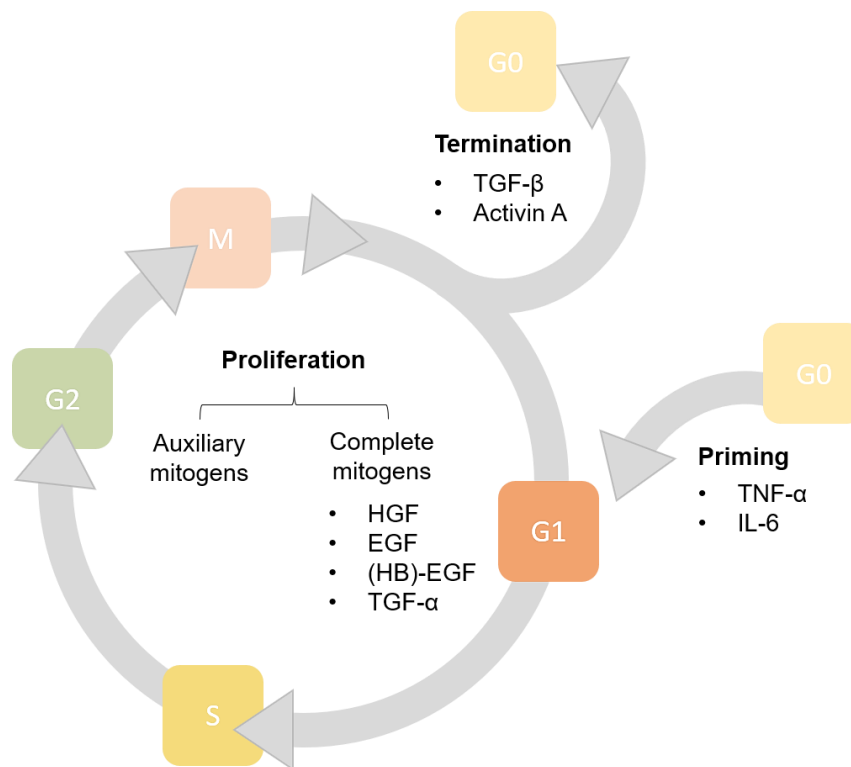


Figure 5 - Liver regeneration process. Identification of the soluble mediators that potentiate the different stages of the cell cycle. Abbreviations: TNF-α (tumour necrosis factor alpha); IL-6 (interleukin 6); HGF (hepatocyte growth factor); EGF (epidermal growth factor); (HB)-EGF (heparin-binding epidermal growth factor); TGF-α (transforming growth factor alpha); TGF-β (transforming growth factor beta); G0, G1, S (synthesis), G2 and M (mitosis) are phases of the cell cycle.

Upon end-stage liver diseases, the liver loses its ability to replace the sheer number of dying hepatocytes and the hepatic resection is not a viable solution. In these situations, liver transplantation is an option with high survival rates. Actually, liver transplantation is the second most common solid organ transplantation, yet the current rate of transplantation only meets 10 % of the global need.⁴⁹ Additionally, the need for long-term use of immunosuppressants after transplantation and the associated high costs make this an impractical option for many patients.⁵⁰ Living donor liver transplantation (LDLT) arises as an alternative treatment, reducing mortality on waiting lists. In LDLT a portion of the liver from a healthy living person (donor) is inserted into a recipient. Both the donor's remaining liver and the transplanted liver grow and restore its normal size.⁵¹ However, this procedure has 38 % risk of complications and the transplanted liver may fail to regenerate to full size, causing liver failure.¹⁴ Therefore, there is a need for innovative therapies that would contribute and enhance the liver healing process, such as cell-based therapies.

1.5. Cell-based therapies for liver regeneration

In the past decades clinical studies have reported that human allogeneic hepatocyte transplantation is a possible treatment for patients with acquired or inherited liver diseases. Resorting to this technique, transplanted hepatocytes from a healthy donor with the functional version of a given dysfunctional disease-causing gene replace the host hepatocytes.⁵² Genetic diseases related with clotting factor deficiencies, hyperlipidaemia and tyrosinemia are examples of successfully treated liver diseases resorting to hepatocyte transplantation. Moreover, this type of treatment can also be used for ALF and CLF, namely, cirrhosis, fulminant hepatic failure and viral failure, avoiding transplantation and abolishing the risk of lifetime immunosuppression associated with allogeneic organ transplantation.⁵³ However, there are still constraints regarding this technology, namely, the limited number and quality of liver tissues as a cell source and the lack of evidence of long-term cure and stability of the cells.¹²

A more alluring alternative is the use of stem cells, which does not rely on the availability of organ donors, due to stem cells ability to self-renew maintaining its undifferentiated state and to differentiate into distinct cell types. Stem cells can be classified into embryonic, fetal, neonatal and adult, according to their origin, and according to their differentiation potential into totipotent, which are able to originate an entire organism and extra-embryonic tissues; pluripotent, which can differentiate into the cell types of the three embryonic germ layers; multipotent, being able to differentiate into the cell types of their original germ layer; and unipotent, which can only give rise to one cell type.

Hepatocyte-like cells (HLCs) can be obtained through the differentiation of embryonic stem cells (ESCs), induced pluripotent stem cells (iPSCs) or mesenchymal stem cells (MSCs) by combining them with specific growth factors and cytokines *in vitro*. ESCs derived from the inner cell mass of the blastocyst were the first to be discovered and studied.⁵⁴ However, ethical concerns have hindered the use of these pluripotent cells in humans.¹² To overcome ethical constraints, mature somatic cells can be reprogrammed into a state of pluripotency generating iPSCs. Additionally, the capability to originate these cells from the patient, enabling autologous transplantation, attract their use in non-genetic diseases. These cells are similar to ESCs in morphology, proliferation and differentiation potential.⁵⁵ However, limitations like reprogramming efficiency, long-term safety, potential formation of teratomas, cost effectiveness and genome instability hinder their application.^{12,36} Alternatively, MSCs with their differentiation capacity, genome stability and absence of ethical concerns, surge as an optimal stem cell type. Furthermore, cultivation of MSCs is possible without feeder layers and high concentrations of serum, as opposed to ESCs.⁵⁶ HLCs have been generated from MSCs derived from human bone marrow⁵⁷, from adipose tissue⁵⁸ and from human umbilical cord matrix⁵⁹.

Several studies have proven the stem cell-derived HLCs capacity to restore hepatic function after injury. Indeed, ESC-derived HLCs enhanced hepatic regeneration, by inducing proliferation and revascularization of host hepatocytes in a CCl₄-induced liver injury mouse model.^{60,61} The *in vivo* transplantation of iPSCs-derived HLCs in mouse models showed to reverse lethal fulminant hepatic failure⁶², enhanced liver regeneration⁶³ and reduced liver fibrosis⁶⁴. Likewise, MSCs-derived HLCs

transplantation in a CCl₄-induced liver failure mouse model restored the hepatic function⁶⁵ and reduced liver fibrosis⁶⁶.

However, *in vitro* stem cell-derived HLCs were not fully functional and mature, displaying a low level of liver repopulation and an associated risk of teratoma formation.^{12,67} Indeed, Wang, H. *et al.* (2014) demonstrated that after differentiation the MSC-derived HLCs lost key properties in comparison to undifferentiated MSCs which revealed to be more therapeutically relevant for liver diseases.⁶⁸ Therefore, the MSCs homing ability to injured tissues and their secretion of soluble factors have been investigated for liver regeneration purposes.

1.5.1. Mesenchymal stem cells therapy for liver regeneration

According to the International Society for Cellular Therapy, MSCs are defined as such if fulfilling a set of three criteria: adherence to plastic when maintained in standard culture conditions using tissue culture flasks; specific surface antigen expression, namely, more than 95 % of the MSC population should express cluster of differentiation (CD) 105, CD73 and CD90 and lack the expression of CD45, CD34, CD14 or CD11b, CD79 α or CD19 and human leukocyte antigen (HLA) class II; and multipotent differentiation potential, i.e., under standard *in vitro* differentiating conditions, MSCs should give rise to osteoblasts, adipocytes and chondroblasts.⁶⁹

MSCs were first isolated from the bone marrow (BM-MSCs) in 1974 by Friedenstein *et al.*⁷⁰, being the principal and best characterized source of MSCs. Afterwards, MSCs were isolated from almost any tissue, either from neonatal tissues – amniotic fluid, placenta, umbilical cord matrix and umbilical cord blood – or from adult tissues – adipose tissue, dental pulp, peripheral blood, synovium and synovial fluid, endometrium, skin and skeletal muscle.⁵⁴

MSCs offer important advantages for their therapeutic application in tissue repair and regeneration since they are easy to obtain, maintain, expand and cryopreserve, without losing their viability neither their replicative capacity.⁷¹ Another advantage of this cell type is their low immunogenicity due to the lack of class II major histocompatibility complex molecules, enabling the allogeneic application without the need for immunosuppression.¹²

The therapeutic potential of allogenic transplanted MSCs relies on the capacity that these cells have to migrate to injured tissues, passaging through the endothelium and engraft, secreting soluble factors which enhance tissue regeneration in a mechanism called homing. Accordingly, MSCs can be administered intravenously or applied *in situ*, being recruited to injury sites in response to chemotactic cues. The homing process is still not fully understood, but it is thought to be similar to leukocyte and hematopoietic stem cell homing cascade due to the involvement of similar cytokines. This process is divided in four steps: tethering/rolling, activation and arrest, transmigration/diapedesis and migration, illustrated in Figure 6.⁷²⁻⁷⁴

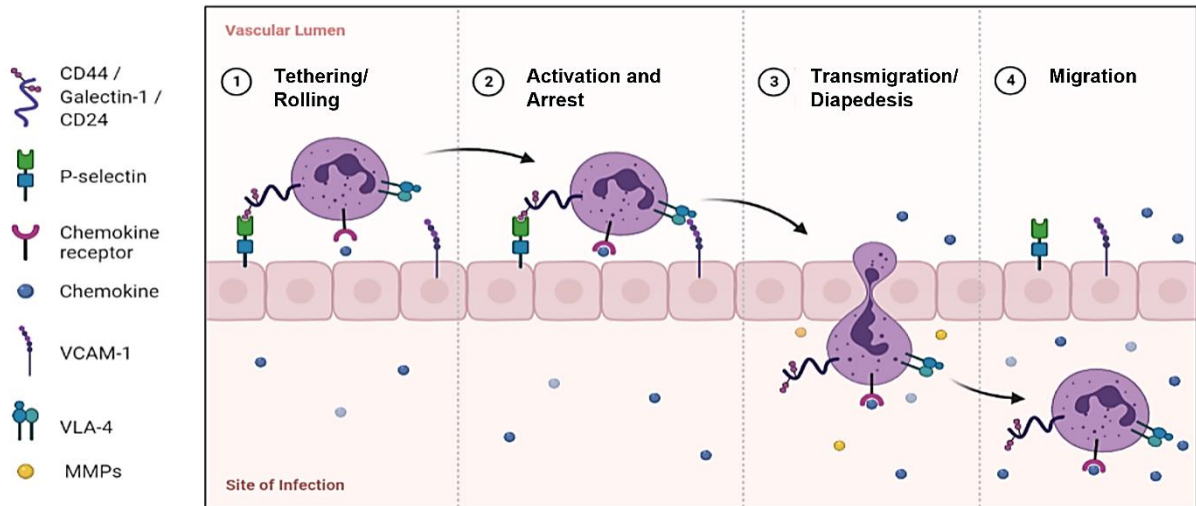


Figure 6 - Mesenchymal stem cell homing mechanism. Steps and molecules involved in the tethering/rolling, activation and arrest, transmigration/diapedesis and migration. Abbreviations: VCAM-1 (vascular adhesion molecule-1); VLA-4 (very late antigen 4); MMPs (matrix metalloproteinases).

Firstly, tethering is performed by a ligand in MSC surface that interacts with P-selectin, a protein in the surface of endothelial cells, inducing MSC rolling along the vasculature wall.⁷² Distinct studies identified CD44⁷⁵, galectin-1⁷⁶ and CD24⁷⁷ as potential P-selectin ligands.

In an inflammatory setting, G protein-coupled chemokine receptors expressed on the surface of MSCs interact with chemokines released in the site of injury and promote the activation step. This interaction is crucial for the arrest step, inducing conformational changes in the MSC extracellular domains of $\alpha_4\beta_1$ very late antigen 4 (VLA-4) integrins, increasing their affinity to chemokines.⁷² Upon CCl₄-induced liver injury condition in mice, Chen, Y. *et al.* (2009) reported the up-regulation of C-C chemokine receptor type 9 (CCR9), type 4 (CXCR4) and c-Met, as well as the respective ligands C-C chemokine ligand 25 (CCL25), stromal cell-derived factor (SDF)-1 and HGF, contributing to the migration of mouse BM-MSCs to the liver.⁷⁸ Moreover, EGF also influenced the MSC chemotaxis and homing.⁷⁹ After activation, the VLA-4 integrin expressed in MSCs binds to vascular adhesion molecule-1 (VCAM-1) on the surface of endothelial cells, arresting the MSCs.⁷²

Subsequently, MSCs transmigrate through the endothelial cell layer, resorting to secreted MMPs, that destroy the endothelial matrix.⁷² MMP-1 is the most described to have a crucial role by degrading collagen-I.⁸⁰

Lastly, within the tissue, MSCs migrate to the site of injury guided by chemotactic signals released upon damage, including the platelet-derived growth factor-AB, the IGF-1 and the inflammatory chemokine IL-8.⁷²

In particular, the homing ability of transplanted MSCs have been applied as a cell-based therapy for liver diseases. *In vivo*, MSCs have the capability to engraft in the recipient's liver and to differentiate into

liver stem cells or mature hepatocytes in both animals (e.g. mice) and humans.^{81,82} This process of MSC engraftment and differentiation was triggered by damaged liver tissue with accumulated collagen. Salomone, F. *et al.* (2013), also demonstrated that transplanted AT-MSCs were effective in healing APAP-induced liver injury.⁸³ In another study, Saito, Y. *et al.* (2014) reported the homing capability of AT-MSCs to the injured liver in mice under stress with hepatectomy and ischemia-reperfusion.⁸⁴ Overall, the success of cell-based therapies mostly relied on the ability of donor cells to access the damaged tissue and survive long enough to display a therapeutic effect. However, many times the levels of engraftment and survival in the injured liver were too low to be therapeutically relevant, what might be related with the delivery route, the number of infused cells and with the MSC culture conditions, among other factors.^{38,67}

Still, MSC cell-based therapies present some issues, namely, the lack of a standardized protocol for isolation and for *ex vivo* expansion, the decline in the engraftment and homing ability, the poor survival rate, the impaired differentiation ability of transplanted MSCs *in vivo* as well as the risks associated with the transplantation of undifferentiated and proliferative cells. Thus, rather than differentiating into liver cells the therapeutic benefit of MSCs in regenerative medicine might be related with cell-free therapies, overcoming the cell culture issues.⁸⁵ Indeed, recent data revealed that MSCs alleviate liver failure mainly through trophic and immunomodulatory factors. These factors induce pro-healing mechanisms after acute damage, altering the tissue microenvironment; support hepatocyte function, promote the proliferation of residual hepatocytes, inhibit hepatocyte apoptosis, reverse liver fibrosis and promote angiogenesis.³⁶ The paracrine factors secreted by MSCs have the capacity to immunomodulate the response of the immune system while having several effects: anti-inflammatory, anti-fibrotic, anti-apoptotic and angiogenic.^{12,38} MSCs suppress the proliferation of PBMCs and decrease the secretion of inflammatory cytokines from immune cells. These trophic and immunomodulatory factors create a regenerative microenvironment and reduce inflammatory injury by restraining life-threatening cytokine storms and immunocyte infiltration. Cell-cell contacts with immune cells might also play a role in immunomodulation, but the primary mechanism lies in MSC-conditioned medium (CM) containing soluble factors rather than cell-cell contacts. Although many trophic and immunomodulatory factors have been characterized from MSC-CM, much remains unclear regarding its constituents.⁸⁶ Thus, the notion of producing CM primed towards a specific microenvironment instead of intact MSCs requires further studies.

In vitro, MSCs secrete cytokines, chemokines, growth factors and immunomodulatory molecules into their culture medium, composing the MSC secretome or CM. These paracrine factors may be encapsulated in extracellular vesicles (EVs) or exosomes (Exo), mediating the communication between the cells and the surrounding tissues.⁸⁵

This cell-free technology has several advantages when compared to MSCs themselves, namely, fewer concerns regarding immunogenicity and tumorigenicity due to administration of undifferentiated and proliferative cells; the storage of CM can be done without any toxic cryopreservatives; the more economical and easier mass-production of CM in comparison to cells; and the simpler safety and efficacy evaluation.^{85,87}

The MSC secretome effect on cell proliferation, modulating the immune system, inhibiting cell death and fibrosis and promoting liver regeneration was reported in several studies. Importantly, the production of MSC-CM in serum-free conditions showed a significant up-regulation of pro-survival and angiogenic factors, namely, VEGF- α , IGF-1 and HGF.⁸⁸ MSC secretion of nitric oxide (NO), prostaglandin E (PGE) 2, indoleamine (IDO) 2, 3-dioxygenase, IL-6 and HLA G had an immunomodulatory effect in the cells of the innate immune system, such as macrophages and NK cells, and of the adaptive immune system, namely, T cells, B cells and lymphocytes. These soluble factors down-regulated T cell and NK cell activation and expansion, while induced regulatory T lymphocytes and modulated the B cell functions, which resulted in a less inflammatory phenotype.^{67,71}

The therapeutic effect of the MSC secretome in ALF was demonstrated in Zagoura, D. *et al.* (2019) in a CCl₄-induced liver injury mouse model. The anti-inflammatory molecule Annexin-A1 (ANXA1) presented in amniotic fluid-derived MSCs secretome ameliorated liver damage by inducing progenitor cell proliferation, migration and differentiation while reducing inflammation.⁸⁹ Moreover, systemic infusion of MSC-CM in a D-galactosamine-induced rat model of acute liver injury reduced apoptotic hepatocellular death by 90 % and stimulated liver regeneration through the secretion of trophic factors.⁹⁰ Also, BM-MSCs secretion of FGF, EGF and HGF inhibited HBV replication and IL-22 secretion had anti-inflammatory effects in HBV infection.⁹¹

An important step towards liver regeneration is the repair of fibrosis caused by the activation of HSCs which are responsible for collagen deposition. MSCs attenuated collagen synthesis through the secretion of the soluble factors, namely, TGF- β 3, TNF- α , IL-10 and HGF and induced the HSC apoptosis through the secretion of HGF and nerve growth factor (NGF).^{92,93} Furthermore, MSCs enhanced the expression of MMPs and inhibited the expression of tissue inhibitors of MMPs, resulting in the regression of liver fibrosis.⁹⁴ In particular, the anti-fibrotic effect of umbilical cord-derived MSCs (UC-MSCs) secretome was demonstrated using a mouse model of hepatic fibrosis induced with thioacetamide (TAA) or CCl₄. The authors verified that, within 3 days of the secretome injection, the fibrotic areas reduced as well as the number of activated HSCs, due to the presence of the anti-fibrotic protein milk fat globule EGF factor 8.⁹⁵

The inhibition of cell apoptosis by MSCs relies on the up-regulation of DNA repair while down-regulating mitochondrial death pathways. Soluble factors such as SDF-1, IGF-1, nuclear factor-erythroid factor 2-related factor (Nrf)-2, HIF, heme oxygenase (HO)-1 and VEGF down-regulated pro-apoptotic factors, namely, Bax, and increased the anti-apoptotic Bcl-2 levels and anti-oxidant activity.^{96,97}

MSCs have also the ability to create new vasculature from pre-existing blood vessels. The angiogenic potential of MSCs was exerted through the secretion of VEGF, FGF-1/2, HGF, Ang-1/3 and SDF-1, contributing to endothelial cell proliferation and improvement of tissue vascularization.⁹⁷ It was reported that the combination of MSCs with a certain growth factor cocktail induced specific angiogenic factors in MSCs, enhancing their therapeutic function in a TAA-induced liver fibrosis model by improving liver function and regeneration.⁹⁸

1.5.1.1. Extracellular vesicles and exosomes

The MSC-EVs are lipid membrane-encapsulated nanoparticles which carry biomolecules, namely, RNAs, enzymes, cytokines, growth factors, lipids and proteins, protecting them from degradation and are involved in cell-to-cell communication. The EVs can interact with the cell surface by receptor-ligand, can be internalized by the cells through phagocytosis or can fuse with the cell membrane.^{67,87}

MSCs-EVs exerted several effects which led to the reduction of fibrosis, inflammation, apoptosis and/or necrosis. For instance, fetal tissue-derived MSCs-EVs ameliorated liver fibrosis in cirrhotic mice, promoting liver regeneration and hepatocytes proliferation in a CCl₄-induced liver injury mouse model.⁹⁹ Moreover, human UC-MSCs-derived Exo reduced hepatic inflammation, collagen deposition and, consequently, fibrosis in a CCl₄-induced fibrotic liver by inhibiting epithelial-to-mesenchymal transition of hepatocytes.¹⁰⁰ Also, the application of human ESC-derived MSC-EVs ameliorated cirrhosis in TAA-induced chronic rat liver injury. The immunomodulatory capacity of EVs resulted in a reduction in fibrosis, collagen deposition and necrosis.¹⁰¹ The anti-inflammatory action was seen in the down-regulation of IL-22 and IL-23 levels along with the increase of the anti-inflammatory molecule PGE2 in mature human regulatory macrophages.¹⁰² The MSCs-Exo might also had a hepatoprotective role with anti-oxidant and anti-apoptotic effects against toxicant-induced injury. Yan, Y. *et al.* (2017) showed that human UC-MSCs-Exo-derived GSH peroxidase 1 detoxified CCl₄ and reduced oxidative stress and apoptosis, promoting the hepatic recovery.¹⁰³

Remarkably, it was shown that exosomes have the ability to accumulate in the liver and not in the lungs, reducing the risk of thromboembolism.⁷¹ However, the inexistence of standardized methods for the production of large quantities of EVs hindered, for now, the application of this cell-free therapy. Even though further research is needed to ensure product biosafety and efficiency, MSC-EVs comprise a promising therapeutic alternative to cell-based therapy.^{71,96}

1.5.1.2. Priming strategies to improvement the clinical outcome of MSCs

The therapeutic effects of MSCs are hampered by the low concentration of the secreted growth factors. MSCs have toll-like receptors which allow them to sense their microenvironment and act accordingly to it, polarizing into a pro-inflammatory or an immunosuppressive phenotype.¹⁰⁴ Therefore, pre-conditioning, commonly designated as priming, of the culture microenvironment with hypoxia or small molecules, three-dimensional (3D) culture systems or genetic manipulations have been performed to enhance the clinical outcome of MSCs and their secretion of paracrine factors into the culture medium.

- **Medium conditioning**

Typically, MSCs are cultured under ambient conditions (21 % oxygen) but the physiological oxygen tension in tissues vary from 1 % (e.g. in cartilage and bone marrow) to 12 % (e.g. in peripheral blood). Importantly, oxygen tension near periportal zones is reported to be 8.5 % and 4 % around pericentral

zones.¹⁰⁵ Moreover, the cell and tissue impairment may occur under hypoxic/ischemic conditions and ischemic/reperfusion injuries are frequently related with hepatic surgical procedure. Therefore, the resistance to hypoxic conditions can be acquired through hypoxic pre-conditioning, helping MSCs adapt to the typically hypoxic diseased site. In fact, MSC culture under hypoxia showed promising results, namely, in terms of cell proliferation and engraftment, as well as improvement in the MSC angiogenic potential and release of microvesicles and trophic factors.^{106,107} The process of hypoxia and reoxygenation led to the up-regulation of pro-survival genes and factors, such as HIF-1 α , which protected the liver against ischemic/reperfusion injury via the inhibition of oxidative stress, inflammation and apoptosis.^{108,109}

Moreover, pre-treatment with pro-inflammatory cytokines and growth factors is a useful tool, mimicking the *in vivo* injury site, since MSCs will answer to the inflammatory environment. Table 1 exhibits the effects on MSCs of some priming agents. Notably, hepatotoxicity may be mitigated by enhancing MSC therapeutic effect with HGF or FGF-2, IGF-2, EGF and VEGF- α priming, resulting in a reduction in liver fibrosis in mice liver injury models.^{98,110} Furthermore, the paracrine factors secreted from the injured liver tissue displayed the capacity to prime MSCs into an increased homing and hepatocyte differentiation ability. Consequently, these MSCs when transplanted into a liver fibrosis CCl₄-induced mouse model revealed an augmented therapeutic potential.¹¹¹

Nevertheless, further research must be developed to understand and define the optimal pre-conditioning conditions that maximizes the therapeutical effect of MSCs paracrine factors, especially in DILI.

Table 1 - Effect of different priming agents in MSCs.

Priming Agent		Effect	Mechanism
Cytokines	IFN- γ	Increased the secretion of immunomodulatory molecules.	Up-regulated secretion of PGE2, HGF and TGF- β . ^{112,113}
		Suppressed T cells.	Up-regulated secretion of programmed death-ligand 1 (PDL-1). ¹¹⁴
	TNF- α	Regulated the survival, proliferation, migration and immunosuppression.	Produced TNF receptor 1, PGE2, TNF stimulated gene (TSG) 6 and TGF- β ; Released HGF, IGF-1, VEGF; Enhanced regulatory T cells (Treg) functions. ¹¹⁵
	IL-17A	Modulated immunological function.	Suppressed effector T cell proliferation; Promoted Tregs. ¹¹⁶
Growth Factors	TGF- β 1	Enhanced proliferation and <i>in vivo</i> survival of UC-MSCs.	Enhanced the expression of ECM components, particularly fibronectin. ¹¹⁷
	HGF	Mitigated CCl ₄ -induced liver injury.	Produced albumin and alpha-fetoprotein; Suppressed transaminase activity and liver fibrosis. ¹¹⁰

	FGF-2, IGF-2, EGF and VEGF- α	Reduced hepatic fibrosis in a TAA-induced rat model.	Inhibited HSCs activation <i>in vitro</i> ; Induced high expression levels of HGF. ⁹⁸
Injured Tissue		Reduced liver fibrosis in a CCl ₄ -induced mouse model.	Induced high expression of albumin, CK8, CK18 and HNF1- α ; Increased homing and differentiation abilities of MSCs. ¹¹¹

- **3D culturing**

Recently, growing evidence has emerged relatively to 3D culturing of MSCs, mimicking the *in vivo* environment and cellular interactions. Indeed, in 3D cultures MSCs enhanced their differentiation, tissue development and therapeutic effects, which resulted from a higher cell-cell contact and cell-ECM interactions. The 3D culture systems enables the cell-to-cell communication, mimics the original physiological properties of stem cells, improves their therapeutic function and increases the homing.¹¹⁸

3D-cultured MSCs enhanced the secretion of immunomodulatory factors, such as TGF- β 1, PGE2 and IL-6 when compared to monolayer cultures.¹¹⁹ Moreover, the entrapment of IFN- γ -bound heparin microparticles within 3D aggregates of MSCs potentiated the spheroids ability to produce IDO and suppress T-cell proliferation.¹²⁰ Additionally, Zhang, X. *et al.* (2016) reported that 3D culture enhanced the expression of anti-fibrotic factors by MSCs – IGF-1, IL-6 and HGF – ameliorated hepatic fibrosis in mice and protected hepatocytes from cell injury and apoptosis more effectively than two-dimensional (2D)-cultured cells.¹²¹

- **Genetic Manipulations**

Genetic engineering is an appealing approach for improving MSCs therapeutic efficacy, either by increasing transplanted MSC survival and residence time, angiogenesis, differentiation potential, homing or anti-inflammatory effects. The genes under possible manipulation are receptors, growth factors and cytokines.⁹⁷ Wang, K. *et al.* (2017) resorted to the lentivirus expression vector to deliver the c-Met gene into BM-MSCs by transfection. The results showed that overexpression of c-Met promoted homing of BM-MSCs to the injured liver of rats after ALF, increasing the survival rate.¹²² Currently, clustered regularly interspaced short palindromic repeat (CRISPR)/Cas9 RNA-based nucleases have been frequently studied and applied as a technology for detailed genetic editing at specific desired sites.¹¹⁸ Other study by Ma, H. C. *et al.* (2014) reported an improvement in the homing of systemically delivered MSCs genetically modified with CXCR4 toward the failing liver. Moreover, the colonization rate of the transplanted MSCs increased as well as the liver regeneration, possibly because of the secretion of HGF and VEGF.¹²³

1.6. Motivation and aims

Liver diseases are responsible for, approximately, 2 million deaths per year worldwide, accounting for 3.5 % of the global mortality.⁴⁹ This number is expected to increase giving the growing population with unhealthy food habits and addictions. In particular, DILI is responsible for 13 % of cases of ALF, being APAP-induced hepatotoxicity the major cause.¹²⁴ Under excessive doses, APAP dysregulates mitochondrial and ER functions, leading to oxidative stress, hepatocyte necrosis and, ultimately, liver failure.

The current therapy for APAP overdose consists in NAC administration, but it relies on the early identification of DILI and on the prompt administration. Liver transplantation is also an alternative treatment. However, the liver transplantation rates do not meet the current need, increasing the burden related with liver diseases. Therefore, there is the need to thoroughly understand the underlying mechanisms of liver injury in order to mimic the liver injury microenvironment in *in vitro* cultures and to develop more efficient alternative therapies.

MSCs, and in particular, their secreted factors with important immunomodulatory and anti-inflammatory effects, have been considered for a variety of pathologies. Since MSCs paracrine activity changes accordingly to their surrounding microenvironment, we hypothesise that the modulation of the MSCs secretome with inflammatory signals from injured liver (mimicking the liver injury microenvironment) would enhance the hepatic regenerative capacity.

As such the objectives of this work were:

- to mimic the liver injury microenvironment resorting to an MSC-derived HLC *in vitro* model of APAP-induced injury; and to produce the inflammatory medium from the APAP-induced liver injury in *in vitro* cultures (SOS medium);
- to modulate the MSC-mediated paracrine mechanisms by incubating MSCs with medium collected from APAP-induced liver injury in *in vitro* cultures (SOS medium); and to produce the primed MSC conditioned medium;
- to evaluate the therapeutical effect of the primed MSC conditioned medium in an MSC-derived HLC *in vitro* model of APAP-induced injury.

2. Materials and methods

2.1. Reagents

Trypsin-EDTA, fetal bovine serum (FBS), insulin-transferrin-selenium (ITS) and penicillin streptomycin were purchased from Gibco®/Thermo Fisher Scientific®. HGF, FGF-2, FGF-4, oncostatin M (OSM), dexamethasone and 5-azacytidine (5-AZA) were purchased from Peptidech®. Amphotericin B was purchased from Biochrom® and bovine serum albumin (BSA) from PanReac®. Lastly, Iscove's modified Dulbecco's medium (IMDM), minimum essential medium eagle alpha modification (α -MEM), EGF, dimethyl sulfoxide (DMSO), nicotinamide, trypan blue and 4-acetamidophenol were acquired from Sigma-Aldrich®.

2.2. Cell culture

Human neonatal umbilical cord matrix-derived MSCs (hnUCM-MSCs) were isolated according to Miranda *et al.* (2015)¹²⁵ and Santos *et al.* (2015)¹¹⁹. In 2D culture, hnUCM-MSCs were expanded as undifferentiated cells in a growing medium consisting in α -MEM with 10 % (v/v) FBS, incubated at 37 °C in 5 % carbon dioxide (CO₂) humidified atmosphere. Cell passage was performed with 0.05 % Trypsin-EDTA incubation for 5 minutes every 2 - 3 days when cell confluence reached 70 - 80 %. Cells were counted under an Olympus CK30-F200 (Olympus Optical®) inverted microscope and cell viability was assessed through trypan blue exclusion method. Cell culture photographs were acquired using a Moticam 2500 5.0 M Pixel (Motic®) camera mounted on Olympus CK30-F200 inverted microscope and images were collected using Motic Images Plus 3.0 software (Motic®).

2.3. Collagen coating

Following the protocol described in Rajan *et al.* (2006)¹²⁶, rat-tail collagen was produced in house for culture flasks and well plates coating. The extracted rat-tail collagen was dissolved in 0.1 % (v/v) acetic acid achieving a stock solution concentration of 1 mg/mL. The stock solution was diluted to 0.2 mg/mL in a volume of phosphate buffered saline (PBS) which assured total culture surface coverage. The collagen polymerization occurred after 1-hour incubation at 37 °C. Afterwards, the cell culture surfaces were washed with PBS before cell inoculation.

2.4. Hepatocyte differentiation protocol

The hepatocyte differentiation protocol herein followed is described in Cipriano *et al.* (2017)^{127,128}. hnUCM-MSCs were seeded in culture flasks pre-coated with rat-tail collagen at a density of 1.5×10^4 cells/cm², reaching a cell confluency of 90 % within 24 hours after inoculation. A three-step

differentiation protocol (Figure 7) was performed to generate HLCs using as basal medium (BM) IMDM with 1 % (v/v) penicillin-streptomycin-amphotericin B. In the first step the cells were incubated for 48 hours in BM supplemented with 2 % (v/v) FBS, 10 ng/mL of EGF and 4 ng/mL of FGF-2, for endoderm commitment and foregut induction. In the second step, hepatoblasts and liver bud formation was induced by maintaining the cells for 10 days in BM supplemented with 4 ng/mL of FGF-2, 10 ng/mL of FGF-4, 20 ng/mL of HGF, 0.61 g/L of nicotinamide and 1 % (v/v) ITS. At day 10 of differentiation (D10), 1 % (v/v) DMSO was added to the medium. Lastly, in the third step, for hepatoblast differentiation and hepatocyte maturation, cells were maintained in BM supplemented with 8 ng/mL of OSM, 1 μ M of dexamethasone, 1 % (v/v) DMSO and 1 % (v/v) ITS from D13 onwards, defined as differentiation medium (DM). At D17, cells were trypsinized with 0.25 % Trypsin-EDTA solution for 3 minutes and re-inoculated in DM containing 20 μ M of 5-AZA and 5 % (v/v) FBS into (1) 2D pre-coated culture flasks for the production of the SOS medium, 96-well plates for cell viability assays and 6-well plates for quantitative real-time polymerase chain reaction (qRT-PCR) analysis at a density of 2×10^4 cells/cm²; and (2) ultra-low attachment plates for 3D spheroid culture at 5.0×10^5 cells/mL. 24 hours after the inoculation, the medium was changed to remove 5-AZA and FBS. Cells were maintained in DM up to D27 of culture with medium replacement every 3 - 4 days.

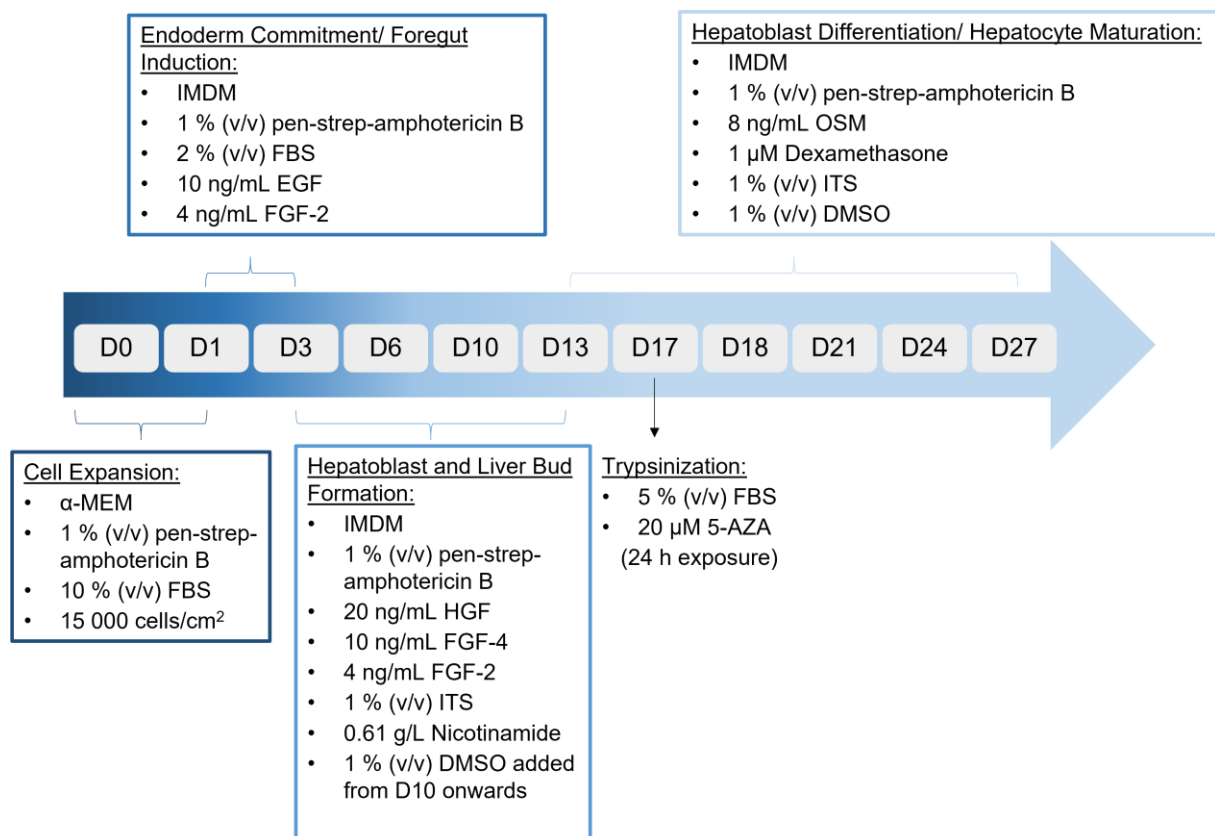


Figure 7 - Hepatocyte differentiation protocol. Description of the three-step differentiation protocol consisting on endoderm commitment/foregut induction, hepatoblast and liver bud formation and hepatoblast differentiation/hepatocyte maturation. Abbreviations: α -MEM (minimum essential medium eagle alpha modification); BM (basal medium); FBS (fetal bovine serum); EGF (epidermal growth factor); FGF (fibroblast growth factor); HGF (hepatocyte growth factor); ITS (insulin-transferrin-selenium); DMSO (dimethyl sulfoxide); 5-AZA (5-azacytidine); OSM (oncostatin M); D0-D27 (days from 0 to 27 of the hepatocyte differentiation protocol).

2.5. Conditioned medium production

2.5.1. SOS medium

At D27, HLCs in 2D culture flasks were incubated with 30 mM APAP. After an 8-hour exposure, cells were washed two times with PBS and the medium was replaced by fresh DM without APAP, at a final volume of 25 mL per 175 cm² t-flask or 10.7 mL per 75 cm² t-flask. After conditioning for 24 hours, the SOS medium was collected under sterile conditions and centrifuged firstly at 300xg, 25 °C, for 10 minutes, and then at 2700xg, 4 °C for 30 minutes. The injured HLCs were harvested for total protein quantification and qRT-PCR analysis.

The same procedure was applied to 3D-cultured HLCs, exposing them for 8 hours to 30 mM APAP at D27 and recovering the medium and the cells 24 hours later.

The SOS medium was concentrated in Amicon® Ultra-15 (Millipore®) 3 kDa cut-off centrifugal concentrators as per manufacture's recommendations. Samples were stored at - 80 °C until further use.

Additionally, samples from 2D-cultured HLCs exposed to 30 mM APAP for 24 hours at D27 were collected for qRT-PCR analysis.

2.5.2. Pre-conditioning of hnUCM-MSCs: production of conditioned medium (MSC-CM)

For the production of MSC-CM, hnUCM-MSCs, with a maximum of 15 passages, were inoculated at a density of 1.0x10⁴ cells/cm² in 175 cm² and 75 cm² t-flasks with α -MEM and 5 % (v/v) FBS. When 60 % confluence was reached, cells were washed with PBS and α -MEM. Afterwards, for priming MSC-CM with the SOS medium, the hnUCM-MSCs medium was replaced by α -MEM without FBS (90 % of the final volume) and with 10 % of SOS medium 50x concentrated, at a final volume of 18 mL per 175 cm² t-flask and 8 mL per 75 cm² t-flask.

After the 24-hour priming, the cells were washed with PBS and α -MEM and the medium was replaced by fresh α -MEM without FBS, at a final volume of 25 mL per 175 cm² t-flask and 10.7 mL per 75 cm² t-flask. After conditioning for 48 hours, primed MSC-CM (pMSC-CM) was collected under sterile conditions and centrifuged as mentioned in section 2.5.1.

Control MSC-CM (cMSC-CM) was produced from a 3-day incubation of hnUCM-MSCs with α -MEM and 5 % (v/v) FBS, followed by 48 hours with α -MEM without FBS at a final volume of 25 mL per 175 cm² t-flask and 10.7 mL per 75 cm² t-flask. Cells were harvested for total protein quantification and qRT-PCR analysis. As described in section 2.5.1, CM was concentrated and stored at - 80 °C until further use.

A summarized outline of the laboratory work developed is presented in Figure 8.

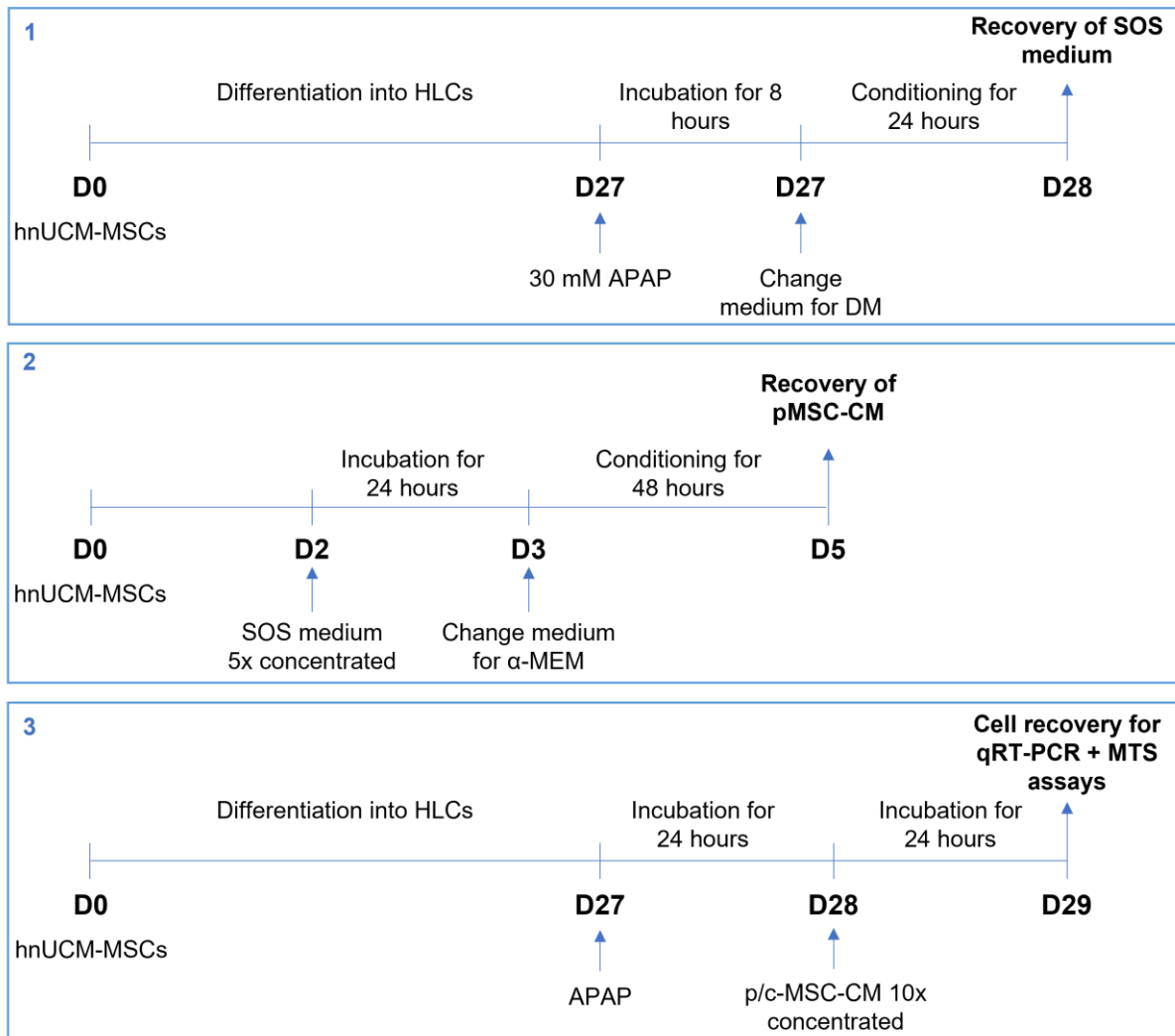


Figure 8 - Outline of the work developed divided in three major phases: 1) production of the SOS medium from hnUCM-MSC-derived HLCs; 2) production of MSC-CM primed with SOS medium 5x concentrated (pMSC-CM); 3) evaluation of MSC-CM, either primed (pMSC-CM) or control (cMSC-CM) 10x concentrated, effect on APAP-injured hnUCM-MSC-derived HLCs through qRT-PCR and MTS assays. Abbreviations: hnUCM-MSCs (human neonatal umbilical cord matrix-derived mesenchymal stem cells); HLCs (hepatocyte-like cells); DM (differentiation medium); SOS medium (hepatocyte-like cells medium with SOS secreted signals after APAP exposure); α -MEM (minimum essential medium eagle alpha modification); pMSC-CM (human neonatal umbilical cord matrix-derived mesenchymal stem cells conditioned medium primed with the hepatocyte-like cell SOS medium); cMSC-CM (human neonatal umbilical cord matrix-derived mesenchymal stem cells conditioned medium); qRT-PCR (quantitative real-time polymerase chain reaction).

2.6. Cell viability assays

APAP cytotoxicity and the effect of CM in HLCs upon APAP exposure were evaluated using the MTS reduction assay (Promega®). Cell viability was measured, according to the manufacturer's instructions. The absorbance was measured at 490 and 690 nm using microplate reader SPECTROstar Omega (BMG Labtech®).

For evaluating APAP cytotoxicity, HLCs at D27 seeded in 96-well plates, were exposed to 0, 5, 10, 15, 20, 30, 50 and 60 mM APAP for 24 hours. The estimated half-maximal inhibitory concentration (IC₅₀) was calculated through a non-linear regression fit.

For assessing the effect of MSC-CM in HLCs viability upon APAP exposure, HLCs were exposed to 0, 5, 15 and 30 mM APAP at D27. After a 24-hour exposure, cells were washed with PBS and the medium was replaced by DM with 10 % (v/v) of pMSC-CM or cMSC-CM 100x concentrated for other 24 hours. 10 % (v/v) DMSO was used as negative control and IMDM as positive control. Results were presented as relative percentages to the positive control, which was considered as 100 % of cellular viability.

2.7. Gene expression

Total RNA was isolated from samples with 0.5 - 1.0 x 10⁶ cells using Trizol® (Life Technologies®) and extracted according to the manufacturer's instructions. RNA concentration was determined by measuring absorbance at 260 nM using LVis Plate mode on SPECTROstar Omega. The 260/280 nm ratio was used as purity measurement for protein presence, considering ratios between 1.8 - 2.0. c-DNA was synthesized from 1 µg of RNA using NZY First-Strand cDNA Synthesis Kit (NZYTech®), following the manufacturer instructions.

qRT-PCR was performed using PowerUp™ SYBR® Green Master Mix (Life Technologies®). Master mix was prepared for a final reaction volume of 15 µL, using 2 µL of template cDNA and 0.333 µM of forward and reverse primers (table A, section 6). The reaction was performed on QuantStudio™ 7 Flex Real-Time PCR System (Applied Biosystems®) consisting of an activation step of Uracil-DNA Glycosylase (UDG) at 50 °C for 2 min, a denaturation step at 95 °C for 10 minutes, followed by 40 cycles of denaturation at 95 °C for 15 seconds and annealing and extension at 60 °C for 1 minute. As a quality and specificity measure, a dissociation stage which determines the melting temperature of a single nucleic acid target sequence was added. Blank controls with no cDNA templates were performed to rule out contamination. The comparative Ct method ($2^{-\Delta\Delta Ct}$) was used to quantify gene expression, which was normalized to the reference gene (β -actin).

2.8. Protein quantification

For total protein quantification, cells were lysed with 0.1 M sodium hydroxide (NaOH) overnight at 37 °C. Protein concentration was determined through the calorimetric Bradford assay with protein assay dye reagent concentrate (Bio-rad®) diluted in 1:5 in Milli-Q® water. The absorbance was measured at 595 nm using microplate mode on SPECTROstar Omega.

2.9. Statistical analysis

Statistical data analysis was performed using GraphPad Prism version 9.0 (GraphPad Software®). The results are shown as the average \pm SD. Data comparisons were analysed by two-way ANOVA with Tukey's or Šidák's test and differences were considered statistically significant for $p < 0.05$.

3. Results and discussion

The high prevalence of APAP hepatotoxicity, accounting for 46 % of all ALF in the US and between 40 to 70 % of all cases in Europe, raised concern worldwide and the mechanisms behind its metabolism have been elucidated in the past years.²⁸ The current therapies rely on the prompt administration of NAC. However, this implies a timely identification of the overdose and many times the DILI diagnosis comes from an exclusion-based method, resulting in a delayed recognition of the insult. Under extreme cases, liver transplantation is the only viable option, although the transplantation rates only meet 10 % of the global need.⁴⁹ Therefore, alternative therapies, particularly related with the liver's regeneration after injury are being studied.

Recently, there has been growing evidence of MSCs therapeutic roles in liver injuries, mainly through their secretome and the stimulation of endogenous repair processes which induce intrinsic hepatocyte regeneration.¹²⁹ Within the various sources of MSCs, hnUCM-MSCs have demonstrated to be more potent immunosuppressors and less immunogenic than hnBM-MSCs.⁷³ Moreover, the CM produced by hnUCM-MSCs had previously been characterized, showing great paracrine activity and potential for regenerative capacity.^{119,130,131} Additionally, the therapeutic effect of MSC secretome can be enhanced with different priming strategies, namely, cytokines and growth factors or injured liver tissue exposure.^{98,110,111}

The study herein presented mimicked the mechanisms related with APAP-induced hepatotoxicity, namely, mitochondrial oxidative stress and ER stress and aimed to modulate and enhance the therapeutic effect of the MSC secretome in hepatic regeneration by priming MSCs with medium from HLCs injured by APAP (SOS medium).

3.1. APAP toxicity in hepatocyte-like cells (HLCs)

Over the years, animal models have been used to study liver mechanisms, mimic liver diseases and assess novel therapeutics, enabling the study of whole organs and living organisms. However, the inherent interspecies differences, the ethical concerns and the impossibility to evaluate molecular mechanisms urged the need for more reliable hepatic models which predicted human toxic events, minimizing the amount of drug failures.¹³² Alternatively, primary human hepatocytes (PHH) resembled the specific metabolism and functionality of the human liver, but their scarcity and suitability only for short-term studies in monolayer cultures due to their rapid loss of functionality hindered their application.¹⁶ Hence, researchers explored hepatocyte immortalized cell lines (e.g. HepG2 and HepaRG) derived from hepatomas or through genetic manipulations. However, these cell lines presented altered metabolic functions and genetic abnormalities, failing to mimic human physiology. Therefore, *in vitro* stem cell-differentiation into HLCs arose, overcoming the limitations related with the aforementioned cell sources.¹³³

HLCs can be differentiated from ESCs, iPSCs and MSCs, but MSCs characteristics and benefits were optimal for *in vitro* models. Indeed, MSC-derived HLCs presented hepatocyte-specific gene expression and functions, namely, urea and glycogen production.¹³⁴ Among the different MSCs sources, hnUCM-MSCs were more favourable to differentiate into HLCs for a human-based *in vitro* liver model, owing to the lack of major ethical issues, the low risk of viral transmission, the low immunogenicity, the abundant and non-invasive availability and to its more primitive origin.¹³⁵

The three-step protocol herein followed for hepatocyte differentiation using hnUCM-MSCs was adapted from the previously described and characterized in Cipriano *et al.* (2017).^{127,128} From D21 onwards HLCs were metabolically competent, displaying drug transporter and phase I and II enzymes expression and activity.^{127,136} Considering the results reported by Cipriano *et al.* (2020)¹³⁶, namely, the expression of genes involved in phase I, II and III of biotransformation of 3D and 2D-cultured HLCs exposed to nevirapine, it was decided that for this study the APAP exposure would be performed at D27 of the differentiation protocol.

To assess the effect of APAP in HLCs, we plotted the APAP dose-response curve in HLCs at D27 through the MTS cell viability assay (Figure 9). The cells were exposed to 5, 10, 15, 20, 30, 50 and 60 mM of APAP for 24 hours.

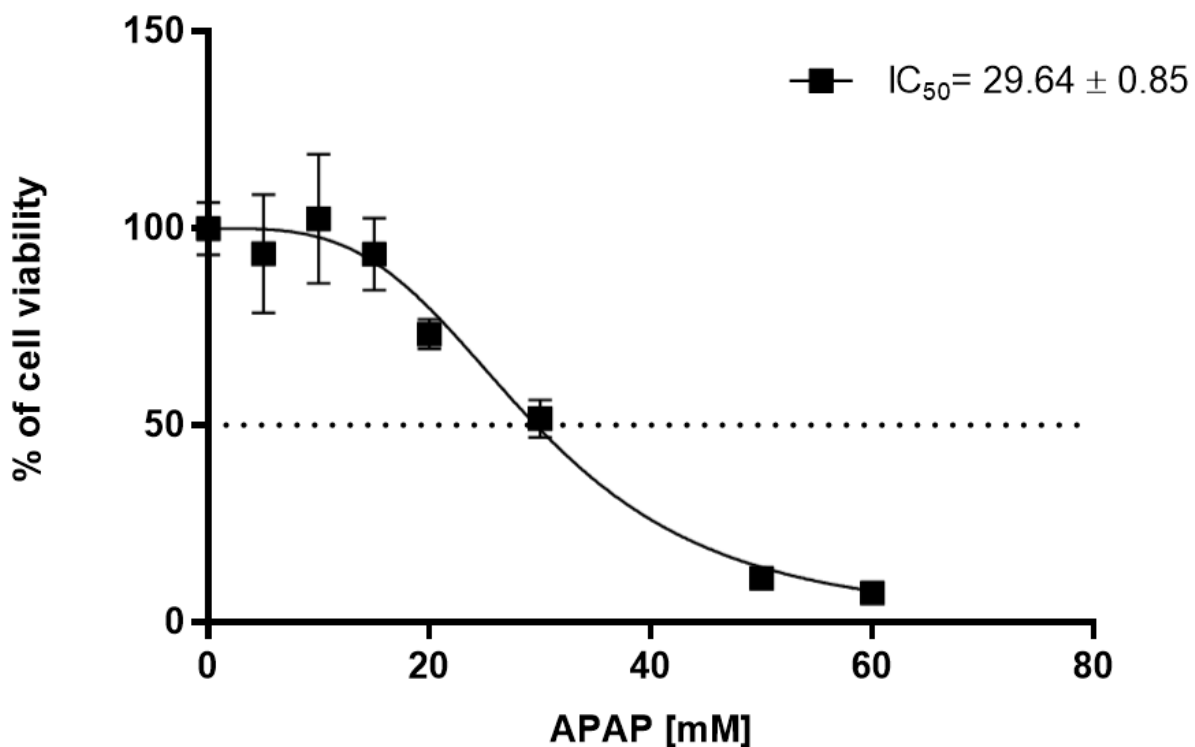


Figure 9 - APAP toxicity in HLCs. The HLCs were incubated with 5, 10, 15, 20, 30, 50 and 60 mM of APAP for 24 hours (n=2) at D27. The percentage of live cells is calculated relatively to non-treated HLCs at D28. Abbreviations: IC₅₀ (half-maximal inhibitory concentration).

From the resulting dose-response curve, the IC₅₀ was determined as 29.64 ± 0.85 mM APAP for a 24-hour exposure in HLCs. Hereafter, we approximated the APAP IC₅₀ value to 30 mM. Therefore, as a starting point, we considered the IC₅₀ value for the APAP-induced liver injury in *in vitro* cultures, namely, for the SOS medium production, since it was a reasonable and sufficient APAP concentration to induce hepatotoxicity while maintaining cells functional.

3.2. APAP-induced injury in 2D and 3D HLC *in vitro* cultures reveal differential liver injury-related gene expression levels

3.2.1. APAP induced morphological changes and altered gene expression in 2D-cultured HLCs

Upon APAP-induced injury human hepatocytes are known to secrete specific cytokines. Indeed, CM from APAP-exposed human ESC-derived HLCs revealed an increase in inflammatory cytokines and activated immune cells, triggering an immune-mediated hepatotoxicity.¹³⁷ Herein, to produce the APAP-induced HLCs injury medium with inflammatory signals (SOS medium), which we hypothesised that could modulate the MSC secretome, we exposed HLCs to 30 mM APAP. Ongoing work in our laboratory group, determined through total protein quantification of HLCs exposed to APAP (data not shown) that the level of cell injury was similar either at 24-hour (the incubation period used for the dose-response curve) or at 8-hour exposure to APAP. Therefore, to ensure minimal loss of injury signals and the presence of the initially produced inflammatory cytokines, we established an 8-hour APAP exposure for the SOS medium production. After an 8-hour APAP exposure, the medium was replaced by fresh medium to remove the presence of APAP. After the 24 hours conditioning period, the conditioned medium was collected (SOS medium), in order to guarantee that HLCs' inflammatory signals consequent of the APAP toxicity were present.

Throughout the differentiation protocol, the hnUCM-MSC-derived HLCs showed significant differences in morphology as a result of the sequential exposure to cytokines, growth factors and small molecules which mimicked the liver embryonic development, transitioning from a fibroblast-like to an epithelial polygonal shape morphology with binucleated cells, seen in Figure 10 a). The HLCs morphology resultant from an 8-hour exposure to 30 mM APAP at D27 is presented in Figure 10 b). Upon APAP exposure, HLCs modified their hepatocellular morphology and the detachment of some cells from the culture flask was visible as a result to the deleterious drug. Their morphology 24 hours after removing APAP, at the end of the conditioning period (Figure 10 c)), exhibited a significant improvement, re-gaining their polygonal shape, suggesting that HLCs had the capacity to recover until a certain extent after the drug removal.

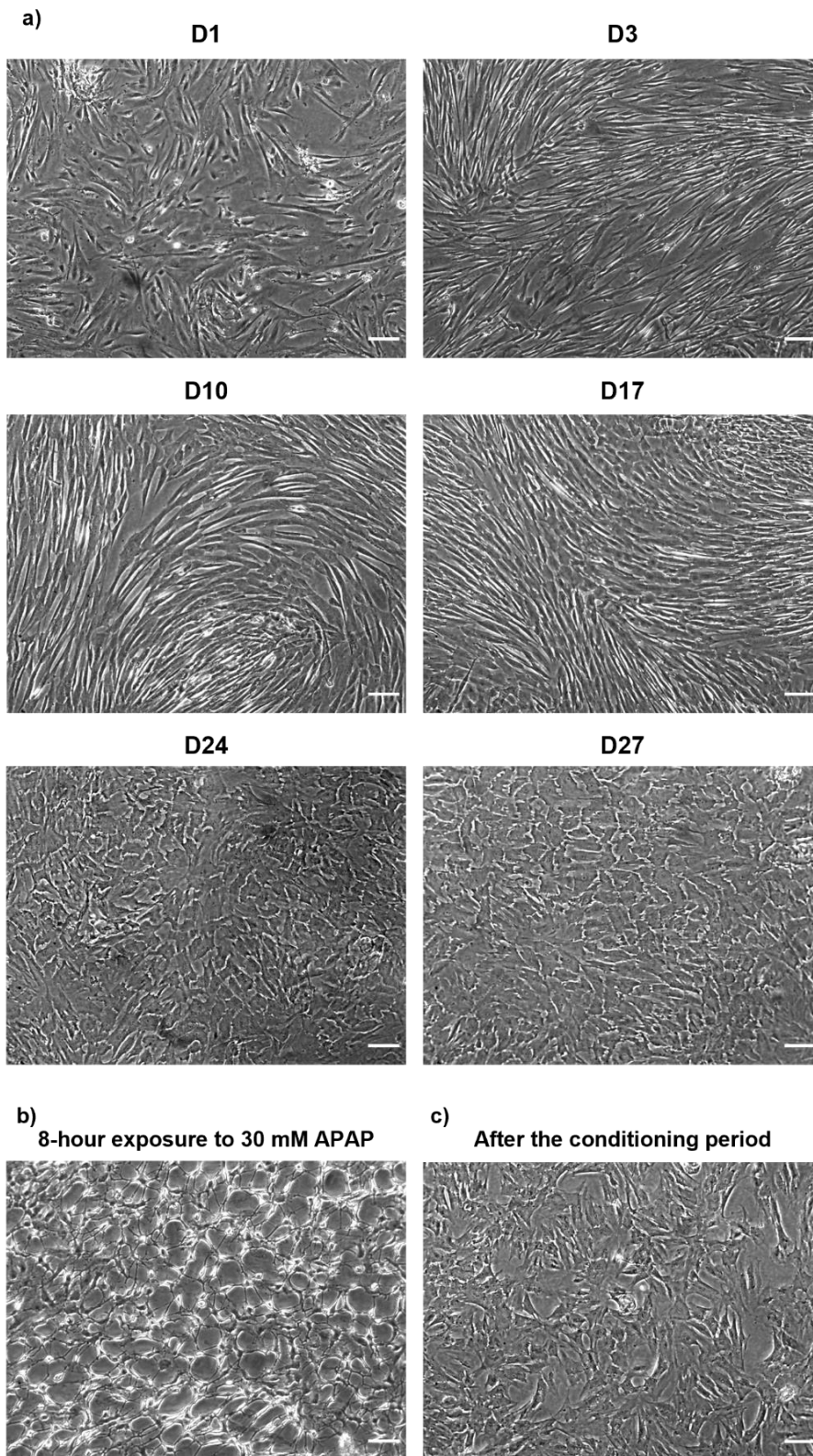


Figure 10 - APAP altered HLCs' polygonal shape morphology and caused detachment. a) morphological changes in 2D-cultured HLCs throughout the differentiation protocol, from D1 to D27; b) HLCs' morphology after an 8-hour exposure to 30 mM APAP; b) HLCs' morphology at the end of the conditioning period to produce the SOS medium. HLCs were exposed to APAP at D27. After APAP exposure, the medium was replaced by fresh medium without APAP. Scale bar = 100 μ m. Abbreviations: D1 - D27 (days 1 to 27 of the hepatocyte differentiation protocol).

Under excessive doses of APAP, the APAP reactive metabolite NAPQI accumulates in the liver, leading to the formation of NAPQI-adducts, causing mitochondrial oxidative stress, ER stress, DNA fragmentation and hepatocyte necrosis. Therefore, to evaluate the effect of APAP in HLCs we assessed the expression level of *ASK1*, *RIPK3*, *ATF-6* and *BAX*, involved in the APAP-induced hepatotoxicity, namely, mitochondrial oxidative stress, necroptosis, ER stress and apoptosis, respectively.

Additionally, expression levels of *HNF4-A* and *TNF-A* were also analysed. The interest in the transcription factor HNF4- α relied on its crucial role in hepatocyte differentiation during embryogenesis, in the maintenance of the hepatic function, in the regulation of the hepatic epithelial morphology and in the enhancement of MSC differentiation. In decompensated livers, in animal models of chronic liver failure and in HCC, the nuclear *HNF4-A* revealed to be significantly down-regulated.^{138,139,140} Moreover, this transcription factor had a crucial role in the termination phase of liver regeneration, since its re-expression after initial decrease was pivotal for hepatocytes exit from the cell cycle.⁴⁸ In regard to TNF- α , this pleiotropic cytokine influenced cell growth, differentiation and metabolism, being involved in both systemic inflammation and regeneration. Indeed, *TNF-A*, one of the most abundant early mediators in injured tissue, showed up-regulation during liver injury.^{90,141} Moreover, TNF- α also prime the hepatic liver regeneration cycle.¹⁴²

Therefore, a panel of genes involved in APAP-induced toxicity were quantified to shed light on the effects of APAP exposure to the cells. The gene expression profile of HLCs was evaluated at the time of the SOS medium collection, i.e., in HLCs exposed for 8 hours to 30 mM APAP followed by a 24-hour conditioning with fresh medium without APAP. Results are shown in Figure 11, relative to non-injured HLCs recovered at D28.

The results presented in Figure 11 showed that only *ATF-6* ($p < 0.001$) and *BAX* ($p < 0.01$) were significantly overexpressed relatively to non-injured cells, suggesting APAP-induced hepatotoxicity through ER stress and apoptosis. Concordantly with the literature, *HNF4- α* was dramatically reduced ($p < 0.001$), relatively to control, indicating the existence of hepatic injury.^{138,139,140}

Since *ASK-1* represents the mitochondrial oxidative stress induced by NAPQI, its inhibition ($p < 0.01$) relatively to non-injured HLCs, might be related with the wash-out of APAP and, consequently, its reactive metabolite NAPQI, during the replacement of medium for the conditioning period. The stress-induced environment triggered by APAP exposure might have stimulated HLCs to intrinsically regenerate and regain their normal phenotype during the following 24-hour conditioning period, seen in the inhibition of *ASK1* and *RIPK3* and in the morphological recovery in Figure 10 c).

The overall presented results seemed to suggest that upon an 8-hour exposure to 30 mM APAP, HLCs suffered damage and activated APAP-related hepatotoxicity pathways, implying that the APAP-induced liver injury *in vitro* culture might have mimicked, to a certain degree, the liver injury microenvironment. Therefore, the SOS medium might display the capacity to prime/modulate the hnUCM-MSCs into a regenerative status.

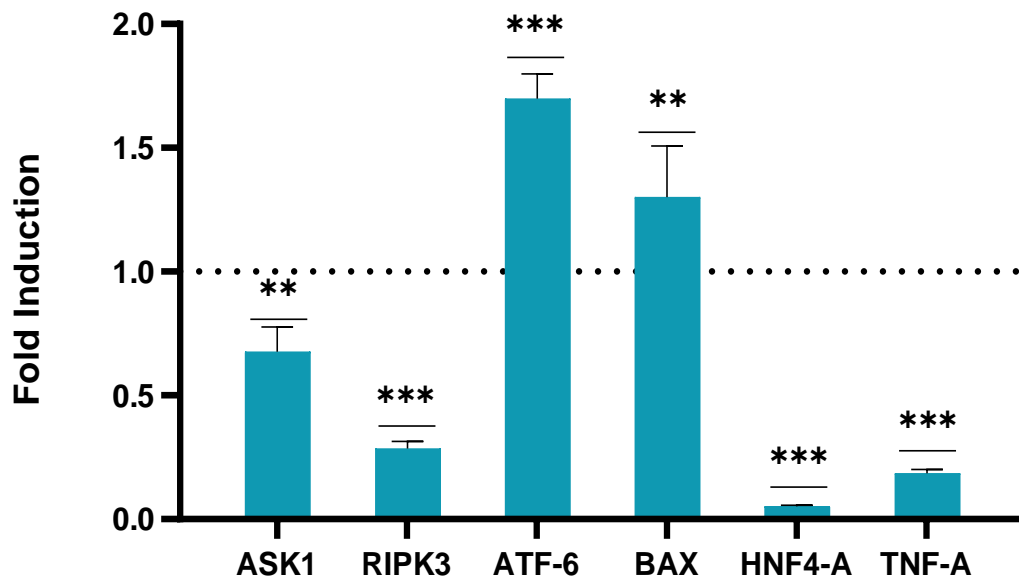


Figure 11 - Endoplasmic reticulum stress and apoptosis were induced in HLCs following APAP exposure. Gene expression of HLCs with an 8-hour exposure to 30 mM APAP, at D27, followed by a 24-hour conditioning with fresh medium without APAP, relative to non-injured HLCs recovered at D28. Data represented as average \pm SD (n=1-3). **, *** significantly differed from the non-injured HLCs gene expression with $p < 0.01$ and $p < 0.001$, respectively. Abbreviations: *ASK1* (apoptosis signal-regulating kinase 1); *RIPK3* (receptor-interacting protein kinases 3); *ATF-6* (activating transcription factor 6); *BAX* (Bcl-2-associated X protein); *HNF4-A* (hepatocyte nuclear factor 4 alpha); *TNF-A* (tumour necrosis factor alpha).

Even though the *in vitro* APAP-induced liver injury through 2D culturing of HLCs seemed to replicate liver injury, several strategies have been studied to identify and further optimize *in vitro* conditions for hepatocyte maturation, assessment of drug toxicities and disease mechanisms, namely, 3D cell culturing.

3.2.2. 3D culturing of HLCs to establish an *in vitro* APAP-induced liver injury model

The advantages of 3D-cultured HLCs rely on a high cell-to-cell and cell-to-ECM contact, on a nutrient and oxygen gradients and on cell polarization which are essential for liver development.¹⁴³ 3D aggregates surge from the adherence of cells to one another, forming a spherical aggregate. Regarding hepatogenic differentiation, 3D culturing of hESCs-derived and iPSCs-derived HLCs improved hepatocyte phenotype, namely, the biotransformation activity.^{144,145} Likewise, the MSC differentiation into HLCs in 3D cultures showed higher liver functional features, namely, phase I and II metabolism capacity and urea and albumin production.¹²⁸

Therefore, taking a step forward in this work, we started the development of an APAP-induced liver injury model in 3D culture. As such, from D17 onwards HLCs were cultured in ultra-low attachment culture plates. The inoculated cells formed clusters which progressively aggregated into small spheroids, as seen in Figure 12 a). At D27, 3D-cultured HLCs were exposed to 30 mM APAP for 8 hours (Figure 12 b)), as in 2D cultures. Afterwards, the medium was replaced to remove APAP and followed by the 24-hour conditioning period (Figure 12 c)), for the production of the SOS medium in 3D culture.

The HLCs aggregates' diameters in different days of the differentiation protocol, upon an 8-hour exposure to 30 mM APAP (at D27) and at the end of the conditioning period (at D28) are presented in Figure 13.

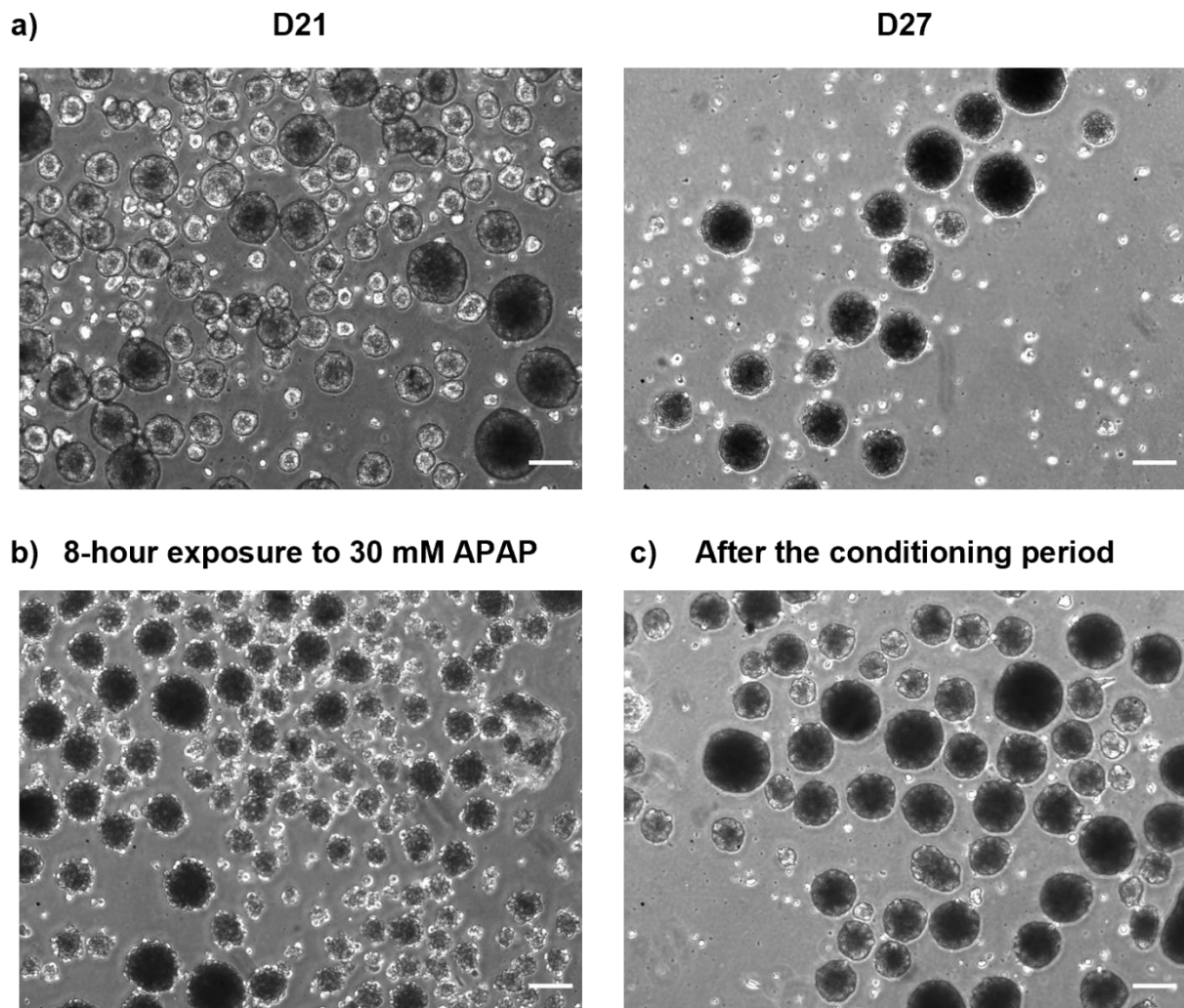


Figure 12 – HLCs aggregates' morphological changes in 3D culturing. a) morphological variation of hnUCM-MSC-derived HLCs aggregates at D21 and D27 cultured in ultra-low attachment plates; b) HLCs aggregates' morphology after an 8-hour exposure to 30 mM APAP, at D27; c) HLCs aggregates' morphology at the end of the 24-hour conditioning period. Scale bar = 100 μ m. Abbreviations: D21, D27 (days 21 and 27 of the hepatocyte differentiation protocol).

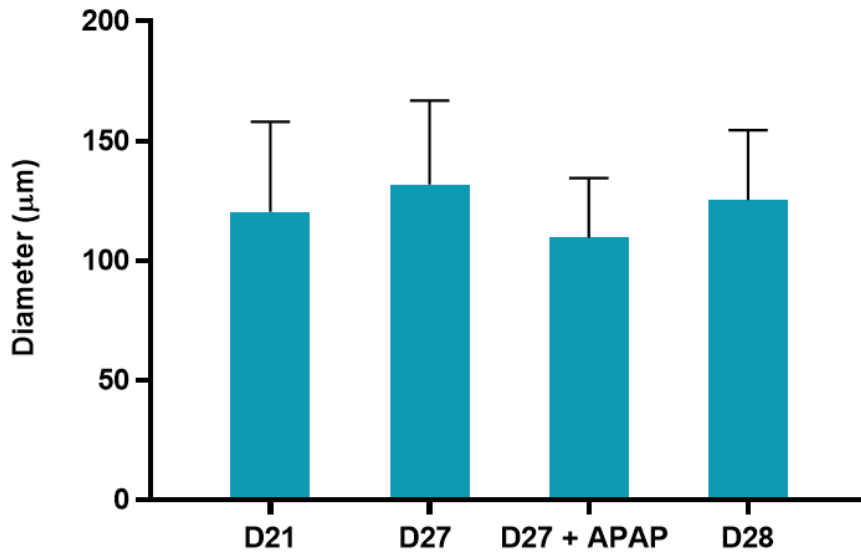


Figure 13 – HLCs aggregates reduced their diameter upon APAP exposure. HLCs aggregates' diameters, in μm , at D21, D27, after an 8-hour exposure to 30 mM APAP at D27 (D27 + APAP) and at D28 at the end of the 24-hour conditioning period. The diameters were measured through phase contrast microscopy images of HLCs inoculated in ultra-low attachment culture plates. Abbreviations: D21 - D28 (days 21 to 28 of the hepatocyte differentiation protocol).

Figure 12 a) illustrates the HLCs aggregates' increased cell density from D21 to D27 which was reflected on the augmentation of their diameter (Figure 13). After an 8-hour exposure to 30 mM APAP (Figure 12 b)), the spheroids showed an irregular border and the number of dead cells in suspension increased, resulting in a slight reduction of their diameter. Alike 2D-cultured HLCs (Figure 10 c)), the aggregates showed improvements in their morphology and diameter size after removing the deleterious drug at the end of the 24-hour conditioning period (Figure 12 c)).

Afterwards, to evaluate if APAP exposure affects differently 2D and 3D-cultured HLCs, a panel of APAP-related hepatotoxicity genes was assessed. In both cultures, the gene expression was quantified after the conditioning of 24 hours in HLCs exposed to 30 mM APAP for 8 hours. The gene expression of 3D injured HLCs are shown in Figure 14 relative to 2D injured HLCs.

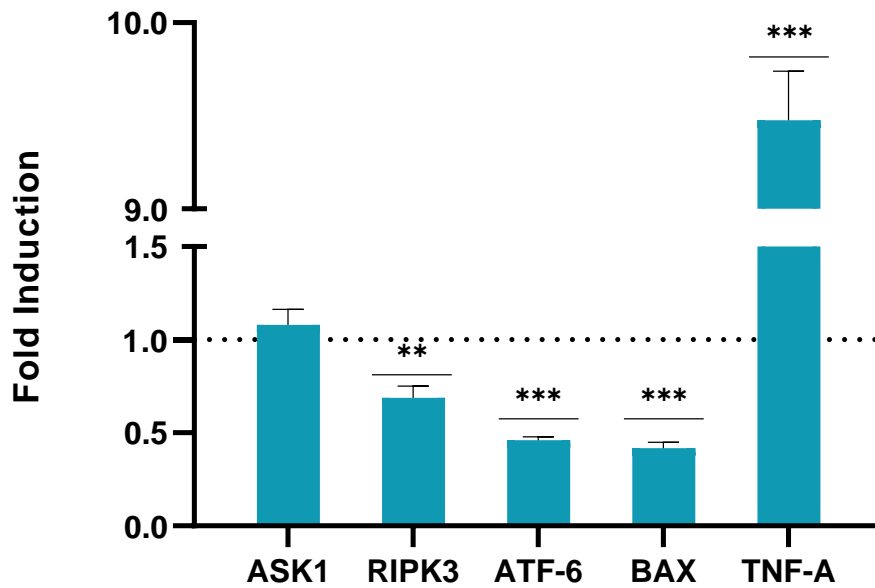


Figure 14 - 3D-cultured HLCs inhibited APAP-related pathways. Gene expression of 3D-cultured HLCs is presented relative to 2D-cultured HLCs both exposed to 30 mM APAP for 8 hours and recovered at the end of the conditioning period. Data represented as average \pm SD (n=1-3). **, *** significantly differs from 2D and 3D-cultured HLCs with $p < 0.01$ and $p < 0.001$, respectively. Abbreviations: *ASK1* (apoptosis signal-regulating kinase 1); *RIPK3* (receptor interacting protein kinases 3); *ATF-6* (activating transcription factor 6); *BAX* (Bcl-2-associated X protein); *HNF4-A* (hepatocyte nuclear factor 4 alpha); *TNF-A* (tumour necrosis factor alpha).

The results showed that 3D-cultured HLCs had lower expression of necroptotic, apoptotic and ER stress genes, i.e., *RIPK3* ($p < 0.01$), *BAX* and *ATF-6* ($p < 0.001$), respectively, than 2D-cultured HLCs. Conversely, *TNF-A* was more up-regulated in 3D cultures ($p < 0.001$). These differences might have been related with the gradients of nutrients, oxygen and, consequently, APAP, generated within the spheroids, not exposing all cells to the same drug concentration as in 2D-cultured HLCs. Moreover, 3D-cultured HLCs might have displayed a higher hepatoprotective potential than 2D-cultured. Likewise, it was previously suggested that 3D cultures might had a higher ability to scavenge reactive species comparing to 2D models.¹³⁶ Therefore, further studies should focus on the APAP-induced mechanisms in 3D-cultured HLCs. Due to time limitations, APAP-induced injury and the effect of the MSC secretome was continued only in 2D-cultured HLCs.

3.3. Priming with the SOS medium exerted pro-angiogenic and regenerative effects in hnUCM-MSCs

The capacity that MSCs have to answer accordingly to their surrounding microenvironment, enabled their pre-conditioning with pro-inflammatory cytokines or injured liver tissue, which resembled the *in vivo* environment, enhancing the secretion of paracrine factors.^{98,104,111} Considering that APAP treatment might have induced the HLCs' secretion of pro-inflammatory cytokines into their medium (SOS medium),

as suggested by the induction of ER stress and apoptosis pathways in HLCs upon APAP exposure (Figure 11), the incubation of hnUCM-MSCs with the SOS medium might modulate them into a more anti-inflammatory and/or pro-regenerative phenotype.

Thus, the next step was to evaluate the effect of priming hnUCM-MSCs with the SOS medium (pMSC-CM) for 24 hours in serum-free conditions. After priming, the medium was replaced by fresh medium without FBS and pMSC-CM was collected 48 hours after. hnUCM-MSCs not exposed to the SOS medium were used as control (cMSC-CM). As a normalization step to ensure that hnUCM-MSCs were always exposed to the same SOS medium conditions, the total protein of HLCs after an 8-hour exposure to 30 mM APAP followed by the 24-hour conditioning period, from which the SOS medium was produced, was quantified (data not shown) and the ratio of total protein per cm² was maintained.

The morphological changes of hnUCM-MSCs during this process are presented in Figure 15. 2 days post-inoculation with 5 % (v/v) FBS (Figure 15 a)), hnUCM-MSCs presented the expected 60 % confluence and fibroblast-like morphology. At day 5 post-inoculation, 72 hours after priming with the SOS medium 5x concentrated (Figure 15 b)), the primed hnUCM-MSCs displayed higher confluency when compared to the non-primed hnUCM-MSCs (Figure 15 c)), as also confirmed by total protein quantification (data not shown), suggesting that the inflammatory signals in the SOS medium might have triggered a proliferative response in hnUCM-MSCs.

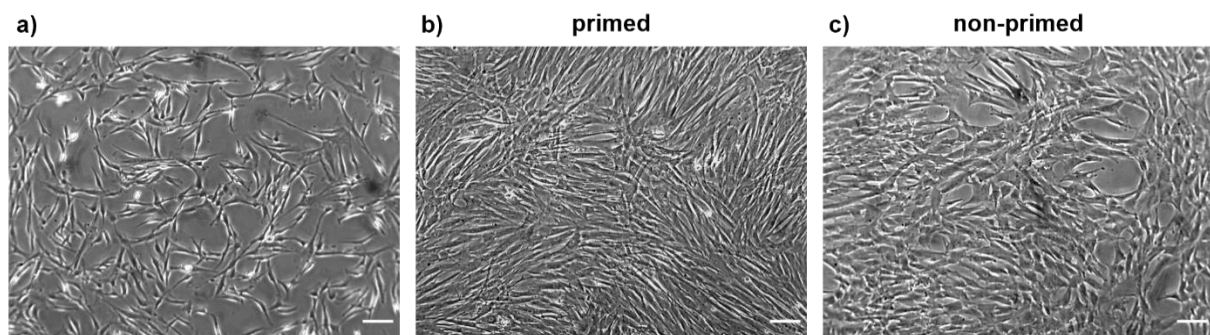


Figure 15 - Priming with the SOS medium increased hnUCM-MSCs' confluency. a) hnUCM-MSCs' morphology 2 days post-inoculation; b) hnUCM-MSCs' morphology 5 days post-inoculation and 72 hours after the priming with the SOS medium; c) non-primed hnUCM-MSCs' morphology 5 days post-inoculation. Scale bar = 100 μ m.

The gene expression profile of the primed hnUCM-MSCs was evaluated and compared to that of non-primed hnUCM-MSCs. From all the known growth factors and cytokines secreted by MSCs, we assessed the expression of key genes (Figure 16) either involved in hepatocyte proliferation and regeneration (*IL-6* and *TNF-A*) or with anti-fibrotic (*HGF*), chemoattractive (*SDF-1*) and pro-angiogenic (*VEGF-A* and *SDF-1*) properties.

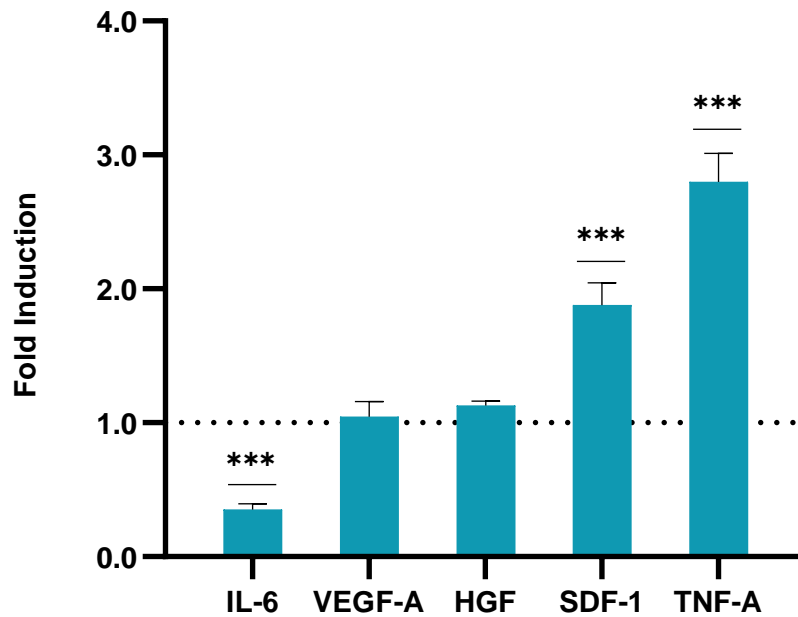


Figure 16 - Enhanced pro-angiogenic effects in hnUCM-MSCs primed with the SOS medium. Gene expression of hnUCM-MSCs primed for 24 hours with the SOS medium following a 48-hour incubation with fresh medium is presented relative to non-primed hnUCM-MSCs. Data represented as average \pm SD (n=2-3). *** significantly differs from the non-primed hnUCM-MSCs gene expression with $p < 0.001$. Abbreviations: *IL-6* (interleukin 6); *VEGF-A* (vascular endothelial growth factor alpha); *HGF* (hepatocyte growth factor); *SDF-1* (stromal cell-derived factor 1); *TNF-A* (tumour necrosis factor alpha).

As seen in Figure 16, *SDF-1* and *TNF-A* ($p < 0.001$) showed a significant up-regulation in primed hnUCM-MSCs comparatively to non-primed hnUCM-MSCs.

SDF-1 has been identified in MSCs amniotic fluid stem cells CM, along with *VEGF*. These two cytokines have been described to act synergically in mediating angiogenesis.¹⁴⁶ Moreover, *SDF-1* has been identified in UC-MSCs CM and its chemoattractive activity induced the recruitment of cells in injured tissue, enhancing the proliferation and exerting therapeutical relevance.¹⁴⁷ Therefore, the *SDF-1* high expression values in primed hnUCM-MSCs showed that its pro-angiogenic effect was activated. Additionally, *TNF- α* has revealed to be pro-angiogenic and cytoprotective.¹⁴⁸ The great expression of *TNF-A* in primed hnUCM-MSCs might be beneficial for the initiation of liver regeneration.

IL-6 is a multifunctional cytokine that mediates cell proliferation, differentiation, survival and apoptosis via the JAK-signal transducer and activator of transcription (STAT) pathway, the MAPK pathway and the PI3K/Akt pathway.¹⁴⁹ *IL-6* has a dual role as a pro-inflammatory cytokine¹⁵⁰ and as a hepatoprotective factor, exerting pro-regenerative¹⁵¹ and anti-apoptotic effects¹⁵² through the suppression of NK T cells in the liver.¹⁵³ Indeed, *IL-6* expressed in MSC-CM had anti-apoptotic effects.¹⁵⁴ Additionally, *IL-6* was essential for the proliferation and immunosuppression capacities of MSCs.¹⁵⁵ Moreover, in the hepatocyte cell cycle, *TNF- α* and *IL-6* are known to initiate the liver regeneration cycle.¹⁴² Therefore, *IL-6* presence in the MSC-CM might stimulate hepatocyte proliferation and

regeneration. However, our results showed *IL-6* inhibition ($p < 0.001$) in primed hnUCM-MSCs. This lower gene expression relatively to control might have been related with the inflammatory signals present in the SOS medium, for instance *ATF-6*, modulating MSCs into a more anti-inflammatory phenotype and suppressing *IL-6* due to its pro-inflammatory role.

MSCs are known to secrete HGF and VEGF- α in high quantities. VEGF- α has an important role in cell protection and survival, being known to induce angiogenesis and HGF is an important anti-fibrotic cytokine known to induce MSCs differentiation into hepatocytes *in vitro*.¹⁵⁶ HGF is recognised by the c-Met receptor in hepatocytes which triggers the activation of a tyrosine kinase signalling cascade, resulting in the stimulation of cell proliferation and in the induction of HSCs apoptosis (anti-fibrotic effect). Indeed, MSC-CM with high levels of HGF inhibited the activation of HSCs *in vitro*.⁹⁸ Moreover, MSCs overexpressing HGF resulted in reduced liver failure and mortality in rats but also improved the functionality of hepatocytes.¹⁵⁷ Furthermore, the secretion of VEGF- α and HGF significantly increased in stress-induced environments, namely in cultures with TNF- α , LPS or hypoxia stimulus.¹⁵⁸ However, in this work, the priming did not enhance the secretion of neither *VEGF- α* or *HGF*, since their expression values were similar to control. This result might suggest that the inflammatory signals presented in the SOS medium were not enough to enhance the expression of these genes, probably related with the intrinsic regeneration of HLCs seen when the SOS medium was collected.

Overall, the expression values of the assessed genes concluded that upon priming with the SOS medium, hnUCM-MSCs were modulated into a more anti-inflammatory phenotype, with pro-angiogenic effect. The pMSC-CM might exert hepatic pro-regenerative effects due to the presence of these soluble mediators, enhancing the formation of new microvasculature from pre-existing blood vessels and priming the hepatocytes cell cycle. Therefore, to assess whether the priming exerts the above-mentioned effects we evaluated the pMSC-CM effect on HLCs.

3.4. Evaluation of the regenerative effect of primed MSC secretome in APAP-induced liver injury *in vitro* model

3.4.1. Inducing liver injury through APAP exposure

The MSC secretome has improved several diseases outcomes through the counterplay between the secreted trophic factors and cells. Bearing in mind the objective of this work, the potential effects of the pMSC-CM secretome in enhancing the regeneration in an APAP-induced HLC *in vitro* model were herein assessed *in vitro*. HLCs were injured at D27 with 30 mM APAP for 24 hours, maintaining the same time of exposure as the established in the APAP dose-response curve. Afterwards, the cells were incubated either with pMSC-CM or cMSC-CM 10x concentrated, for other 24 hours.

To evaluate the hepatic injury in HLCs exposed to 30 mM APAP for 24 hours (prior to treatment with MSC-CM), we analysed the panel of genes involved in APAP-induced hepatotoxicity. Results are shown in Figure 17 relative to non-injured HLCs recovered at D28.

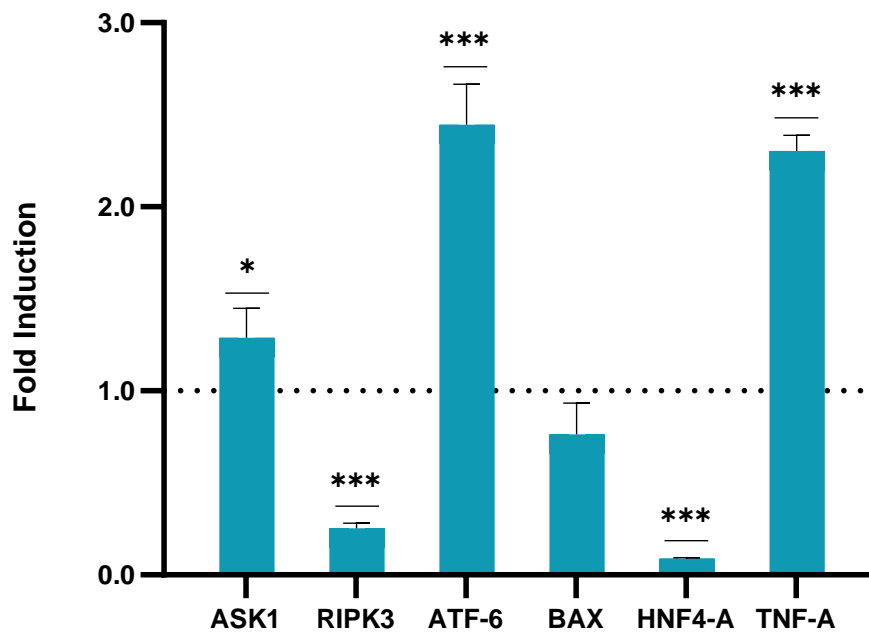


Figure 17 - Mitochondrial and oxidative stress were induced in HLCs following APAP exposure. Gene expression of HLCs exposed to 30 mM APAP for 24 hours is presented relative to non-injured HLCs recovered at D28. Data represented as average \pm SD (n=1-3). *, *** significantly differs from the non-injured HLCs gene expression with $p < 0.05$ and $p < 0.001$, respectively. Abbreviations: *ASK1* (apoptosis signal regulating kinase 1); *RIPK3* (receptor-interacting protein kinases 3); *ATF-6* (activating transcription factor 6); *BAX* (Bcl-2-associated X protein); *HNF4-A* (hepatocyte nuclear factor 4 alpha); *TNF-A* (tumour necrosis factor alpha).

The results presented in Figure 17 showed that *ASK1* ($p < 0.05$), *ATF-6* and *TNF-A* ($p < 0.001$) were significantly overexpressed relatively to non-injured cells, indicating the APAP-induced hepatotoxicity, as expected, namely, the mitochondrial and ER stress. Moreover, the *HNF4-A* ($p < 0.001$) is dramatically reduced, relatively to control, indicating the existence of hepatic injury. After inducing the injury, we must evaluate the regenerative effect of pMSC-CM in injured HLCs.

3.4.2. pMSC-CM displayed a regenerative effect in APAP-induced injury *in vitro* model

To evaluate the MSC secretome (MSC-CM) effect on the HLCs regeneration after APAP-induced injury, we analysed the expression of key genes involved in hepatocyte proliferation (*C-MET* and *CCND1* (gene for cyclin D1)) and angiogenesis (*FGF-2* and *VEGF-A*). Additionally, to assess the effect of the MSC secretome in apoptotic pathways, *BAX* expression was analysed. Gene expression of HLCs exposed to 30 mM APAP for 24 hours and incubated with the primed MSC secretome (pMSC-CM) or the control MSC secretome (cMSC-CM) for other 24 hours is presented in Figure 18. Results are presented relative to HLCs injured with 30 mM APAP for 24 hours and incubated with their basal medium for other 24 hours (control).

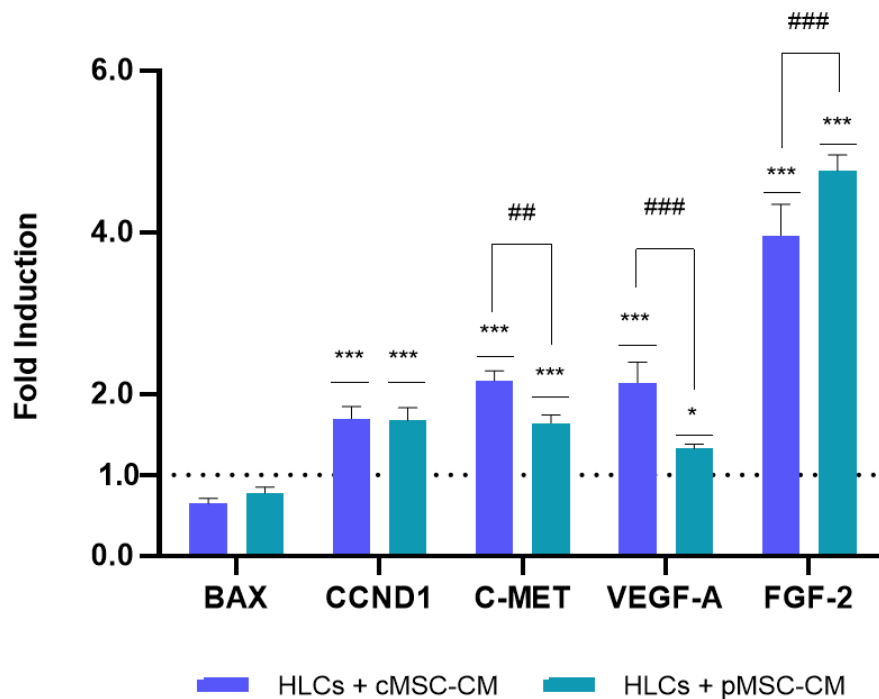


Figure 18 - Regenerative genes were up-regulated in HLCs exposed to the MSC secretome. Gene expression of HLCs with cMSC-CM and pMSC-CM 10x concentrated, after a 24-hour exposure to 30 mM APAP, is presented relative to HLCs exposed to 30 mM APAP for 24 hours incubated with their basal medium (control) for other 24 hours. Data represented as average \pm SD (n=2-3). *, *** significantly differs from the control gene expression with $p < 0.05$ and $p < 0.001$, respectively. ##, ### significant difference between injured HLCs with cMSC-CM and with pMSC-CM with $p < 0.01$ and $p < 0.001$, respectively. Abbreviations: HLCs (hepatocyte-like cells); *BAX* (Bcl-2-associated X protein); *CCND1* (cyclin D1); *VEGF-A* (vascular endothelial growth factor alpha); *FGF-2* (fibroblast growth factor 2); cMSC-CM (human neonatal umbilical cord matrix-derived mesenchymal stem cells conditioned medium not primed); pMSC-CM (human neonatal umbilical cord matrix-derived mesenchymal stem cells conditioned medium primed with the hepatocyte-like cell SOS medium).

The genes involved in the hepatic regeneration, proliferation and angiogenesis – *CCND1*, *C-MET*, *VEGF- α* and *FGF-2* – were overexpressed ($p < 0.05$) in both MSC secretome conditions when compared to control. Nevertheless, the expression level of *BAX* was maintained, indicating that both primed and non-primed MSC secretome did not influence apoptosis.

The priming phase of liver regeneration is mediated by $TNF-\alpha$ and IL-6, which induce the transcription of cyclin D1, for instance. Even though *CCND1* expression increased upon treatment with both MSC-CM conditions relatively to control, the results showed no significant differences between *CCND1* expression in HLCs exposed to pMSC-CM and cMSC-CM. This seemed to suggest that the higher overexpression of *TNF-A* in primed MSCs (Figure 16, section 3.3) did not enhance the *CCND1* expression.

Under inflammatory status, the regenerative genes induce the release of HGF and, consequently, the activation of its hepatocyte receptor c-Met. This receptor plays a crucial role in liver regeneration,

activating CDKs and enhancing cell proliferation and survival. Since MSCs expressed *HGF* (Figure 16, section 3.3), the higher available quantity of HGF predictably induced the up-regulation of *C-MET*, relatively to control, in HLCs exposed to the MSC secretome.

Within the pro-regenerative signalling pathways, VEGF- α and FGF-2 are responsible for angiogenesis and duplication of hepatic endothelial cells in the injured liver. These cytokines are crucial to restore the vessel wall (endothelial cells, smooth muscle cells and fibroblast cells) of the liver.⁴⁵ Thus, the significant overexpression of *VEGF-A* and *FGF-2* in injured HLCs exposed to the MSC secretome, relatively to control, may suggest that the hepatocyte regeneration was enhanced. This result is concordant with the observed in Du, Z. *et al.* (2013) in which *VEGF-A* higher expression was associated with hepatocyte proliferation after MSC-CM therapy.¹⁵⁹

The MSC secretome seemed to be beneficial on injured HLCs by enhancing their regenerative pathways. However, the gene expression of HLCs exposed to 30 mM APAP for 24 hours did not evidence clearly which CM condition (cMSC-CM or pMSC-CM) improved the hepatic regeneration to a greater extent, since *VEGF-A* and *C-MET* were more induced in HLCs exposed to cMSC-CM ($p < 0.01$) while *FGF-2* ($p < 0.001$) had a higher induction in HLCs treated with pMSC-CM. This might be related with the level of injury, which corresponded to the APAP IC_{50} , being too high and in this case the CM cannot exert more notorious therapeutic effects.

Given these results, we hypothesized that the MSC secretome therapeutical action could be enhanced under lower APAP concentrations. Thus, in an attempt to distinguish the benefits of the two MSC secretome conditions, we tested their proliferative effect under lower levels of HLC injury.

The APAP concentrations herein analysed consisted of the concentration used until this point, the IC_{50} (30 mM); an intermediate (15 mM) and a lower concentration (5 mM); and a control with HLCs not exposed to APAP (0 mM) tested upon a 24-hour incubation. After inducing the injury, the medium was replaced by fresh medium with either pMSC-CM or cMSC-CM 10x concentrated, exposing the cells for 24 hours to the MSC secretome. Finally, the cell viability was measured (Figure 19). The results are presented as a normalization to the positive control (HLCs not exposed to APAP with their basal medium).

The results show that the MSC secretome was not toxic for HLCs. Indeed, in HLCs exposed to 5 mM and 15 mM APAP, both cMSC-CM and pMSC-CM, revealed to be beneficial in comparison to not treated HLCs, showing higher cell viability percentages ($p < 0.05$). However, non-injured HLCs (0 mM APAP) and HLCs exposed to 30 mM APAP, incubated with either cMSC-CM or pMSC-CM did not display significative cell viability alterations. This result seemed to indicate that until a certain concentration of APAP and, consequently, a certain degree of APAP-induced injury, the therapeutic effect of both primed and non-primed MSC secretomes is stimulated. Therefore, the MSC secretome therapeutical action appeared to be between 5 and 15 mM APAP.

Notably, the cell viability percentages presented in Figure 19 did not correspond to the estimated by the APAP dose-response curve (Figure 9, section 3.1). The cell viability in HLCs exposed to 30 mM APAP was superior to the calculated IC_{50} . This result was concordant with the cell morphology seen 24

hours after removing APAP in Figure 10 c), section 3.2.1., reinforcing the hypothesis that HLCs were able to recover until a certain extension of injury even with their basal medium.

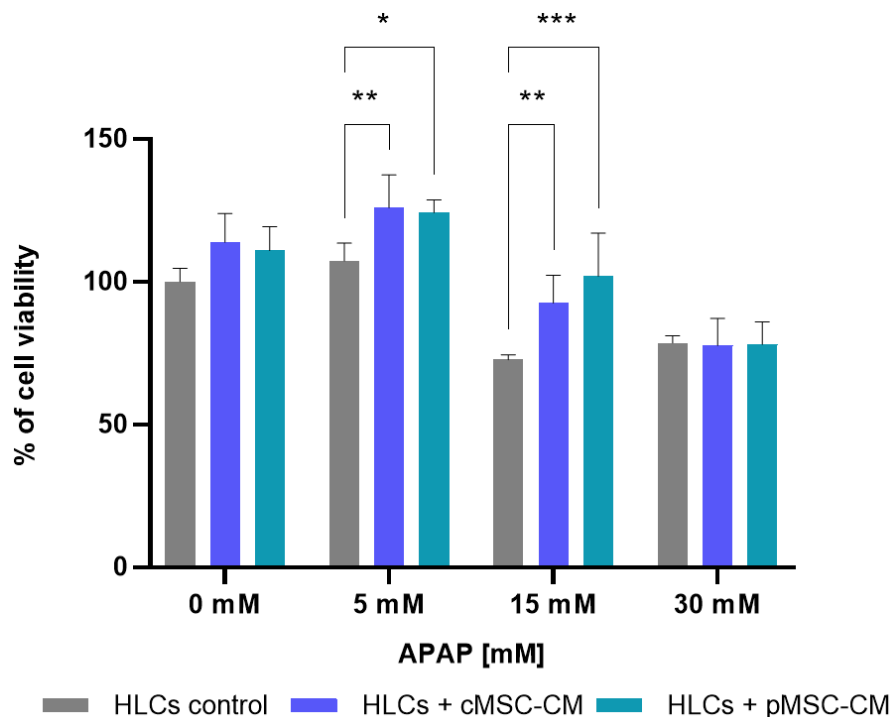


Figure 19 - MSC secretome enhanced HLCs proliferation in lower APAP concentrations. Cell viability of HLCs exposed to different APAP concentrations for 24 hours and incubated with cMSC-CM or pMSC-CM, 10x concentrated, or with their basal medium, for 24 hours. Cell viability percentage was normalized to the positive control (HLCs not exposed to APAP). Data represented as average \pm SD (n=1). *, **, *** significantly differs from the injured HLCs control, cMSC-CM or pMSC-CM gene expression with $p < 0.05$, $p < 0.01$ and $p < 0.001$, respectively. Abbreviations: HLCs (hepatocyte-like cells); cMSC-CM (human neonatal umbilical cord matrix-derived mesenchymal stem cells conditioned medium); pMSC-CM (human neonatal umbilical cord matrix-derived mesenchymal stem cells conditioned medium primed with the hepatocyte-like cell SOS medium).

Regarding the priming strategy, in intermediate injuries (15 mM APAP), the pMSC-CM exerted more beneficial effects than cMSC-CM, suggesting that the secreted pro-angiogenic and pro-regenerative factors (Figure 16, section 3.3) seemed to enhance the cell proliferation. Conversely, in a lesser extent of injury (5 mM APAP) the priming did not seem crucial for HLCs regeneration, since cMSC-CM revealed a higher enhancement in cell proliferation.

Concordantly with the up-regulation of regenerative genes in HLCs exposed to the MSC secretome (Figure 18), this CM therapy appeared to be beneficial and enhance the regeneration of APAP-injured HLCs. Particularly, the priming strategy herein applied to hnUCM-MSCs seemed to indicate that in an intermediate APAP concentration (15 mM) the hepatic regeneration was potentiated, appearing to be a favourable liver regenerative therapy.

4. Conclusions and future perspectives

To develop efficient therapies for APAP-induced liver injury, the underlying mechanisms of hepatotoxicity and liver regeneration need to be thoroughly understood. In particular, MSC paracrine activity, which can be modulated according to the surrounding microenvironment, has been demonstrated to present important immunomodulatory and anti-inflammatory effects, representing an interesting therapeutic approach.

Firstly, injury was induced by exposing HLCs to APAP IC_{50} (30 mM) in 2D and 3D cultures. In 2D cultures, it was observed that mitochondrial and ER stress and apoptosis were activated. In contrast, 3D-cultured HLCs had lower expression of necroptotic, apoptotic and ER stress genes and increased upregulation of *TNF-A* when compared to 2D cultures. These differences might be related with gradients of APAP generated within the spheroids and possible hepatoprotective effects previously described in 3D cultures. As such, further studies should focus on the APAP-induced toxicity mechanisms in 3D-cultured HLCs. Nevertheless, given the resultant hepatotoxicity upon APAP incubation, 2D-cultured HLCs were used to evaluate MSC secretome therapeutic effect. Accordingly, the resultant medium from APAP-injured HLCs with inflammatory signals (SOS medium) was then used to prime MSC-derived secretome (pMSC-CM) into a more regenerative phenotype. It was observed that MSCs exposed to SOS medium presented a more pro-regenerative phenotype, activating pro-angiogenic pathways.

The next step was to evaluate the effect of the MSC secretome in APAP-injured HLCs. Overall, both primed MSC secretome (pMSC-CM) and non-primed (cMSC-CM) induced regeneration, proliferation and angiogenic pathways in HLCs. In particular, pMSC-CM induced higher *FGF-2* overexpression than cMSC-CM, which is related to angiogenesis. On the other hand, cMSC-CM induced higher overexpression of *C-MET* and *VEGF-A*, related to cell proliferation and angiogenesis, respectively. As both secretomes exerted beneficial effects on HLCs injured with 30 mM of APAP, lower levels of injury were studied to assess if differential effects could be observed in cell viability. In fact, in an intermediate level of injury (15 mM), pMSC-CM induced higher HLC proliferation while cMSC-CM stimulated higher cell proliferation in a lower injury level (5 mM). Therefore, our results suggest that at lower levels of injury, MSC secretome does not need to be modulated to produce effects at the cell proliferation level but MSC priming strategy seemed to be best suited for intermediate levels of HLC injury.

As differences in cell proliferation upon MSC secretome treatment were observed with different levels of HLC injury, future work should include a broader characterization of HLCs and MSC secretome. Specifically, HLCs should be analysed regarding gene expression, secreted factors and mitochondrial and ER functionality. Moreover, the specific paracrine mediators present in the SOS medium, in the pMSC-CM and in the cMSC-CM should also be determined, through e.g. proteomic analysis.

Furthermore, our results suggested that HLCs were able to activate intrinsic regenerative mechanisms in the 24 hours of conditioning for the production of the SOS medium. Therefore, to increase the presence of inflammatory signals in the SOS medium, we might consider the reduction of the conditioning time.

In the present work, we tested MSC-CM 10x concentrated, corresponding to 10 % of the final volume, since it was previously established in our group as an optimized concentration. However, Poll, D. et al. (2008), noticed that low concentrations of MSC-CM in the culture medium revealed a direct anti-apoptotic effect on hepatocytes. Actually, 2% MSC-CM in the culture medium revealed to have better results than 8 %.⁹⁰ Thus, it might be interesting to assess the regenerative effect of different MSC-CM concentrations in the HLCs regeneration in future work.

In conclusion, this work demonstrated that the medium obtained from an APAP-induced liver injury *in vitro* model (SOS medium) was capable of mimicking the liver injury microenvironment and successfully modulated hnUCM-MSCs into a pro-regenerative phenotype. Therefore, the primed MSC secretome revealed to enhance the hepatic regeneration in intermediate degrees of APAP-induced injury. Although further studies are needed to better understand the regenerative mechanisms potentiated by the primed MSC secretome and in which conditions it is best applied as a hepatic therapy, the work herein achieved showcased the first steps towards establishing a stem cell free-based therapy for hepatic regeneration.

5. References

1. Kalra, A., Yetiskul, E., Wehrle, C. J. & Tuma, F. Physiology, Liver. in (2021).
2. Meyer, D. J. The Liver. in *Canine and Feline Cytology* vol. 27 226–248 (Elsevier, 2010).
3. Tsung, A. & Geller, D. A. Gross and Cellular Anatomy of the Liver. in 3–6 (2011). doi:10.1007/978-1-4419-7107-4_1.
4. Kusminski, C. M. & Scherer, P. E. New zoning laws enforced by glucagon. *Proc. Natl. Acad. Sci. U. S. A.* **115**, 4308–4310 (2018).
5. Hijmans, B. S., Grefhorst, A., Oosterveer, M. H. & Groen, A. K. Zonation of glucose and fatty acid metabolism in the liver: Mechanism and metabolic consequences. *Biochimie* **96**, 121–129 (2014).
6. Wild, S. L. *et al.* The Canonical Wnt Pathway as a Key Regulator in Liver Development, Differentiation and Homeostatic Renewal. *Genes (Basel)*. **11**, 1163 (2020).
7. Perugorria, M. J. *et al.* Wnt– β -catenin signalling in liver development, health and disease. *Nat. Rev. Gastroenterol. Hepatol.* **16**, 121–136 (2019).
8. Soto-Gutierrez, A., Gough, A., Verneti, L. A., Taylor, D. L. & Monga, S. P. Pre-clinical and clinical investigations of metabolic zonation in liver diseases: The potential of microphysiology systems. *Exp. Biol. Med.* **242**, 1605–1616 (2017).
9. Ben-Moshe, S. & Itzkovitz, S. Spatial heterogeneity in the mammalian liver. *Nat. Rev. Gastroenterol. Hepatol.* **16**, 395–410 (2019).
10. Almazroo, O. A., Miah, M. K. & Venkataramanan, R. Drug Metabolism in the Liver. *Clin. Liver Dis.* **21**, 1–20 (2017).
11. Liu, L. & Liu, X. *Drug Transporters in Drug Disposition, Effects and Toxicity. Advances in Experimental Medicine and Biology* vol. 1141 (Springer Singapore, 2019).
12. Boyd, A., Newsome, P. & Lu, W.-Y. The role of stem cells in liver injury and repair. *Expert Rev. Gastroenterol. Hepatol.* **13**, 623–631 (2019).
13. Cordero-Espinoza, L. & Huch, M. The balancing act of the liver: tissue regeneration versus fibrosis. *J. Clin. Invest.* **128**, 85–96 (2018).
14. de Miguel, M. P., Prieto, I., Moratilla, A., Arias, J. & Aller, M. A. Mesenchymal Stem Cells for Liver Regeneration in Liver Failure: From Experimental Models to Clinical Trials. *Stem Cells Int.* **2019**, 1–12 (2019).
15. Zhao, R.-H., Shi, Y., Zhao, H., Wu, W. & Sheng, J. Acute-on-chronic liver failure in chronic hepatitis B: an update. *Expert Rev. Gastroenterol. Hepatol.* **12**, 341–350 (2018).
16. Serras, A. S. *et al.* A Critical Perspective on 3D Liver Models for Drug Metabolism and Toxicology Studies. *Front. Cell Dev. Biol.* **9**, 1–30 (2021).
17. Andrade, R. J. *et al.* Drug-induced liver injury. *Nat. Rev. Dis. Prim.* **5**, 58 (2019).
18. Roh, J. S. & Sohn, D. H. Damage-Associated Molecular Patterns in Inflammatory Diseases. *Immune Netw.* **18**, 1–14 (2018).
19. Katarey, D. & Verma, S. Drug-induced liver injury. *Clin. Med. (Northfield. Ill)*. **16**, s104–s109 (2016).
20. Babai, S., Auclert, L. & Le-Louët, H. Safety data and withdrawal of hepatotoxic drugs. *Therapie* (2018) doi:10.1016/j.therap.2018.02.004.
21. Verneti, L. A., Vogt, A., Gough, A. & Taylor, D. L. Evolution of Experimental Models of the Liver to Predict Human Drug Hepatotoxicity and Efficacy. *Clinics in Liver Disease* vol. 21 197–214 (2017).

22. Hoofnagle, J. H. & Björnsson, E. S. Drug-Induced Liver Injury — Types and Phenotypes. *N. Engl. J. Med.* **381**, 264–273 (2019).
23. Roth, R. A. & Ganey, P. E. Intrinsic versus Idiosyncratic Drug-Induced Hepatotoxicity—Two Villains or One? *J. Pharmacol. Exp. Ther.* **332**, 692–697 (2010).
24. Schomaker, S. *et al.* Serum glutamate dehydrogenase activity enables early detection of liver injury in subjects with underlying muscle impairments. *PLoS One* **15**, e0229753 (2020).
25. Korver, S. *et al.* The application of cytokeratin-18 as a biomarker for drug-induced liver injury. *Arch. Toxicol.* **95**, 3435–3448 (2021).
26. Fisher, K., Vuppalanchi, R. & Saxena, R. Drug-Induced Liver Injury. *Arch. Pathol. Lab. Med.* **139**, 876–887 (2015).
27. Yoon, E., Babar, A., Choudhary, M., Kutner, M. & Pyrsopoulos, N. Acetaminophen-Induced Hepatotoxicity: a Comprehensive Update. *J. Clin. Transl. Hepatol.* **4**, 131–142 (2016).
28. Lee, W. M. Acetaminophen (APAP) hepatotoxicity—Isn't it time for APAP to go away? *J. Hepatol.* **67**, 1324–1331 (2017).
29. Bunchorntavakul, C. & Reddy, K. R. Acetaminophen (APAP or N-Acetyl-p-Aminophenol) and Acute Liver Failure. *Clin. Liver Dis.* **22**, 325–346 (2018).
30. Mazaleuskaya, L. L. *et al.* PharmGKB summary: pathways of acetaminophen metabolism at the therapeutic versus toxic doses. *Pharmacogenet. Genomics* **25**, 416–26 (2015).
31. Ramachandran, A. & Jaeschke, H. Acetaminophen Toxicity: Novel Insights Into Mechanisms and Future Perspectives. *Gene Expr.* **18**, 19–30 (2018).
32. Yan, M., Huo, Y., Yin, S. & Hu, H. Mechanisms of acetaminophen-induced liver injury and its implications for therapeutic interventions. *Redox Biol.* **17**, 274–283 (2018).
33. Liu, X. & Green, R. M. Endoplasmic reticulum stress and liver diseases. *Liver Res.* **3**, 55–64 (2019).
34. Nguyen, G. C., Sam, J. & Thuluvath, P. J. Hepatitis C is a predictor of acute liver injury among hospitalizations for acetaminophen overdose in the United States: A nationwide analysis. *Hepatology* **48**, 1336–1341 (2008).
35. Yaghi, C. *et al.* Influence of acetaminophen at therapeutic doses on surrogate markers of severity of acute viral hepatitis. *Gastroentérologie Clin. Biol.* **30**, 763–768 (2006).
36. Duncan, A. W., Dorrell, C. & Grompe, M. Stem Cells and Liver Regeneration. *Gastroenterology* **137**, 466–481 (2009).
37. Gao, C. & Peng, J. All routes lead to Rome: multifaceted origin of hepatocytes during liver regeneration. *Cell Regen.* **10**, 1–10 (2021).
38. Zhang, Y., Li, Y., Zhang, L., Li, J. & Zhu, C. Mesenchymal stem cells: potential application for the treatment of hepatic cirrhosis. *Stem Cell Res. Ther.* **9**, 59 (2018).
39. Bangru, S. & Kalsotra, A. Cellular and molecular basis of liver regeneration. *Semin. Cell Dev. Biol.* **100**, 74–87 (2020).
40. Wang, B., Zhao, L., Fish, M., Logan, C. Y. & Nusse, R. Self-renewing diploid Axin2+ cells fuel homeostatic renewal of the liver. *Nature* **524**, 180–185 (2015).
41. Pu, W. *et al.* Mfsd2a+ hepatocytes repopulate the liver during injury and regeneration. *Nat. Commun.* **7**, 13369 (2016).
42. Valizadeh, A., Majidinia, M., Samadi-Kafil, H., Yousefi, M. & Yousefi, B. The roles of signaling pathways in liver repair and regeneration. *J. Cell. Physiol.* **234**, 14966–14974 (2019).
43. Fausto, N., Campbell, J. S. & Riehle, K. J. Liver regeneration. *Hepatology* **43**, S45–S53 (2006).
44. Gilgenkrantz, H. & Collin de l'Hortet, A. Understanding Liver Regeneration: From Mechanisms

- to Regenerative Medicine. *Am. J. Pathol.* **188**, 1316–1327 (2018).
45. Abu Rmilah, A. *et al.* Understanding the marvels behind liver regeneration. *WIREs Dev. Biol.* **8**, 1–46 (2019).
 46. Apte, U., Limaye, P. B. & Michalopoulos, G. K. Extracellular Signals Involved in Liver Regeneration. in *Liver Regeneration* 65–75 (Elsevier, 2015). doi:10.1016/B978-0-12-420128-6.00005-1.
 47. Kaur, S. & Anita, K. Angiogenesis in liver regeneration and fibrosis: “a double-edged sword”. *Hepatol. Int.* **7**, 959–968 (2013).
 48. Huck, I., Gunewardena, S., Espanol-Suner, R., Willenbring, H. & Apte, U. Hepatocyte Nuclear Factor 4 Alpha Activation Is Essential for Termination of Liver Regeneration in Mice. *Hepatology* **70**, 666–681 (2019).
 49. Asrani, S. K., Devarbhavi, H., Eaton, J. & Kamath, P. S. Burden of liver diseases in the world. *J. Hepatol.* **70**, 151–171 (2019).
 50. Preziosi, M. & Monga, S. Update on the Mechanisms of Liver Regeneration. *Semin. Liver Dis.* **37**, 141–151 (2017).
 51. Goldaracena, N. & Barbas, A. S. Living donor liver transplantation. *Curr. Opin. Organ Transplant.* **24**, 131–137 (2019).
 52. Dwyer, B. J., Macmillan, M. T., Brennan, P. N. & Forbes, S. J. Cell therapy for advanced liver diseases: Repair or rebuild. *J. Hepatol.* **74**, 185–199 (2021).
 53. Gramignoli, R., Vosough, M., Kannisto, K., Srinivasan, R. C. & Strom, S. C. Clinical Hepatocyte Transplantation: Practical Limits and Possible Solutions. *Eur. Surg. Res.* **54**, 162–177 (2015).
 54. Berebichez-Fridman, R. & Montero-Olvera, P. R. Sources and Clinical Applications of Mesenchymal Stem Cells: State-of-the-art review. *Sultan Qaboos Univ. Med. J. [SQUMJ]* **18**, 264 (2018).
 55. Takahashi, K. *et al.* Induction of Pluripotent Stem Cells from Adult Human Fibroblasts by Defined Factors. *Cell* **131**, 861–872 (2007).
 56. Weiss, M. L. & Troyer, D. L. Stem Cells in the Umbilical Cord. *Stem Cell Rev.* **2**, 155–162 (2006).
 57. Dong, X. *et al.* Modification of Histone Acetylation Facilitates Hepatic Differentiation of Human Bone Marrow Mesenchymal Stem Cells. *PLoS One* **8**, e63405 (2013).
 58. Li, X. *et al.* Direct Differentiation of Homogeneous Human Adipose Stem Cells Into Functional Hepatocytes by Mimicking Liver Embryogenesis. *J. Cell. Physiol.* **229**, 801–812 (2014).
 59. Campard, D., Lysy, P. A., Najimi, M. & Sokal, E. M. Native Umbilical Cord Matrix Stem Cells Express Hepatic Markers and Differentiate Into Hepatocyte-like Cells. *Gastroenterology* **134**, 833–848 (2008).
 60. Woo, D. *et al.* Direct and Indirect Contribution of Human Embryonic Stem Cell–Derived Hepatocyte-Like Cells to Liver Repair in Mice. *Gastroenterology* **142**, 602–611 (2012).
 61. Yamamoto, H. Differentiation of embryonic stem cells into hepatocytes: Biological functions and therapeutic application. *Hepatology* **37**, 983–993 (2003).
 62. Chen, Y.-F. *et al.* Rapid generation of mature hepatocyte-like cells from human induced pluripotent stem cells by an efficient three-step protocol. *Hepatology* **55**, 1193–1203 (2012).
 63. Espejel, S. *et al.* Induced pluripotent stem cell–derived hepatocytes have the functional and proliferative capabilities needed for liver regeneration in mice. *J. Clin. Invest.* **120**, 3120–3126 (2010).
 64. Asgari, S. *et al.* Differentiation and Transplantation of Human Induced Pluripotent Stem Cell–derived Hepatocyte-like Cells. *Stem Cell Rev. Reports* **9**, 493–504 (2013).
 65. Kuo, T. K. *et al.* Stem Cell Therapy for Liver Disease: Parameters Governing the Success of

- Using Bone Marrow Mesenchymal Stem Cells. *Gastroenterology* **134**, 2111-2121.e3 (2008).
66. Li, T. Z. *et al.* Therapeutic Potential of Bone-Marrow-Derived Mesenchymal Stem Cells Differentiated with Growth-Factor-Free Coculture Method in Liver-Injured Rats. *Tissue Eng. Part A* **16**, 2649–2659 (2010).
 67. Kang, S. H., Kim, M. Y., Eom, Y. W. & Baik, S. K. Mesenchymal Stem Cells for the Treatment of Liver Disease: Present and Perspectives. *Gut Liver* **14**, 306–315 (2020).
 68. Wang, H. *et al.* How important is differentiation in the therapeutic effect of mesenchymal stromal cells in liver disease? *Cytotherapy* **16**, 309–318 (2014).
 69. Dominici, M. *et al.* Minimal criteria for defining multipotent mesenchymal stromal cells. The International Society for Cellular Therapy position statement. *Cytotherapy* **8**, 315–317 (2006).
 70. Friedenstein, A. J., Gorskaja, J. F. & Kulagina, N. N. Fibroblast precursors in normal and irradiated mouse hematopoietic organs. *Exp. Hematol.* **4**, 267–74 (1976).
 71. Watanabe, Y., Tsuchiya, A. & Terai, S. The development of mesenchymal stem cell therapy in the present, and the perspective of cell-free therapy in the future. *Clin. Mol. Hepatol.* **27**, 70–80 (2021).
 72. Ullah, M., Liu, D. D. & Thakor, A. S. Mesenchymal Stromal Cell Homing: Mechanisms and Strategies for Improvement. *iScience* **15**, 421–438 (2019).
 73. Bárcia, R. N. *et al.* What Makes Umbilical Cord Tissue-Derived Mesenchymal Stromal Cells Superior Immunomodulators When Compared to Bone Marrow Derived Mesenchymal Stromal Cells? *Stem Cells Int.* **2015**, 583984 (2015).
 74. Petit, I., Ponomaryov, T., Zipori, D. & Tsvee, L. G-CSF induces stem cell mobilization by decreasing bone marrow SDF-1 and up-regulating CXCR4. *Nat. Immunol.* **3**, 687–694 (2002).
 75. Sackstein, R. *et al.* Ex vivo glycan engineering of CD44 programs human multipotent mesenchymal stromal cell trafficking to bone. *Nat. Med.* **14**, 181–187 (2008).
 76. Suila, H. *et al.* Human Umbilical Cord Blood-Derived Mesenchymal Stromal Cells Display a Novel Interaction between P-Selectin and Galectin-1. *Scand. J. Immunol.* **80**, 12–21 (2014).
 77. Bailey, A. M., Lawrence, M. B., Shang, H., Katz, A. J. & Peirce, S. M. Agent-Based Model of Therapeutic Adipose-Derived Stromal Cell Trafficking during Ischemia Predicts Ability To Roll on P-Selectin. *PLoS Comput. Biol.* **5**, e1000294 (2009).
 78. Chen, Y. *et al.* Recruitment of endogenous bone marrow mesenchymal stem cells towards injured liver. *J. Cell. Mol. Med.* **14**, 1494–1508 (2009).
 79. Liesveld, J. L., Sharma, N. & Aljitawi, O. S. Stem cell homing: From physiology to therapeutics. *Stem Cells* **38**, 1241–1253 (2020).
 80. Chen, M.-S. *et al.* IL-1 β -Induced Matrix Metalloprotease-1 Promotes Mesenchymal Stem Cell Migration via PAR1 and G-Protein-Coupled Signaling Pathway. *Stem Cells Int.* **2018**, 1–11 (2018).
 81. Theise, N. D. *et al.* Liver from bone marrow in humans. *Hepatology* **32**, 11–16 (2000).
 82. Dai, L.-J., Li, H. Y., Guan, L.-X., Ritchie, G. & Zhou, J. X. The therapeutic potential of bone marrow-derived mesenchymal stem cells on hepatic cirrhosis. *Stem Cell Res.* **2**, 16–25 (2009).
 83. Salomone, F., Barbagallo, I., Puzzo, L., Piazza, C. & Li Volti, G. Efficacy of adipose tissue-mesenchymal stem cell transplantation in rats with acetaminophen liver injury. *Stem Cell Res.* **11**, 1037–1044 (2013).
 84. Saito, Y. *et al.* Homing effect of adipose-derived stem cells to the injured liver: the shift of stromal cell-derived factor 1 expressions. *J. Hepatobiliary. Pancreat. Sci.* **21**, 873–880 (2014).
 85. L., P. K. *et al.* The mesenchymal stem cell secretome: A new paradigm towards cell-free therapeutic mode in regenerative medicine. *Cytokine Growth Factor Rev.* **46**, 1–9 (2019).

86. Alm, J. J., Qian, H. & Le Blanc, K. Clinical Grade Production of Mesenchymal Stromal Cells. in *Tissue Engineering* 427–469 (Elsevier, 2014). doi:10.1016/B978-0-12-420145-3.00013-4.
87. Zhou, Y., Yamamoto, Y., Xiao, Z. & Ochiya, T. The Immunomodulatory Functions of Mesenchymal Stromal/Stem Cells Mediated via Paracrine Activity. *J. Clin. Med.* **8**, 1025 (2019).
88. Oskowitz, A., McFerrin, H., Gutschow, M., Carter, M. L. & Pochampally, R. Serum-deprived human multipotent mesenchymal stromal cells (MSCs) are highly angiogenic. *Stem Cell Res.* **6**, 215–225 (2011).
89. Zagoura, D. *et al.* Functional secretome analysis reveals Annexin-A1 as important paracrine factor derived from fetal mesenchymal stem cells in hepatic regeneration. *EBioMedicine* **45**, 542–552 (2019).
90. Van Poll, D. *et al.* Mesenchymal stem cell-derived molecules directly modulate hepatocellular death and regeneration in vitro and in vivo. *Hepatology* **47**, 1634–1643 (2008).
91. Park, O. *et al.* In vivo consequences of liver-specific interleukin-22 expression in mice: Implications for human liver disease progression. *Hepatology* **54**, 252–261 (2011).
92. Wang, J. *et al.* Inhibition of hepatic stellate cells proliferation by mesenchymal stem cells and the possible mechanisms. *Hepatol. Res.* **39**, 1219–1228 (2009).
93. ZHANG, L.-T. *et al.* Bone marrow-derived mesenchymal stem cells inhibit the proliferation of hepatic stellate cells by inhibiting the transforming growth factor β pathway. *Mol. Med. Rep.* **12**, 7227–7232 (2015).
94. Rabani, V. *et al.* Mesenchymal stem cell infusion therapy in a carbon tetrachloride-induced liver fibrosis model affects matrix metalloproteinase expression. *Cell Biol. Int.* **34**, 601–605 (2010).
95. An, S. Y. *et al.* Milk Fat Globule-EGF Factor 8, Secreted by Mesenchymal Stem Cells, Protects Against Liver Fibrosis in Mice. *Gastroenterology* **152**, 1174–1186 (2017).
96. Vizoso, F., Eiro, N., Cid, S., Schneider, J. & Perez-Fernandez, R. Mesenchymal Stem Cell Secretome: Toward Cell-Free Therapeutic Strategies in Regenerative Medicine. *Int. J. Mol. Sci.* **18**, 1852 (2017).
97. Saeedi, P., Halabian, R. & Imani Fooladi, A. A. A revealing review of mesenchymal stem cells therapy, clinical perspectives and Modification strategies. *Stem Cell Investig.* **6**, 34–34 (2019).
98. Choi, J. S., Ryu, H. A., Cheon, S. H. & Kim, S. W. Human Adipose Derived Stem Cells Exhibit Enhanced Liver Regeneration in Acute Liver Injury by Controlled Releasing Hepatocyte Growth Factor. *Cell. Physiol. Biochem.* **52**, 935–950 (2019).
99. Tan, C. *et al.* Mesenchymal stem cell-derived exosomes promote hepatic regeneration in drug-induced liver injury models. *Stem Cell Res. Ther.* **5**, 76 (2014).
100. Li, T. *et al.* Exosomes Derived from Human Umbilical Cord Mesenchymal Stem Cells Alleviate Liver Fibrosis. *Stem Cells Dev.* **22**, 845–854 (2013).
101. Mardpour, S. *et al.* Extracellular vesicles derived from human embryonic stem cell-MSCs ameliorate cirrhosis in thioacetamide-induced chronic liver injury. *J. Cell. Physiol.* **233**, 9330–9344 (2018).
102. Hyvärinen, K. *et al.* Mesenchymal stromal cells and their extracellular vesicles enhance the anti-inflammatory phenotype of regulatory macrophages by downregulating the production of interleukin (IL)-23 and IL-22. *Front. Immunol.* **9**, 1–13 (2018).
103. Yan, Y. *et al.* hucMSC Exosome-Derived GPX1 Is Required for the Recovery of Hepatic Oxidant Injury. *Mol. Ther.* **25**, 465–479 (2017).
104. Waterman, R. S., Tomchuck, S. L., Henkle, S. L. & Betancourt, A. M. A New Mesenchymal Stem Cell (MSC) Paradigm: Polarization into a Pro-Inflammatory MSC1 or an Immunosuppressive MSC2 Phenotype. *PLoS One* **5**, e10088 (2010).
105. Kietzmann, T. Metabolic zonation of the liver: The oxygen gradient revisited. *Redox Biol.* **11**,

- 622–630 (2017).
106. Haque, N., Rahman, M. T., Abu Kasim, N. H. & Alabsi, A. M. Hypoxic Culture Conditions as a Solution for Mesenchymal Stem Cell Based Regenerative Therapy. *Sci. World J.* **2013**, 1–12 (2013).
 107. Noronha, N. C. *et al.* Hypoxia priming improves in vitro angiogenic properties of umbilical cord derived-mesenchymal stromal cells expanded in stirred-tank bioreactor. *Biochem. Eng. J.* **168**, 107949 (2021).
 108. Levy, O. *et al.* Shattering barriers toward clinically meaningful MSC therapies. *Sci. Adv.* **6**, eaba6884 (2020).
 109. Hu, C. & Li, L. Preconditioning influences mesenchymal stem cell properties in vitro and in vivo. *J. Cell. Mol. Med.* **22**, 1428–1442 (2018).
 110. Oyagi, S. *et al.* Therapeutic effect of transplanting HGF-treated bone marrow mesenchymal cells into CCl₄-injured rats. *J. Hepatol.* **44**, 742–748 (2006).
 111. Mohsin, S. *et al.* Enhanced hepatic differentiation of mesenchymal stem cells after pretreatment with injured liver tissue. *Differentiation* **81**, 42–48 (2011).
 112. English, K., Barry, F. P., Field-Corbett, C. P. & Mahon, B. P. IFN- γ and TNF- α differentially regulate immunomodulation by murine mesenchymal stem cells. *Immunol. Lett.* **110**, 91–100 (2007).
 113. Ryan, J. M., Barry, F., Murphy, J. M. & Mahon, B. P. Interferon- γ does not break, but promotes the immunosuppressive capacity of adult human mesenchymal stem cells. *Clin. Exp. Immunol.* **149**, 353–363 (2007).
 114. Sheng, H. *et al.* A critical role of IFN γ in priming MSC-mediated suppression of T cell proliferation through up-regulation of B7-H1. *Cell Res.* **18**, 846–857 (2008).
 115. Yan, L., Zheng, D. & Xu, R. H. Critical role of tumor necrosis factor signaling in mesenchymal stem cell-based therapy for autoimmune and inflammatory diseases. *Front. Immunol.* **9**, 1–13 (2018).
 116. Sivanathan, K. N. *et al.* Interleukin-17A-Induced Human Mesenchymal Stem Cells Are Superior Modulators of Immunological Function. *Stem Cells* **33**, 2850–2863 (2015).
 117. Li, D. *et al.* Low levels of TGF- β 1 enhance human umbilical cord-derived mesenchymal stem cell fibronectin production and extend survival time in a rat model of lipopolysaccharide-induced acute lung injury. *Mol. Med. Rep.* **14**, 1681–1692 (2016).
 118. Lee, B.-C. & Kang, K.-S. Functional enhancement strategies for immunomodulation of mesenchymal stem cells and their therapeutic application. *Stem Cell Res. Ther.* **11**, 397 (2020).
 119. Santos, J. M. *et al.* Three-dimensional spheroid cell culture of umbilical cord tissue-derived mesenchymal stromal cells leads to enhanced paracrine induction of wound healing. *Stem Cell Res. Ther.* **6**, 90 (2015).
 120. Zimmermann, J. & McDevitt, T. C. Engineering the 3D MSC Spheroid Microenvironment to Enhance Immunomodulation. *Cytotherapy* **20**, S106 (2018).
 121. Zhang, X., Hu, M.-G., Pan, K., Li, C.-H. & Liu, R. 3D Spheroid Culture Enhances the Expression of Antifibrotic Factors in Human Adipose-Derived MSCs and Improves Their Therapeutic Effects on Hepatic Fibrosis. *Stem Cells Int.* **2016**, 1–8 (2016).
 122. Wang, K. *et al.* Overexpression of c-Met in bone marrow mesenchymal stem cells improves their effectiveness in homing and repair of acute liver failure. *Stem Cell Res. Ther.* **8**, 162 (2017).
 123. Ma, H.-C., Shi, X.-L., Ren, H.-Z., Yuan, X.-W. & Ding, Y.-T. Targeted migration of mesenchymal stem cells modified with CXCR4 to acute failing liver improves liver regeneration. *World J. Gastroenterol.* **20**, 14884 (2014).
 124. Suk, K. T. & Kim, D. J. Drug-induced liver injury: present and future. *Clin. Mol. Hepatol.* **18**, 249

- (2012).
125. Miranda, J. P. *et al.* The Human Umbilical Cord Tissue-Derived MSC Population UCX ® Promotes Early Motogenic Effects on Keratinocytes and Fibroblasts and G-CSF-Mediated Mobilization of BM-MSCs when Transplanted In Vivo. *Cell Transplant.* **24**, 865–877 (2015).
 126. Rajan, N., Habermehl, J., Coté, M.-F., Doillon, C. J. & Mantovani, D. Preparation of ready-to-use, storable and reconstituted type I collagen from rat tail tendon for tissue engineering applications. *Nat. Protoc.* **1**, 2753–2758 (2006).
 127. Cipriano, M. *et al.* The role of epigenetic modifiers in extended cultures of functional hepatocyte-like cells derived from human neonatal mesenchymal stem cells. *Arch. Toxicol.* **91**, 2469–2489 (2017).
 128. Cipriano, M. *et al.* Self-assembled 3D spheroids and hollow-fibre bioreactors improve MSC-derived hepatocyte-like cell maturation in vitro. *Arch. Toxicol.* **91**, 1815–1832 (2017).
 129. Chiabotto, G., Pasquino, C., Camussi, G. & Bruno, S. Molecular Pathways Modulated by Mesenchymal Stromal Cells and Their Extracellular Vesicles in Experimental Models of Liver Fibrosis. *Front. Cell Dev. Biol.* **8**, 1–13 (2020).
 130. Miranda, J. P. *et al.* The Secretome Derived From 3D-Cultured Umbilical Cord Tissue MSCs Counteracts Manifestations Typifying Rheumatoid Arthritis. *Front. Immunol.* **10**, 1–14 (2019).
 131. Miranda, J. P. *et al.* The Human Umbilical Cord Tissue-Derived MSC Population UCX ® Promotes Early Motogenic Effects on Keratinocytes and Fibroblasts and G-CSF-Mediated Mobilization of BM-MSCs when Transplanted In Vivo. *Cell Transplant.* **24**, 865–877 (2015).
 132. Liu, Y. *et al.* Animal models of chronic liver diseases. *Am. J. Physiol. Liver Physiol.* **304**, G449–G468 (2013).
 133. Zeilinger, K., Freyer, N., Damm, G., Seehofer, D. & Knöspel, F. Cell sources for in vitro human liver cell culture models. *Exp. Biol. Med.* **241**, 1684–1698 (2016).
 134. Lee, C.-W., Chen, Y.-F., Wu, H.-H. & Lee, O. K. Historical Perspectives and Advances in Mesenchymal Stem Cell Research for the Treatment of Liver Diseases. *Gastroenterology* **154**, 46–56 (2018).
 135. Yin, F., Wang, W.-Y. & Jiang, W.-H. Human umbilical cord mesenchymal stem cells ameliorate liver fibrosis in vitro and in vivo: From biological characteristics to therapeutic mechanisms. *World J. Stem Cells* **11**, 548–564 (2019).
 136. Cipriano, M. *et al.* Nevirapine Biotransformation Insights: An Integrated In Vitro Approach Unveils the Biocompetence and Glutathiolomic Profile of a Human Hepatocyte-Like Cell 3D Model. *Int. J. Mol. Sci.* **21**, 3998 (2020).
 137. Kim, D. E. *et al.* Prediction of drug-induced immune-mediated hepatotoxicity using hepatocyte-like cells derived from human embryonic stem cells. *Toxicology* **387**, 1–9 (2017).
 138. Florentino, R. M. *et al.* Cellular Location of HNF4 α is Linked With Terminal Liver Failure in Humans. *Hepatol. Commun.* **4**, 859–875 (2020).
 139. Nishikawa, T. *et al.* Resetting the transcription factor network reverses terminal chronic hepatic failure. *J. Clin. Invest.* **125**, 1533–1544 (2015).
 140. Lazarevich, N. L. *et al.* Progression of HCC in mice is associated with a downregulation in the expression of hepatocyte nuclear factors. *Hepatology* **39**, 1038–1047 (2004).
 141. Parameswaran, N. & Patial, S. Tumor Necrosis Factor- α Signaling in Macrophages. *Crit. Rev. Eukaryot. Gene Expr.* **20**, 87–103 (2010).
 142. Fausto, N. & Riehle, K. J. Mechanisms of liver regeneration and their clinical implications. *J. Hepatobiliary. Pancreat. Surg.* **12**, 181–189 (2005).
 143. Pinheiro, P. F. *et al.* Hepatocyte spheroids as a competent in vitro system for drug biotransformation studies: nevirapine as a bioactivation case study. *Arch. Toxicol.* **91**, 1199–

- 1211 (2017).
144. Takayama, K. *et al.* 3D spheroid culture of hESC/hiPSC-derived hepatocyte-like cells for drug toxicity testing. *Biomaterials* **34**, 1781–1789 (2013).
 145. Ramasamy, T. S., Yu, J. S. L., Selden, C., Hodgson, H. & Cui, W. Application of Three-Dimensional Culture Conditions to Human Embryonic Stem Cell-Derived Definitive Endoderm Cells Enhances Hepatocyte Differentiation and Functionality. *Tissue Eng. Part A* **19**, 360–367 (2013).
 146. Mirabella, T., Cilli, M., Carlone, S., Cancedda, R. & Gentili, C. Amniotic liquid derived stem cells as reservoir of secreted angiogenic factors capable of stimulating neo-arteriogenesis in an ischemic model. *Biomaterials* **32**, 3689–3699 (2011).
 147. SHEN, C. *et al.* Conditioned medium from umbilical cord mesenchymal stem cells induces migration and angiogenesis. *Mol. Med. Rep.* **12**, 20–30 (2015).
 148. Kelly, M. L. *et al.* TNF receptor 2, not TNF receptor 1, enhances mesenchymal stem cell-mediated cardiac protection following acute ischemia. *Shock* **33**, 602–7 (2010).
 149. HEINRICH, P. C. *et al.* Principles of interleukin (IL)-6-type cytokine signalling and its regulation. *Biochem. J.* **374**, 1–20 (2003).
 150. Bourdi, M. *et al.* Role of IL-6 in an IL-10 and IL-4 Double Knockout Mouse Model Uniquely Susceptible to Acetaminophen-Induced Liver Injury. *Chem. Res. Toxicol.* **20**, 208–216 (2007).
 151. James, L. P., Lamps, L. W., McCullough, S. & Hinson, J. A. Interleukin 6 and hepatocyte regeneration in acetaminophen toxicity in the mouse. *Biochem. Biophys. Res. Commun.* **309**, 857–863 (2003).
 152. Kovalovich, K. *et al.* Interleukin-6 Protects against Fas-mediated Death by Establishing a Critical Level of Anti-apoptotic Hepatic Proteins FLIP, Bcl-2, and Bcl-xL. *J. Biol. Chem.* **276**, 26605–26613 (2001).
 153. Sun, R., Tian, Z., Kulkarni, S. & Gao, B. IL-6 Prevents T Cell-Mediated Hepatitis via Inhibition of NKT Cells in CD4 + T Cell- and STAT3-Dependent Manners. *J. Immunol.* **172**, 5648–5655 (2004).
 154. Hoek, J. B. & Pastorino, J. G. Cellular Signaling Mechanisms in Alcohol-Induced Liver Damage. *Semin. Liver Dis.* **24**, 257–272 (2004).
 155. Dorransoro, A. *et al.* Intracellular role of IL-6 in mesenchymal stromal cell immunosuppression and proliferation. *Sci. Rep.* **10**, 21853 (2020).
 156. Lai, L. *et al.* Transplantation of MSCs Overexpressing HGF into a Rat Model of Liver Fibrosis. *Mol. Imaging Biol.* **18**, 43–51 (2016).
 157. Kim, M. D. *et al.* Therapeutic effect of hepatocyte growth factor-secreting mesenchymal stem cells in a rat model of liver fibrosis. *Exp. Mol. Med.* **46**, e110-10 (2014).
 158. Crisostomo, P. R. *et al.* Human mesenchymal stem cells stimulated by TNF- α , LPS, or hypoxia produce growth factors by an NF κ B- but not JNK-dependent mechanism. *Am. J. Physiol. Physiol.* **294**, C675–C682 (2008).
 159. Du, Z. *et al.* Mesenchymal stem cell-conditioned medium reduces liver injury and enhances regeneration in reduced-size rat liver transplantation. *J. Surg. Res.* **183**, 907–915 (2013).

6. Annexes

Table A - Primers used for qRT-PCR.

Name	Sequence
ASK1_F	CTGCATTTTGGGAAACTCGACT
ASK1_R	AAGGTGGTAAAACAAGGACGG
RIPK3_F	CCAAATCCAGTAACAGGGCG
RIPK3_R	TCTTTAGGGCCTTCTTGCGA
ATF-6_F	GACAGTACCAACGCTTATGCC
ATF-6_R	CTGGCCTTTAGTGGGTGCAG
BAX_F	CCCGAGAGGTCTTTTTCCGAG
BAX_R	CCAGCCCATGATGGTTCTGAT
TNF-A_F	AAGCACACTGGTTTCCACACT
TNF-A_R	TGGGTCCCTGCATATCCGTT
HNF4-A_F	ATTGACAACCTGTTGCAGGA
HNF4-A_R	CGTTGGTTCCCATATGTTCC
IL-6_F	ACTCACCTCTTCAGAACGAATTG
IL-6_R	CCATCTTTGGAAGGTTCAAGTTG
HGF_F	GCTATCGGGTAAAGACCTACA
HGF_R	CGTAGCGTACCTCTGGATTGC
SDF-1_F	ATTCTCAACACTCCAAACTGTGC
SDF-1_R	ACTTTAGCTTCGGGTCAATGC
VEGF-A_F	AGGGCAGAATCATCACGAAGT
VEGF-A_R	AGGGTCTCGATTGGATGGCA
C-MET_F	AGCAATGGGGAGTGTAAGAGG
C-MET_R	CCCAGTCTTGTA CT CAGCAAC
CCND1_F	GCTGCGAAGTGGAACCATC
CCND1_R	CCTCCTTCTGCACACATTTGAA
FGF-2_F	AGAAGAGCGACCCTCACATCA
FGF-2_R	CGGTTAGCACACACTCCTTTG